NTNU

Norwegian University of
Science and Technology

Power Production from Low-Temperature Aluminium Electrolysis Cell Off-Gases

Kraftproduksjon fra lavtemperatur aluminium elektrolysecelle avgasser

Monica Andrea Børgund

Master of Science in Energy and Environment
Submission date: June 2009
Supervisor: Erling Næss, EPT

Problem Description

Purpose: The purpose of this thesis is to come up with solutions for power production from low temperature raw gas at Hydro Aluminium, Øvre Årdal.

The thesis is written based on the following points:

1. The energy content and temperature level of the raw gas exiting the pot rooms in Årdal are to be presented. Furthermore, limitations governing the exploitation of this energy are to be evaluated.

2. Power production from the available heat source is to be evaluated. In this context the following is to be done:

a. An investigation and evaluation of different power production technologies relevant for the given heat source is to be performed. If information about relevant existing installations exists, they are to be given.

b. A power production system based on the organic Rankine cycle (ORC), adapted to the given heat source is to be developed. Relevant working fluids are to be evaluated and a recommendation should be given. Furthermore, cycle simulations are to be done to determine power plant efficiency and expected power output.

c. A suggestion of practical layout of a power production unit containing all main components is to be given. Local conditions (such as space limitation, access to cooling water etc.) are to be maintained. Net power production, compensated for increased fan work, pump work etc. is to be estimated. If information is available, a cost estimate for the given power production unit is to be done.

3. Suggestions for further work are to be given.

Assignment given: 28. January 2009
Supervisor: Erling Næss, EPT

Norges teknisk-
naturvitenskapelige universitet
NTNU

Institutt for energi- og prosessteknikk

EPT-H-2009-12

HOVEDOPPGAVE

for

Student Monica Andrea Børgund

Våren 2009

Kraftproduksjon fra lavtemperatur aluminium elektrolysecelle avgasser

Power production from low-temperature aluminum electrolysis cell off-gases

Bakgrunn

Hydro Aluminium AS, Årdal Verk produserer rå-aluminium i prebake elektrolyseceller, og videreforedler aluminiumen ved legering, utstøping og varmebehandling av aluminiumbolter. Store energimengder går i dag tapt i form av varm rågass fra elektrolysecellene. Det er ønskelig å gjenvinne denne energien, og da primært i form av elektrisk kraft. På grunn av rågassens lave temperaturnivå må kraftsykluser med spesielle arbeidsmedier egnet for disse temperaturområdene benyttes.

Mål

Oppgavens mål er å utarbeide forslag til løsninger for kraftproduksjon fra lavtemperatur rågass ved Øvre Årdal Verk.

Oppgaven er en videreføring av prosjektarbeidet.

Oppgaven bearbeides ut fra følgende punkter:

1. Med basis i Hydros aluminiumsverk i Øvre Årdal skal energimengder samt temperaturnivå og gassmengder fra elektrolysecellene presenteres. Det skal også vurderes hvilke begrensninger som gjelder i utnyttelse av den tilgjengelige energien.

2. Produksjon av elektrisk kraft fra den tilgjengelige spillvarmen skal vurderes. I denne sammenhengen skal følgende utføres:
    a. Det skal gjennomføres en undersøkelse og vurdering av ulike teknologier for kraftproduksjon fra den aktuelle spillvarmekilden. I den grad informasjon er tilgjengelig skal relevante eksisterende installasjoner beskrives, og nøkkeldata oppgis.
    b. Et kraftproduksjonssystem basert på Organisk Rankine Syklus-prinsippet (ORC) tilpasset den aktuelle anvendelsen skal utarbeides. Aktuelle arbeidsmedium for kraftprosessen skal vurderes og en anbefaling skal foretas. Det skal videre gjennomføres syklusberegninger for å bestemme energi- og anleggsvirkningsgrader, samt forventet kraftproduksjon.
    c. Det skal utarbeides et forslag til praktisk utforming av en kraftproduksjonsenhet inneholdenede alle hovedkomponenter. Lokale forhold (plassbegrensninger, tilgang på kjølevann etc) skal ivaretas. Netto kraftproduksjon, kompensert for økt

viftearbeid, pumpearbeid etc. skal estimeres. I den grad informasjon er tilgjengelig skal kostnadsestimat for aktuelle kraftproduksjonsanlegg.

3.   Forslag til videre arbeid skal utarbeides.

Senest 14 dager etter utlevering av oppgaven skal kandidaten levere/sende instituttet en detaljert fremdrift- og evt. forsøksplan for oppgaven til evaluering og evt. diskusjon med faglig ansvarlig/ veiledere. Detaljer ved evt. utførelse av dataprogrammer skal avtales nærmere i samråd med faglig ansvarlig.

Besvarelsen redigeres mest mulig som en forskningsrapport med et sammendrag både på norsk og engelsk, konklusjon, litteraturliste, innholdsfortegnelse etc. Ved utarbeidelsen av teksten skal kandidaten legge vekt på å gjøre teksten oversiktlig og velskrevet. Med henblikk på lesning av besvarelsen er det viktig at de nødvendige henvisninger for korresponderende steder i tekst, tabeller og figurer anføres på begge steder. Ved bedømmelsen legges det stor vekt på at resultatene er grundig bearbeidet, at de oppstilles tabellarisk og/eller grafisk på en oversiktlig måte, og at de er diskutert utførlig.

Alle benyttede kilder, også muntlige opplysninger, skal oppgis på fullstendig måte. (For tidsskrifter og bøker oppgis forfatter, tittel, årgang, sidetall og evt. figurnummer.)

Det forutsettes at kandidaten tar initiativ til og holder nødvendig kontakt med faglærer og veileder(e). Kandidaten skal rette seg etter de reglementer og retningslinjer som gjelder ved alle (andre) fagmiljøer som kandidaten har kontakt med gjennom sin utførelse av oppgaven, samt etter eventuelle pålegg fra Institutt for energi- og prosessteknikk.
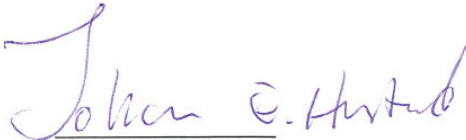
I henhold til "Utfyllende regler til studieforskriften for teknologistudiet/sivilingeniørstudiet" ved NTNU § 20, forbeholder instituttet seg retten til å benytte alle resultater i undervisnings- og forskningsformål, samt til publikasjoner.

Ett -1 komplett eksemplar av originalbesvarelsen av oppgaven skal innleveres til samme adressat som den ble utlevert fra. (Det skal medfølge et konsentrert sammendrag på maks. en maskinskrevet side med dobbel linjeavstand med forfatternavn og oppgavetittel for evt. referering i tidsskrifter).
Til Instituttet innleveres to - 2 komplette, kopier av besvarelsen. Ytterligere kopier til evt. medveiledere/oppgavegivere skal avtales med, og evt. leveres direkte til, de respektive.
Til instituttet innleveres også en komplett kopi (inkl. konsentrerte sammendrag) på CD-ROM i Word-format eller tilsvarende.

Institutt for energi og prosessteknikk, 12. januar 2009

Johan E. Hustad
Instituttleder

Erling Næss
Faglig ansvarlig/veileder

Kontaktperson/medveileder:
    Pia Magnussen, Hydro Aluminium
    Gunn Iren Müller, Hydro Aluminium
    Håkon Skistad, Sintef Energiforskning AS
    Yves Ladam, Sintef Energiforskning AS

Preface

This thesis is a continuation of the project thesis, "Energy Flow Analysis in an Aluminium Plant and Survey of Material Balance", written by Marianne Brekke Tabuk and Monica Andrea Børgund (the writer) in the fall 2008. The project thesis mapped the energy flow at AAM, and found that 16.9 % of the incoming energy to produce aluminium ends up as heat in the exhaust gas. The project report identified the exhaust gas as one of the potential sources for energy recovery and concluded that "the most relevant technologies and working fluids together with component design and cost should be mapped". It was with this in mind the layout of this thesis was formed.

I would like to thank my supervisors at Hydro, Pia Magnussen and Gunn Iren Muller, for making me see the practical use of my thesis, for encouragement and for letting me sit at their offices at Steinshagen in Oslo for a month. I would also like to thank Erling Næss, my main supervisor, and Yves Ladam (SITNEF), for their time and guidance throughout the semester. Finally I would like to thank Håkon Skistad (SINTEF), who first presented me to the world of aluminium and showed me all the possibilities it holds.

Trondheim June 24,2009

Monica Andrea Børgund

Abstract

The objective of this report is to determine the feasibility of installing a waste heat power production unit in connection to the fume treatment plants at AAM and to determine its performance characteristics.

The specific cycles for electricity production suited for low temperature heat sources were discussed, these include the Stirling cycle, the organic Rankine cycle (ORC) and the Kalina cycle. The ORC proved to be the best suited technology for power production from low temperature waste heat. This is due to its superior thermodynamic properties to the steam Rankine cycle. Furthermore, the cycle is better developed and documented than the Stirling and the Kalina cycle. However, the industry for producing power from industrial waste heat is under rapid development, and the same conclusion might not be valid in a couple of years.

The ORC unit was adapted for flue gas heat recovery in connection to the ÅI fume treatment plant (FTP) by identifying the properties of the heat source and heat sink. Furthermore, working fluids contained in the REFPROP 8.0 database were simulated and an optimization to find the optimal working fluid for a direct and an indirect system design was done. R227ea proved to be the best performer both in the direct and the indirect system design with an average power output of 2262 kW and 2153 kW, respectively. This resulted in a 5 % lower power output for the indirect design.

The outline of the power production unit was found by looking at the local conditions and the layout of the future ÅI FTP. The result was an indirect system with four raw gas heat exchangers connected in parallel to a water circuit supplying hot water to the ORC unit. Even tough R227ea proved to be the best performer in the working fluid simulations, R134a was chosen as the working fluid for the final system design based on ORC manufacturer's practical experience with the working fluids. The net power output from the power production unit was identified by adding additional system restrictions to the ORC simulation model, and including power consumption from all auxiliary system components. The final system design had an average net power output of 1726 kW, 21% lower than in the preliminary indirect design.

Four system solutions received from ORC manufacturers Opcon and Turboden were compared based on system performance and financial viability. The performance estimates all had inferior power outputs to the simulated ORC. This was partially due to different system constraints, but mostly due to the different simulation targets. While the commercial units are optimized for minimum cost per kW, the simulations done in this thesis are optimized for maximum power output. Only one of the commercial performance estimates fulfilled the minimum rate of return requirement set by Hydro (11 %). The installation of two Opcon Powerbox modules with ammonia as working fluid is profitable with a financial support of 16.25 % (4 062 708 NOK). Moreover, if the ORC unit is to be installed in connection to the construction of a new FTP, the investment costs of the ORC are expected to be smaller as a gas cooling system is likely to be installed nevertheless.

Table of Contents

List of Figures

List of Tables

Nomenclature

Latin letters

Cp	Specific heat capacity at constant pressure	kJ/kgK
d	Diameter	m
H	Enthalpy	kJ/kg
$\dot{m}$	Mass flow rate	kg/s
p	Pressure	Pa or bar
P	Power, electrical	kWe, kW
Q	Energy, thermal	kJ
$\dot{Q}$	Power, thermal	kW
S	Entropy	kJ/kgK
T	Temperature	°C
$\dot{V}$	Volume flowrate	kg/s
W	Energy, mechanical	kJ

Greek letters

Δ	Differential	
η	Efficiency	
ρ	Density	kg/m^3
v	Specific volume	m^3/kg

Subscripts

c	Condensation, cold
e	Evaporation
h	High, hot
net	Net
th	Thermal
vap	Vaporization

Abbreviations

AAM	Hydro Aluminium Årdal
FTP	Fume Treatment Plant
GWP	Global Warming Potential
HE	Heat Exchanger
HP	High side Pressure (referring to the evaporation pressure)
IHE	Internal Heat Exchanger
LFL	Lower Flammability Limit
LP	Low Pressure (referring to the condensation pressure)
ODP	Ozone Depletion Potential
ORC	Organic Rankine Cycle
PPU	Power Production Unit
TLV	Treshold Limit Value

1 Introduction

1.1 Background

The production of aluminium from alumina is done through electrolysis which is an energy-intensive process. In one year, Hydro Aluminium Årdal (AAM) uses about 2.7 TWh of electricity to produce aluminium, and only 40% of the energy remains chemically bound in the aluminium, while the rest is lost as heat to the cell exhaust gases and the electrolysis hall ventilation air (Tabuk and Børgund, 2008). Because of the high energy loss, increased energy efficiency at AAM can give Hydro both financial savings and strengthen their image as an environmentally conscious company.
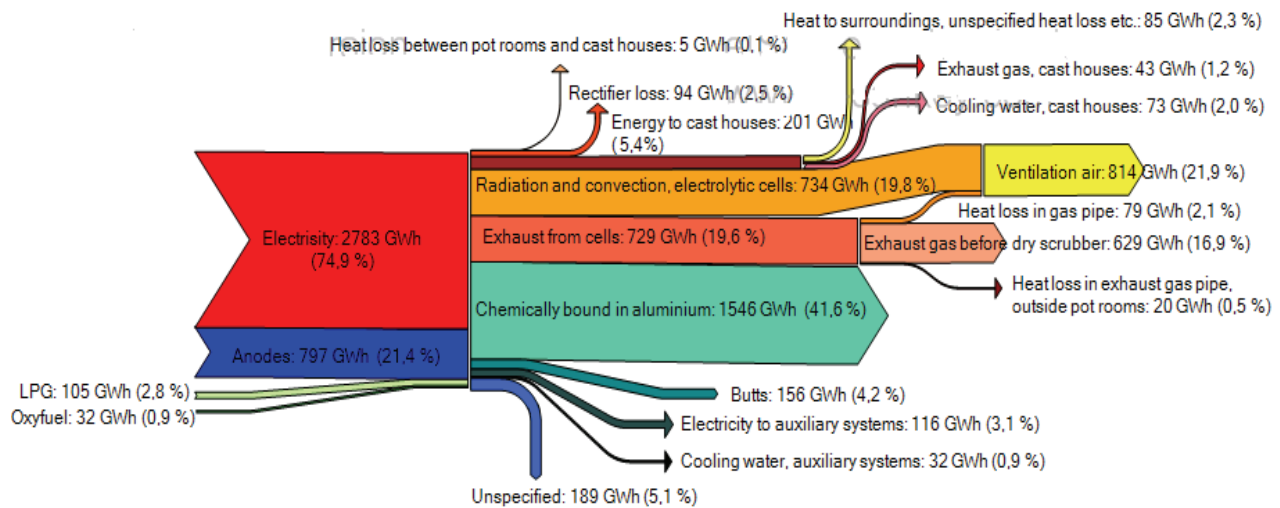
Figure 1.1: AAM energy flow diagram

This thesis is a continuation of the project thesis, "Energy Flow Analysis in an Aluminium Plant and Survey of Material Balance", written by Marianne Brekke Tabuk and Monica Andrea Børgund (the writer). The project thesis mapped the energy flow at AAM, and the result is displayed in Figure 1.1. As seen from the figure, 16.9 % of the incoming energy ends up as heat in the exhaust gas. The project report identified the exhaust gas as one of the potential sources for energy recovery and concluded that "the most relevant technologies and working fluids together with component design and cost should be mapped". It was with this in mind the layout of this thesis was formed.

1.2 Objective

The objective of this report is to determine the feasibility of installing a waste heat power production unit in connection to the fume treatment plants at AAM and to determine its performance characteristics.

The scope of this thesis is narrowed down to electricity production from the raw gas at AAM. As such the performance estimates found in this report are best applicable to AAM, but can also be relevant for aluminium production plants with similar operating conditions. It is not applicable, however, to plants in hotter climates, such as the new aluminium plant in Qatar, where other heat source and heat sink temperatures applies.

1.3 Report Outline

Chapter 2: The theory behind a heat engine is first investigated and then the specific cycles for electricity production suited for low temperature heat sources are discussed. Examples of different power production units using low temperature heat sources are presented along with the current technology status of the different cycles.

Chapter 3: The organic Rankine cycle (ORC) unit was adapted for a flue gas heat source application by identifying the properties of the heat source and heat sink. Furthermore, working fluids contained in the REFPROP 8.0 database were simulated and an optimization to find the optimal working fluid for a direct and an indirect system design was done.

Chapter 4: The outline of the power production unit was found by looking at the local conditions and the layout of the future ÅI FTP. The net power output from the power production unit was found by adding additional system restrictions to the ORC simulation model in Chapter 3, and including power consumption from all auxiliary system components. Furthermore, several system solutions received from ORC manufacturers were compared based on system performance and financial viability.

Chapter 5: Conclusion and suggestions to further work.

2 Low-temperature Power Production Cycles

In this chapter, the theory behind a heat engine is investigated and the specific cycles for electricity production suited for low temperature heat sources are discussed. Examples of different power production units using low temperature heat sources are presented along with the current technology status of the different cycles.

2.1 Theory behind a Heat Engine

A heat engine works by extracting heat from a hot reservoir to a cold reservoir and exploiting the temperature difference between the reservoirs to produce mechanical work (Figure 2.1). The amount of mechanical work produced by the heat engine is dependent on factors such as the ideal cycle efficiency, the amount of heat extracted from the heat source and the component efficiencies. How the different terms are defined, and how they influence the work output is discussed in the next section.
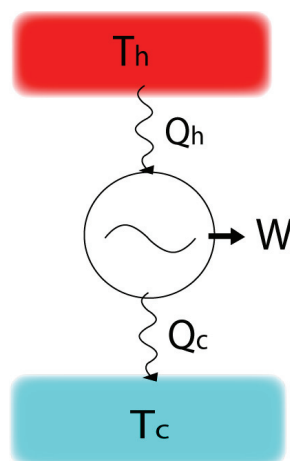
Figure 2.1: A heat engine

2.1.1 Carnot Cycle Efficiency

The thermodynamic cycle efficiency is a measure on how efficiently the transferred flue gas heat (Q_h) is converted to work (W):

$$\eta_{cycle} = \frac{W}{Q_h} \tag{2.1}$$

The maximum cycle efficiency is the Carnot cycle efficiency, which describes how much work you ideally can obtain from a heat engine operating between two reservoirs of different temperatures (Figure 2.1.) It is the second law of thermodynamics that puts quantitative limits on how much useful work that can be obtained by the heat engine.

$$\eta_{Carnot} = \frac{W_{max}}{Q_h} = \frac{T_h - T_c}{T_h} \tag{2.2}$$

Where, T_h and T_c are the temperatures of the high- and low-temperature reservoir, respectively. For sources with gliding temperature during heat extraction, the Carnot efficiency has to be modified. This is the case for electrolysis flue gas as its temperature decreases as heat is removed. Integrating over the temperature range T_h-T_c, the modified Carnot efficiency equation for gliding temperatures becomes:

$$\eta_{Carnot,gliding} = \int_{T_c}^{T_h} \frac{T - T_c}{T} dT = \left[T - T_c \ln(T) \right]_{T_c}^{T_h} = 1 - \frac{T_c \ln\left(\dfrac{T_h}{T_c}\right)}{T_h - T_c} \tag{2.3}$$

Clearly, the ideal cycle efficiency for gliding heat source temperatures is lower than for constant heat source temperatures. This is shown in Figure 2.2, where the isothermal Carnot efficiency is plotted together with the gliding temperature Carnot efficiency (heat sink temperature is set to 7°C).
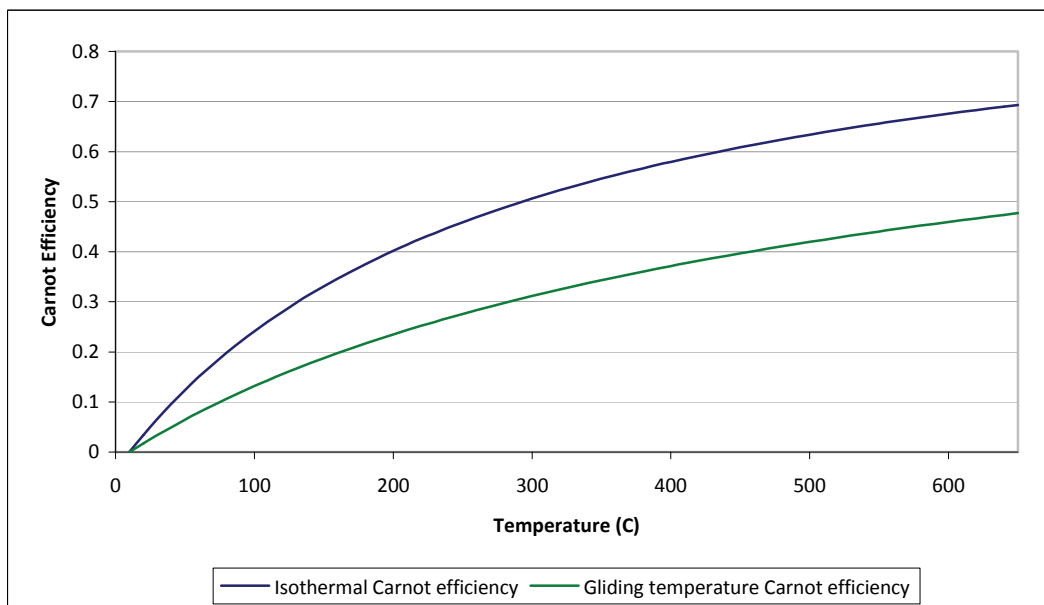
Figure 2.2: Maximum theoretical efficiency for constant and gliding heat source temperatures

Equation   (2.3) displays how the cycle efficiency is dependent on the temperature of the hot and cold reservoir. When (T_h-T_c) goes to infinity, the Carnot efficiency equals 1 (100%). In other words, a large temperature difference between the hot and cold reservoirs results in high cycle efficiency. In this context it is important to see the effect changes in hot and cold reservoir temperature have on cycle efficiency. In Figure 2.3 a. the cold reservoir is set to 0 °C and the Carnot cycle efficiency is plotted for hot reservoir temperatures varying from 80 °C to 140 °C. The graph is nearly linear and the cycle efficiency increases about 0.12% per degree Celsius hot reservoir temperature rise. In Figure 2.3 b. the hot reservoir temperature is set to 100 °C while the cold reservoir temperature varies between -20 °C to 40 °C. In this case, the cycle efficiency increases about 0.16% per degree Celsius cold reservoir temperature drop.   This result is important to remember when designing a power production unit with a low temperature heat source, where the focus tends to be to maximize the hot reservoir temperature. It shows that to minimize the cold reservoir temperature is just as important, and can actually have a greater effect on the cycle efficiency than a hot reservoir temperature rise.
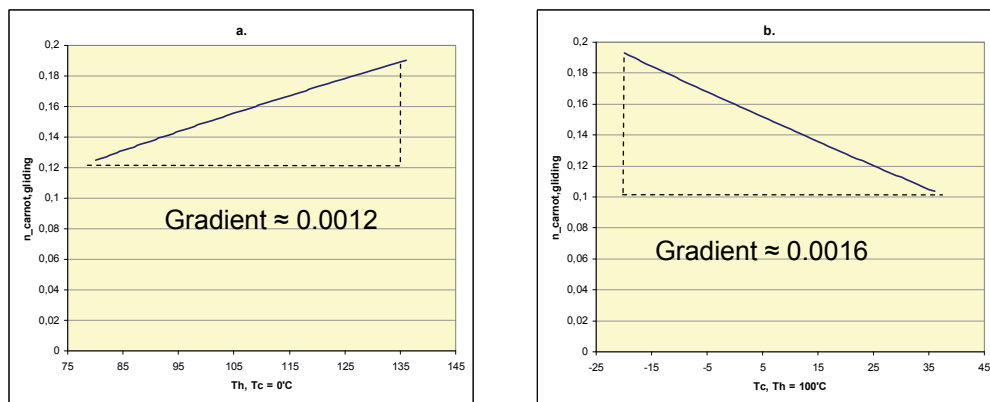
Figure 2.3: Reservoir temperature influence on cycle efficiency

2.1.2 Source Utilization

The work output of a heat engine is dependent on both the Carnot cycle efficiency and the amount of heat extracted from the heat source. As stated earlier, the cycle efficiency is a measure on how much of the heat transferred to the heat engine, Q_h, is eventually transformed to work. Because of the temperature limitation for low temperature heat sources, the ideal cycle efficiency has a tendency to be small (under 20%). For power production units exploiting low temperature heat sources it is therefore important to utilize as much of the energy available as possible from the heat source to get a satisfying work output. This relationship, between work output and available energy, is best displayed by the source utilization factor, η_{source}.

Exergy, or available energy, is the amount of energy that through a reversible process can be transformed to any other energy state (electricity, work, heat etc.). The source utilization factor

is defined as the amount of work produced compared to the total available energy, $Q_{available}$, of the heat source (Milora and Tester, 1977) and describes how well the system utilizes the heat source to produce work:

$$\eta_{source} = \frac{W}{Q_{available}} = \frac{W}{\dot{m}Cp(T_h - T_{ambient})} \qquad (2.4)$$

Where $\dot{m}$ is the mass flow rate of the source, Cp its specific heat and T_{source} its temperature. $T_{ambient}$ is the temperature of the surroundings.

The source utilization factor includes all irreversibilities in the cycle including losses in pumps, compressors, expanders and heat exchangers. To get a high source utilization factor it is therefore important to try and minimize these losses. Investment costs and source utilization are thereby closely linked, as a high utilization factor demands very efficient power converting equipment (heat exchangers, pumps, turbines), which tends to be expensive (Milora and Tester, 1977). A low temperature heat source, such as the electrolysis flue gas, often has costly installations exactly for this reason. Because the installations have low cycle efficiencies, they have to compensate with a high source utilization to produce enough electricity for commercial use.

2.2 Stirling Cycle

The Stirling engine was invented in 1816 by Robert Stirling, and was the first regenerative cycle heat engine (Kontragool and Wongwises, 2003). It was popular in the 19th century due to the engine's safe and silent operation and fuel flexibility. However, its first era came to an abrupt end with the development of the internal combustion engine and electric motor. In the 1940's, as knowledge about materials and working fluids increased, the Stirling engine was re-discovered and great advances in performance were done. Today Stirling cycle-based systems are used in cryogenic refrigeration, air liquefaction and electric generation systems. The Stirling technology is as such a well developed technology, but electricity production from industrial waste heat is a new area of application.

With the current technology the Stirling engine can achieve 65 – 70% of Carnot cycle efficiency (Thombare and Verma, 2008). The main irreversibilities in a Stirling engine are:
- Ineffectiveness in the regenerator (regenerator holdup)
- Irreversibilities in the heat exchangers
- Fluid friction

To minimize the losses, the engine working fluid should have low viscosity, low density, high thermal conductivity and high specific heat capacity (Thombare and Verma, 2008). The predominant working fluids are hydrogen and helium, but new composite working fluids are under investigation. As helium is an inert gas, it has a practical advantage over hydrogen, which is a highly reactive gas. However, Stirling engines with hydrogen as working fluid has a better

efficiency and performance than helium. Both hydrogen and helium have low molecular weights and can be difficult to operate in a pressurized system because of the leakage hazard. A real system installed by Single-Phase Power (SPP) with 1kg Helium as working fluid has a leakage rate of 10% in a year (Høeg, 2009). The leakage does not seem to be a problem, though, as the system can be refilled under routine maintenance.

2.2.1 Basic Configuration

The Stirling engine is composed of two compartments at different temperatures connected to each other through two heat exchangers and a regenerator (see Figure 2.4). The ideal Stirling engine's main processes are:

1 – 2: Isothermal compression. At point 1 (see Figure 2.4) the cold piston is at the outer dead point, the compression volume is at maximum and the pressure and temperature is at their minimum values. During the isothermal compression the cold piston moves upwards, compressing the working fluid, and heat is rejected to the heat sink at constant temperature.
2 – 3: Isochoric heat addition. In the next step the hot and cold piston moves simultaneously to maintain a constant volume. The fluid moves from the cold space to the hot space through the regenerator. The regenerator transfers stored heat to the fluid raising its temperature and pressure.
3 – 4: Isothermal expansion. The cold piston is at its inner dead point, but the hot piston keeps moving outwards as heat is transferred from the heat source to the working fluid. Work is done by the working fluid on the piston equal in magnitude to the heat supplied.
4 – 1: Isochoric heat rejection. The hot and cold piston moves simultaneously to maintain a constant volume. The fluid moves from the hot space to the cold space through the regenerator. The regenerator absorbs heat from the fluid lowering its temperature and pressure.

a. Temperature - entropy diagram   b. Schematic diagram, alpha configuration
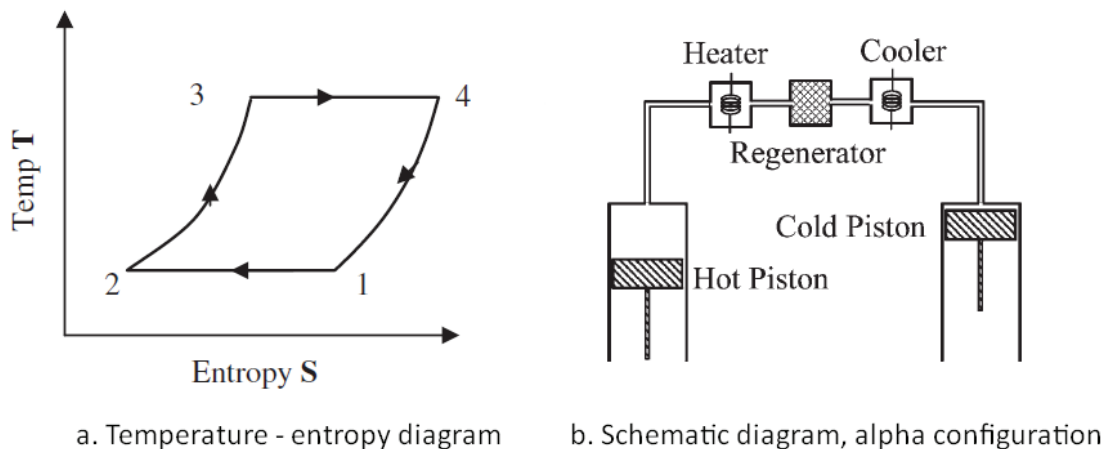
Figure 2.4: Stirling engine basic configuration (a. Thombare and Verma, 2008 b. Kontragool and Wongwises, 2003)

2.2.2 Available Technology

At the moment, the Stirling engine is not commercially competitive to the steam engine or ORC for power outputs larger than 1 MW and heat source temperatures above 250°C. But as this is a technology in constant development, the situation can change rapidly.

The two leading Stirling engine suppliers are Kockums and Stirling DK with mass-produced Stirling engines up to 75kW in size. In Norway, SPP is the leading supplier of Stirling engines. They develop systems for waste incineration plants, bio cogeneration plants and low temperature waste heat. Their current technology specifications are listed in Table 2.1.

Table 2.1: Single-Phase Power enigne's operating criteria

Max. module size	250 kW
Max. power output [1]	1-2 MW
Max. heat source temperature	250 °C
1) For low temperature waste heat applications	

The units are module based and, for greater power output, several modules can be combined. SPP has a pilot plant in Hurum with a max high inlet temperature of 180 °C and a heat sink temperature of 0 °C – 20 °C. The inlet temperature has been adjusted down to 70 °C for research purposes with good results. The already installed unit has helium as working fluid, but hydrogen may be used for the lowest temperature applications in the future. One of their prototypes is shown in Figure 2.5.
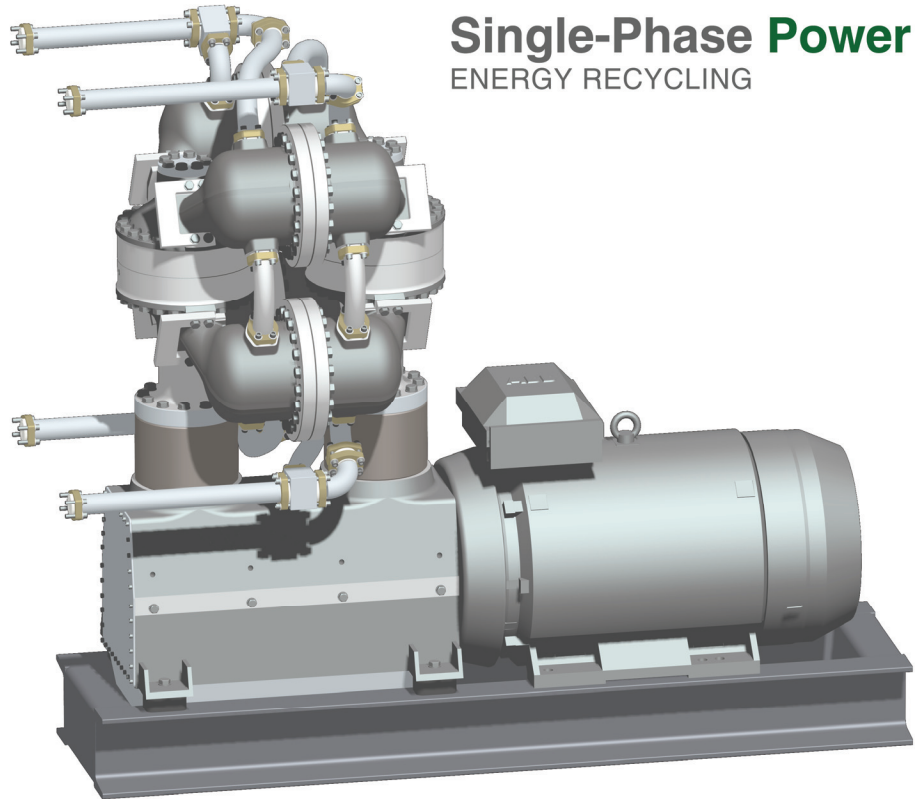
Figure 2.5: Prototype Stirling engine from Single-Phase Power

For flue gas heat recovery, their units should be used with an indirect heat supply system (as shown in Figure 3.3a). As SPP does not have any commercially installed units yet, no data is available from a full-scale Stirling engine in operation. Table 2.2 displays a performance estimate for a Stirling engine installation in connection to a waste incineration plant.

Table 2.2: Performance estimate for a Stirling engine used at a waste incineration plant (Single-Phase Power)

Source: Excess steam in the summer can be used for power production. The steam goes directly to the Stirling engine's heat exchanger.	
Steam mass flow rate	4.3 kg/s
Steam pressure	24 bar
Steam temperature	222 °C
Heat sink temperature (sea water)	15 °C
Power output	1.6 MW
Electricity production	6.2 GWh/year
Investment (excl. coupling)	18.5 MNOK

2.3 Rankine Cycle

The Rankine cycle was first described by the Scottish engineer William J.M. Rankine in 1859. It is a thermodynamic cycle that converts heat into usable work. The most common Rankine cycle is the steam cycle, but in recent years the organic Rankine cycle (ORC) has come to attention because of its superiority in power production from low temperature heat sources.

2.3.1 Basic Configuration

Processes of the ideal Rankine cycle (see Figure 2.6):

1 – 2: Liquid compression; the working fluid is brought from the condensation pressure to the evaporation pressure by a feed water pump.

2 – 3: Evaporator; the liquid is heated and vaporized at constant pressure by an external heat source.

3 – 4: Turbine; the dry saturated vapor expands through a turbine, generating power, and temperature and pressure decreases.

4 – 1: Condenser; the gas is cooled down and condensed in contact with the heat sink, at a constant pressure and temperature.
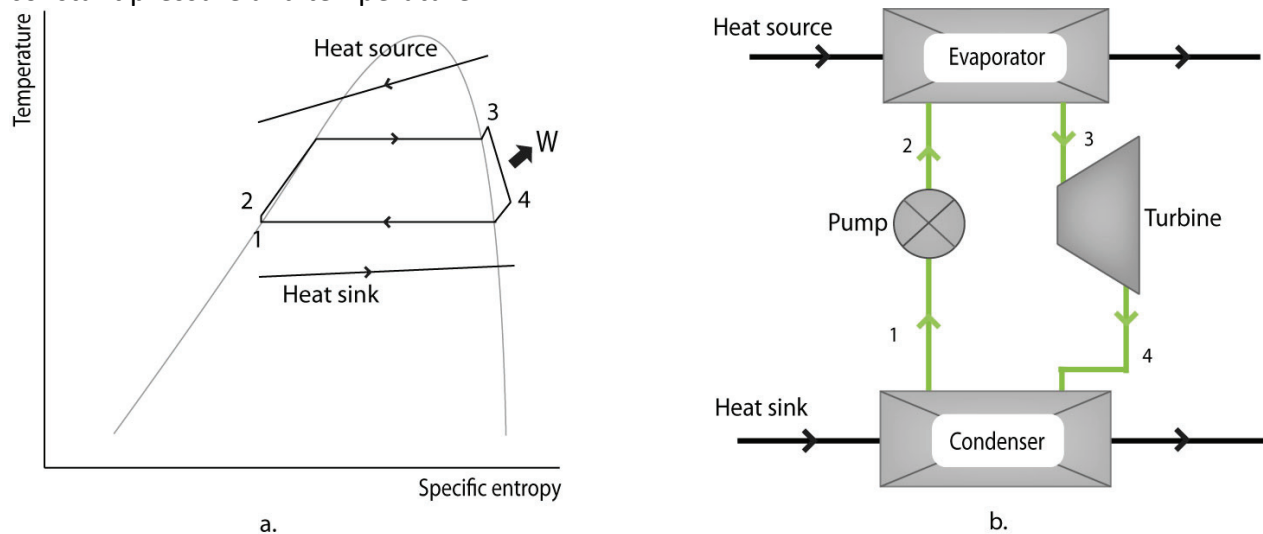
Figure 2.6: The Rankine cycle basic configuration represented by (a) temperature – entropy diagram and (b) schematic diagram.

2.3.2   Steam Cycle

Water has been used as working fluid in Rankine cycle power plants in more than a century. It is today the most commonly used working fluid and the steam cycle technology is highly developed and documented. The advantages of water as working fluid are that it is cheap, inflammable, non-toxic, has good heat transfer properties, low pump work and high thermal stability (Hornnes and Bolland, 1991). The major disadvantages of water are its very low pressure and large specific vapor volume at low temperatures. As a consequence water is not suitable for low to moderate temperature heat sources below 350°C (Hornnes and Bolland, 1991).

2.3.3   Organic Rankine Cycle

The organic Rankine cycle (ORC) is a version of the Rankine cycle that is especially suitable for low temperature heat sources. Instead of having water as working fluid as the original Rankine cycle, the ORC uses an organic working fluid. The organic compounds used have higher condensation pressures, and also higher molecular weights than water which allows for more compact turbines. The working fluid must be selected in accordance to the temperature level of the heat source.

Producers

The major producers of ORC technology for low temperature heat sources are Ormat, GMK and Turboden. Opcon and UTC Power are also in the field. Under is a brief description of the different companies and a presentation of their technology.

Ormat
The American company Ormat is a world leader in the geothermal power industry and ORC technology. They have designed and supplied more than 900 MW of geothermal and heat recovery power plants in the past 25 years with a wide range of source temperatures and power outputs (Bronicki, 2007). Ormat only designs customized ORC units and do not have any standard equipment. As such, they obtain the highest power output possible, but may have more expensive units to offer where a standard unit from another company can be used.

GMK
GMK is a German company founded in 1994 and is a subsidiary of Germania Technologieholding GmbH. It is one of the leading companies in ORC module development and production for waste heat and geothermal power applications in Europe. It's standard module technology for industrial waste heat applications, INDUCAL, has electrical power outputs ranging from 0.5 MW to 5 MW and is aimed at heat source temperatures below 300 °C (GMK, 2009). Figure 2.7 is an illustration of their INDUCAL module.
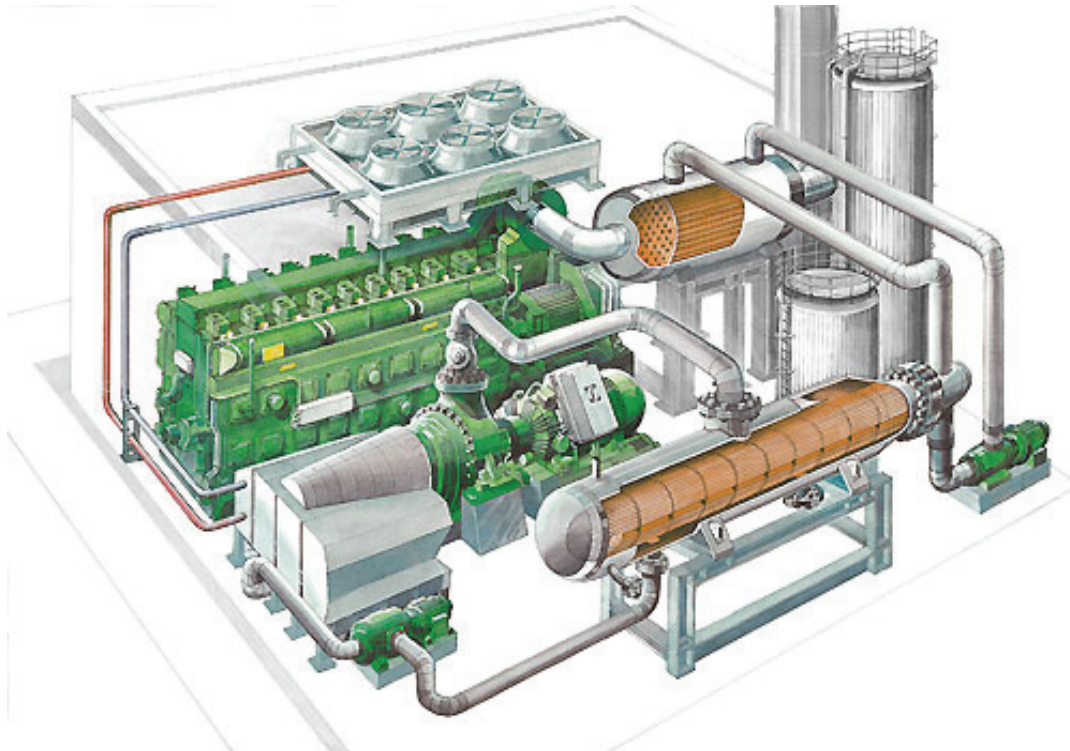
Figure 2.7: GMK ORC module for industrial waste heat applications, INDUCAL (GMK, 2009)

Turboden

Turboden is an Italian company with a leading position within ORC technology in Europe. They have manufactured turbogenerators based on the ORC for nearly 30 years and as of January 2009 they have 93 ORC units in operation throughout Europe (Turboden, 2009a). Their standard heat recovery units have electric power outputs ranging from 400 kW to 2.2 MW, but they are aimed at heat sources at temperatures close to 300 °C. They also design and produce customized units for applications where their standard units cannot be used. Figure 2.8 displays the sizes and typical performances of their standard heat recovery modules.

Heat Recovery application - Standard Sizes and typical performances *

		TURBODEN 6 HR	TURBODEN 7 HR	TURBODEN 10 HR	TURBODEN 14 HR	TURBODEN 18 HR	TURBODEN 22 HR
INPUT- thermal oil							
thermal oil nominal temperature (in/out)	°C	260/150	270/150	270/150	275/150	280/150	280/150
thermal power input	kW	2850	3450	4500	6450	8700	11000
OUTPUT - hot water							
cooling water temperature (in/out)	°C	25/35	25/35	25/35	25/38	25/40	25/42
thermal power to the cooling water circuit	kW	2253	2728	3563	5096	6860	8682
PERFORMANCES							
gross electric power	kW	567	687	898	1302	1762	2220
gross electric efficiency		0.199	0.199	0.199	0.202	0.203	0.202
captive power consumption	kW	22	27	33	52	62	80
net active electric power output	kW	545	660	865	1250	1700	2140
net electric efficiency		0.191	0.191	0.191	0.192	0.196	0.195
electrical generator		asynch.3 phase L.V.	asynch.3 phase L.V.	asynch.3 phase L.V.	asynch.3 phase L.V.	asynch.3 phase L.V.	asynch.3 phase L.V.
size of plant		15x3x3,1m single skid	15x3x3,1m single skid	15x4,5x3,3m single skid	13x6x6,2m multiple skid	15x7x5m multiple skid	15x7x5m multiple skid

*Data indicated could change taking into account the actual features of the specific project (optimization of heat recovery application).

Figure 2.8: Turboden heat recovery application. Standard sizes and typical performances (Turboden, 2009a)

Opcon

Opcon is a Swedish company with a newly founded subsidiary, Opcon Energy Systems, who specializes in developing technology for small-scale production of electricity from waste heat. Opcon Energy Systems developed the Opcon Powerbox, an ORC technology based unit designed to exploit water-based heat sources in the 50 °C – 95 °C temperature range, based on the company's extensive knowledge of screw compressor technology. The Opcon Powerbox was launched in 2007 and the first Powerbox was in operation in 2008. Figure 2.9 displays the net power output from an Opcon Powerbox for different cooling and hot water temperatures.
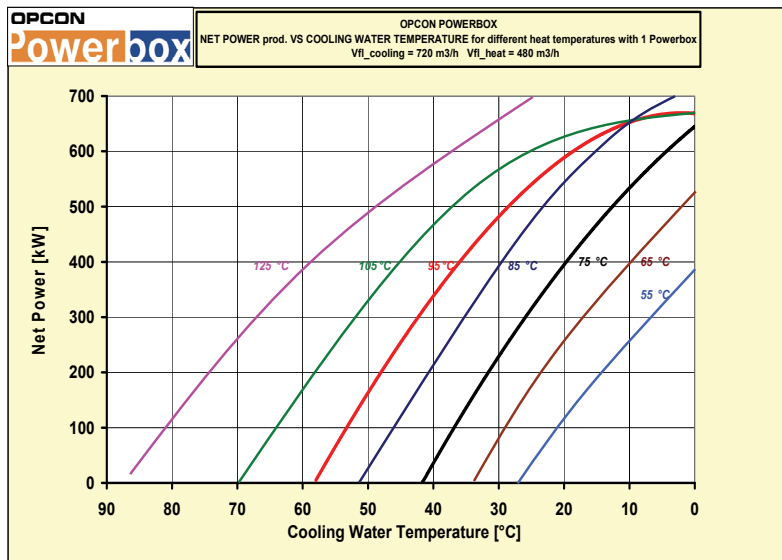
Figure 2.9: Opcon Powerbox net power output versus cooling water temperature for different hot water supply temperatures (Gustavsson, 2009)

UTC Power

UTC Power is part of the United Technology Corporation and has over 50 years of experience as a products and services provider for the building and aerospace industries in the US. As part of their commitment to environmentally responsible power solutions, UTC power has developed the PureCycle Power system. It is an ORC based system that can operate with liquid heat source temperatures down to 91 °C. The system can generate a maximum of 280 kW (gross) of electrical power and uses R134a as working fluid (UTC Power, 2009a). UTC Power has installed a Pure Cycle system at Chena Hot Springs Resort in Alaska. With a heat source temperature of only 74 °C, this is the lowest temperature geothermal resource used for commercial power production in the world (UTC Power, 2009b)

Figure 2.10: The UTC Power PureCycle (UTC Power, 2009b)

Existing Installations

Most existing installations with heat source temperatures below 150 °C are geothermal power production units. They can easily be used as reference examples, as the ORC technology remains the same for waste heat and geothermal applications. The main difference is, off course, the heat source integration design. Geothermal water is usually very aggressive, salty and corrosive so it is very important to know the composition of the water in order to avoid scaling and fouling in the heat exchangers. The material used for the heat exchangers can therefore be more expensive than standard units. Furthermore, the water composition also puts a lower limitation on the water temperature as scaling occurs at lower temperatures. As such, the source utilization of geothermal plants is low.

For aluminium electrolysis raw gas heat recovery, the same problem of fouling and scaling occurs as the gas is full of particles and reactive chemicals. However, the temperature limit is set to 40 °C, much lower than most geothermal plants. The heat source utilization is therefore higher for the raw gas heat recovery system. The raw gas has a disadvantage, however, in that it is a gas and not a fluid, as the heat transfer properties of gases are inferior of those of liquids.

Reference example 1 (Turboden, 2009b):

Plant type:	Heat recovery from waste incinerator
Producer:	Turboden
Location:	Roeselare, Belgum
In operation since:	2008
Heat source:	Hot water at 180 °C
Heat sink:	Water / air
Total electric power:	3 MW
Net efficiency:	16.5 %

Reference example 2 (Turboden, 2009b):

Plant type:	Geothermal
Producer:	Turboden
Location:	Altheim, Austria
In operation since:	2001
Heat source:	Hot water at 106 °C
Heat sink:	Water at 10 °C – 18 °C
Total electric power:	1 MW
Net efficiency:	-

Reference example 3 (Holdman, 2007)

Plant type:	Geothermal
Producer:	UTC Power
Location:	Alaska, USA
In operation since:	2006
Heat source:	Hot water at 74 °C
Heat sink:	Water at 4 °C
Total electric power:	400 kW
Thermal efficiency:	8.2 %

2.3.4 Kalina Cycle

The Kalina cycle was invented by Dr. Alexander Kalina in the 1980's and is therefore a relatively new technology. Main applications are for low temperature heat sources, preferably between 100 °C and 200 °C (Exorca, 2008). It uses a mixed working fluid of ammonia and water, to provide a better temperature match between the working fluid and the heat source in the evaporator. The difference between a subcritical ORC and a Kalina cycle evaporator is shown in Figure 2.11.
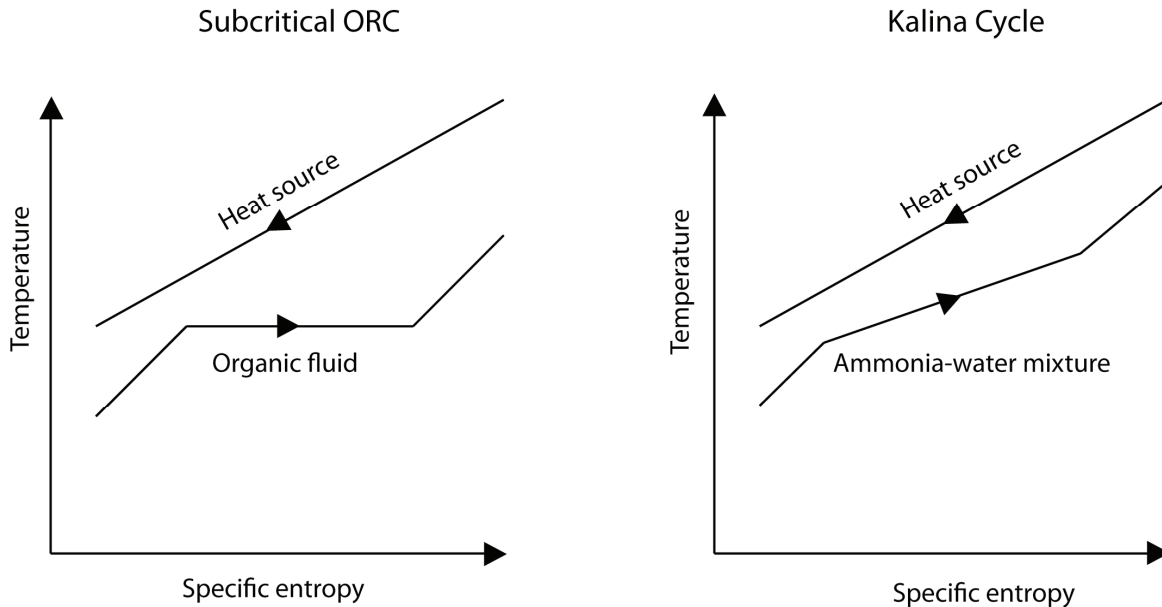
Figure 2.11: Basic sketch of the evaporator temperature profile of a subcritical ORC and a Kalina cycle.

In ORC units the main exergy losses seem to occur due to the finite temperature difference in the heat exchangers. The benefit of the non-isothermal evaporation of the Kalina cycle is therefore evident, as a close temperature fit reduces the exergy losses in the heat exchanger. Theoretically it is assumed that the Kalina cycle can achieve 20-40 % better efficiency, than the ORC (Renz, 2006). However, published comparisons have showed that Kalina- and organic Rankine cycles get approximately the same results (Dippipo, 2004).

Producers

The Kalina process is a patented technology and companies wanting to produce Rankine cycles based on the Kalina technology must posses a license. Because of this, there are not many companies delivering commercial Kalina power plants. The companies currently in possession of a license are:
- Siemens and Exorca in Europe
- MAP resources in the U.S.
- Geodynamics in Australia
- Ebara Corp. in Japan

Existing Installations

One of the first full-scale Kalina plants were erected at Husavik, Iceland in 2000. The main characteristics of the plant are as follows (Dippipo, 2004):

Plant type:	Geothermal
Producer:	Exorca
In operation since:	2000
Heat source:	Hot water at 122 °C
Heat sink:	Water at 5 °C
Net electric power:	1.7 MW
Thermal efficiency:	10.6 %

The plant experienced some "child diseases" in its first years of operation, such as turbine corrosion and leaking safety valves (Valdimarsson, 2006). However, improved Kalina cycles are under development (Renz, 2006).

2.3.5 Internal Heat Exchanger

An internal heat exchanger (IHE) can be used in some cases to improve the Rankine cycle efficiency. The IHE transfers heat from the fluid after the turbine outlet (4-4a in Figure 2.12) to the fluid before the boiler (2-2a in Figure 2.12). This increases the average boiler temperature and decreases the average condenser temperature. Because this heat is not supplied from, or delivered, to the outside the IHE increases the thermal efficiency of the cycle.
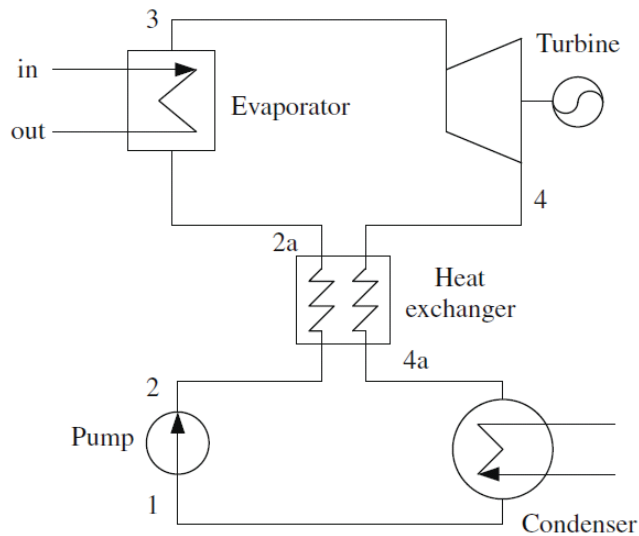
Figure 2.12: ORC with internal heat exchanger (Dai et al., 2008)

Even though the IHE increases the thermal efficiency of the cycle it should only be used when the temperature T_4 is significantly higher than the temperature T_1 (Saleh et al., 2007). This because the gain in cycle efficiency has to make up for the extra costs associated with the IHE.

For fluids with bell-shaped phase equilibrium curves, this can only be obtained by superheating the fluid in the evaporator (Figure 2.13.a). This requires a large heat transfer area as heat transfer during boiling is much more efficient than heat transfer for gas. The extra heat transfer area increases the investment costs, and again, this is an optimization between the gain in cycle efficiency and the increased investment costs.

| a. Bell-shaped coexistence curve | b. Overhaning coexistence curve |
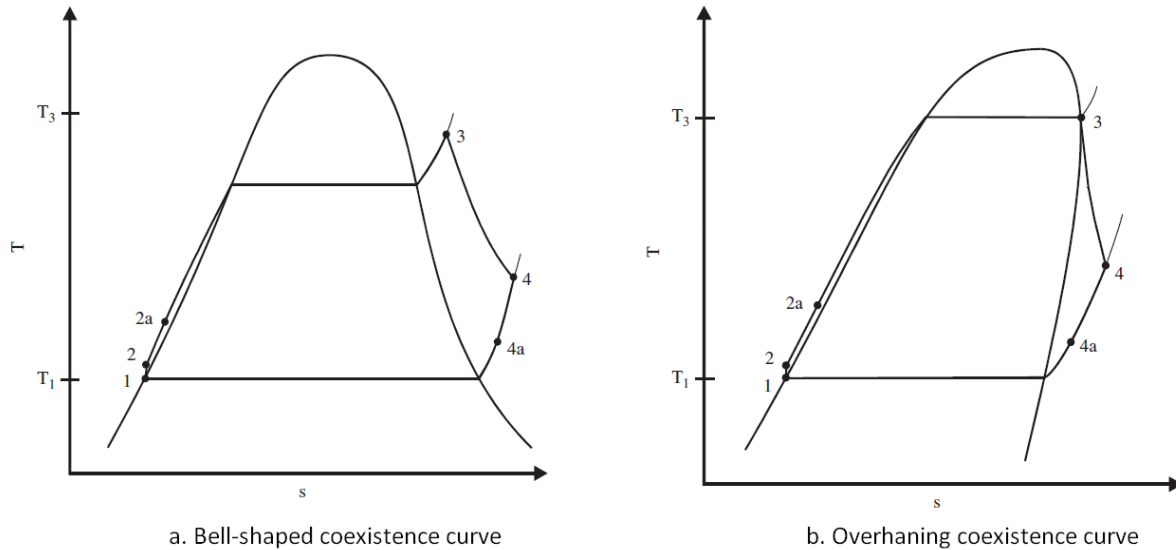
Figure 2.13: Rankine cycle T,s diagrams for a fluid with a) bell-shaped phase-equilibrium curve and b) overhanging phase-equilibrium curve (Saleh et al., 2007)

Because of the positive slope of the saturated vapor curve of the fluids with overhanging phase-equilibrium curves, superheating in the evaporator is not necessary (Figure 2.13.b) and would actually lead to a decrease in cycle efficiency (Saleh et al., 2007). Retrograde fluids are normally already in the super heated region when exiting the turbine, and have to be cooled down to reach the saturation point and start to condense. Without an IHE, the superheated vapor exiting the turbine has to be cooled down in the condenser. If the cooling water source is limited, this is an unwanted use of it. In addition, it augments the average temperature in the condenser leading to a decrease in thermal efficiency. Because of this, it is almost always profitable to install an IHE when using a retrograde working fluid in an ORC.

The IHE can be favorable in more than one way. As pointed out in Chapter 3.1.1, there is a lower temperature limit on the working fluid heat exchanging with the flue gas. In the direct system design (see Chapter 3.1.2) this temperature limit can be avoided by pre-heating the fluid entering the evaporator through an IHE.

3 Evaluation of Working Fluid Candidates

When it comes to electricity production from low temperature heat sources, the ORC technology is the most well proven technology available with several reliable suppliers with many years of experience in the field (see Chapter 2.3.3). In this chapter, the ORC unit was adapted for flue gas heat recovery by identifying the properties of the heat source and heat sink. Both a direct and indirect system design approach was discussed. Furthermore, working fluids contained in the REFPROP 8.0 database were simulated within the boundaries set by the two different system designs and an optimization to find the optimal working fluid for the two system designs was done.

3.1 Background Information and Theory

3.1.1 The Heat Source

The heat source to the power production unit (PPU) is waste heat from the electrolysis cells producing aluminium. About 50% of the waste heat is contained in the raw gas which is sucked away from the cells and treated in a fume treatment plant (FTP). It is in connection with the FTP the heat extraction for electricity production can take place.

The Fume Treatment Plant

AAM has three FTP that process the raw gas before it is released into the atmosphere, belonging to the pot rooms ÅI, ÅIIC and ÅIIC Extension, respectively. As seen in Table 3.1, ÅI has the oldest and largest FTP. It processes flue gas from 216 electrolytic cells, and has a flue gas volume flow rate of 1 456 000 Nm^3/h. The exergy content of the raw gas treated in the ÅI FTP is calculated to be 480 GWh/year based on the mean outdoor temperature in Årdal (5.7 °C, Tabuk and Børgund, 2008).

Currently, the ÅI FTP runs at full capacity as a consequence of the increased cell amperage (and thereby production) the recent years. Before the amperage can be further increased, the ÅI FTP

has to be replaced with a larger, more modern FTP unit. As ÅI FTP is the FTP at AAM with the largest capacity and because a PPU unit would be easier integrated in the design of a new FTP, this report will investigate the possibilities for installing a PPU in connection with the new FTP at ÅI.

Table 3.1: FTP Overview (Tabuk and Børgund, 2008)

FTP	ÅI	ÅIIC	ÅIIC extension	Total
Year of construction	1971	1976 (1991)	1997	-
Flue gas volume flow rate [Nm³/h]	1 456 000	530 000	160 000	2 146 000
Flue gas energy content[i] [GWh/year]	480	191	58	729

i) Based on the temperature and volume flow of the exhaust gas just after leaving the cells

Heat Exchanger Placement

A general sketch of an FTP is illustrated in Figure 3.1. A heat exchanger (HE) can either be placed near the cell (position A), before the dry scrubber (position B) or after the dry scrubber (position C). The next section will discuss the pros and cons of the three possible placements.
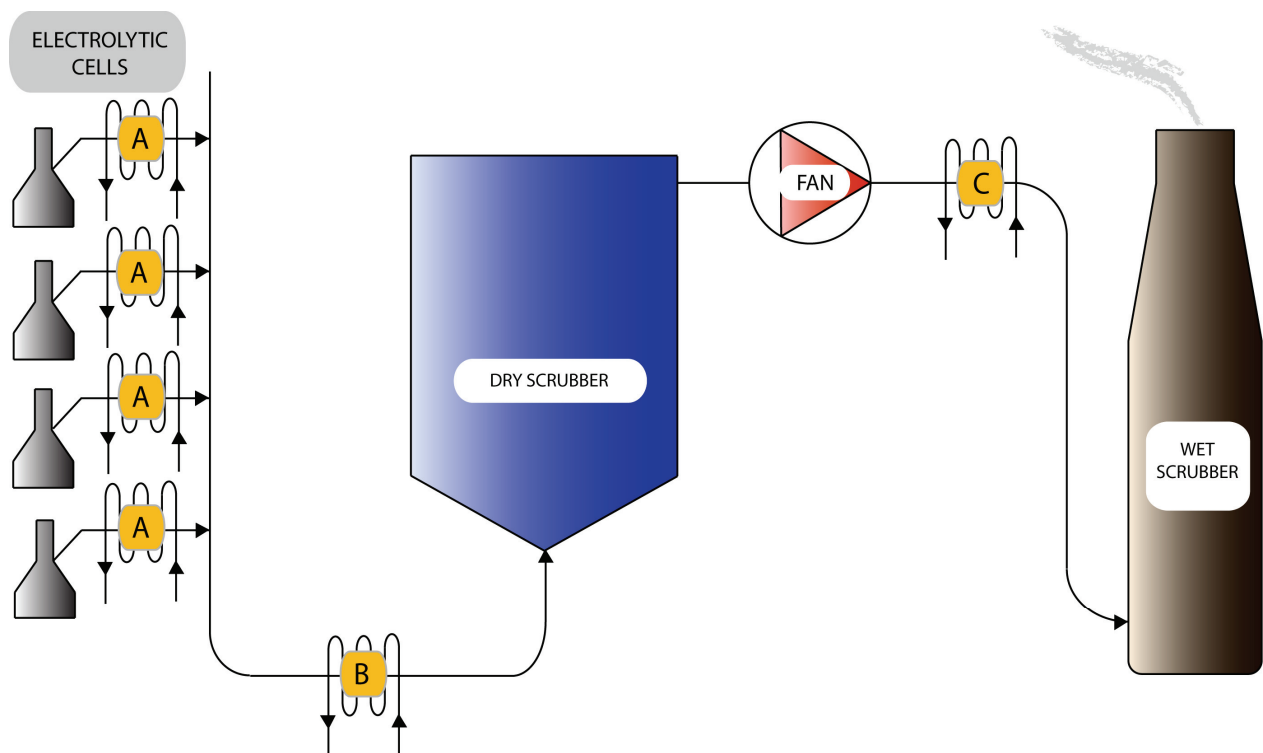
Figure 3.1: FTP setup with three possible heat exchanger placements

The closer the HE is placed to the cell, the higher the supply temperature and thus the thermal efficiency of the PPU will be. However, because ÅI is an old pot room heat exchangers in position A are not plausible. First, one HE for each cell is space demanding and would require

space in the already crowded pot room basement. Second, the HE would be hard to install in the gas ducts while the cells are in operation. Third, installing individual HE requires additional piping and the complexity would result in high investment and maintenance cost. As such, position A is not considered as a realistic option. It could be considered, however, if the power production was related to the construction of a new pot room.

A HE in position B is thermodynamically favorable to a HE in position C as the raw gas is on average 20 °C higher here than after the dry scrubber. The reason lies in the dry cleaning process to remove fluorine from the gas. In the dry scrubber the gas gets mixed with alumina particles before it is sucked through a bag filter leaving the fluorine and the alumina particles behind. The alumina particles, and air that comes with them, are at outdoor temperature, and when blended with the raw gas, the temperature of the raw gas falls. The high temperature before the dry scrubber is favorable to maximize the available heat for power production and the thermal efficiency of the PPU.

Other benefits of a HE in position B include decreased FTP maintenance and operating costs due to the reduced dry scrubber inlet temperature. The reduced temperature decreases the strain on the bag filters in the dry scrubber and reduces the volume flow and pressure drop through the FTP (Tabuk and Børgund, 2008), thus increasing the bag filter lifetime and reducing fan work. On the other hand, a HE also adds to the pressure drop due to friction and form drag on the HE surfaces.

Furthermore, the operating conditions of a HE in position B are more challenging than for a HE in position C. The reason is particles in the raw gas, which at high speeds can act abrasive and grind on the HE surfaces. In addition, the gas contains other substances and moisture, which can cause fouling under certain conditions. Even though the raw gas is not an ideal environment for a HE, several installations exist. An example is the raw gas heat exchanger at Elkem's ferrosilisium plant in Thamshavn, another is heat exchangers in connection with power plants using biofuel (Åmand et al., 2006).

In position C the gas is considered clean, as all solid particles, alumina and fluoride has been removed from the gas by the dry scrubber. This facilitates heat exchange and several clean gas HE are already in operation at Hydro Sunndalsøra to produce hot water for district heating.

The net power output from an ORC process is primarily dependent on the thermal efficiency (η_{th}) and the available heat (Q_h). These parameters are again dependent on the heat source supply temperature. Therefore, to maximize power output, the heat source supply temperature should be maximized. Table 3.2 compares the electricity production potential for a HE installed in position B with a HE in position C in the ÅI FTP. The result is from "Energy Flow Analysis in an Aluminium Plant and Survey of Material Balance" by Tabuk and Børgund, 2008.

Table 3.2: Conclusion Project Report (Tabuk and Børgund, 2008)

	Position B	Position C	Ratio B / C
Electricity production potential [MWh/year]	18 777	11 181	1.68
Fan power consumption increase [MWh/year]	- 2 284	3 461	-
Net electricity gain potential [MWh/year]	20 060	7 720	2.60

As seen from Table 3.2, heat exchange in position B produces 68% more electricity than heat exchange in position C. If the effect on fan power is included the difference is even higher, and position B produces 2.60 times more than position C. Electricity production from low temperature heat sources is a challenge as electricity still is a relatively cheap commodity in Norway. As such, position B presents a more economically viable option than position C as it can produce more electricity and pay back the investment costs faster than position C. In the future both options will be more attractive as the old power price agreements between the state and the industry (including Hydro) expires, and more environmental responsibility is put on the producers.

Because of the superior power production potential of a HE in position B, it will be the position used in the subsequent analyses in this chapter.

Temperature

The temperature at the entrance of the ÅI FTP is monitored throughout the year and recorded approximately every hour. In addition, the ÅI FTP has eight different entrances so for every hour there are eight recorded temperatures. As such, the temperature of the raw gas can be said to be well documented. The data set used in this report originates from measurements done from from May 4th 2008 to May 3rd 2009.
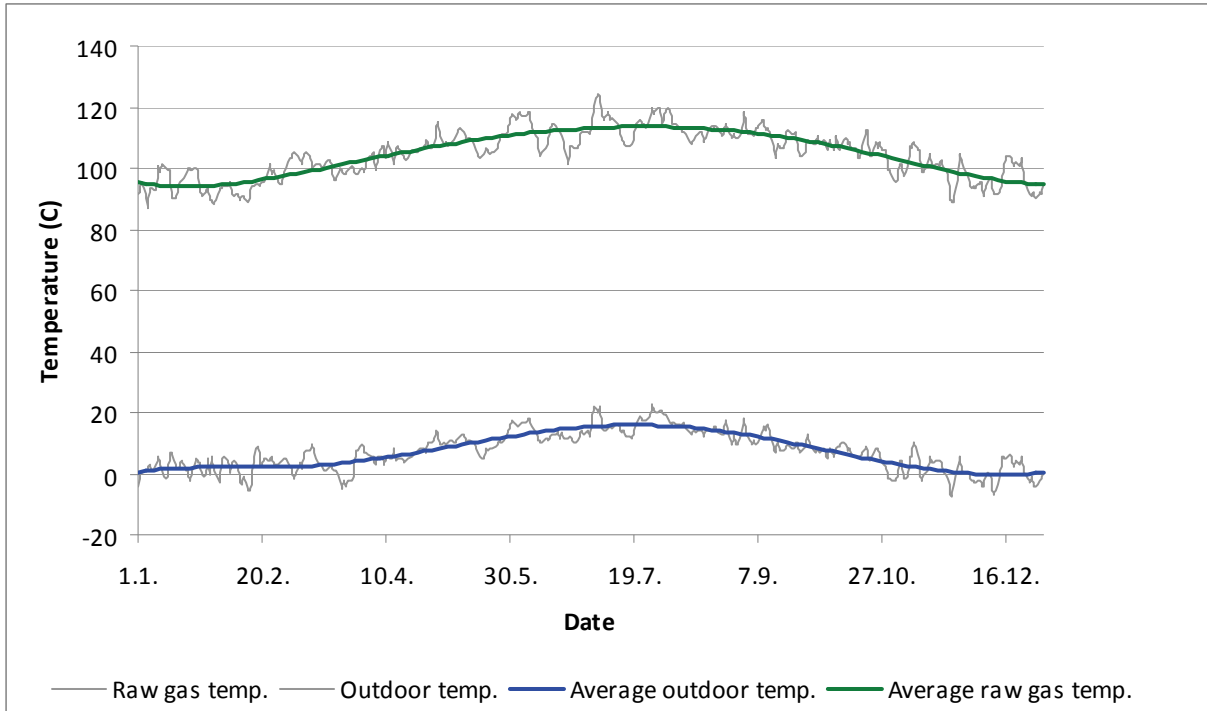
Figure 3.2: Ål FTP raw gas temperature versus Lærdal outdoor temperature

Figure 3.2 displays the raw gas temperature fluctuations throughout the year. The outdoor temperature is also displayed in the graph to illustrate the relation between the exhaust gas and outdoor temperatures[1]. Throughout the year temperature fluctuations occur due to changes in outdoor temperature and disturbances in cell operation (such as anode change, tapping of metal, anode effects and shutdown/startup of a cell). However, the raw gas temperature is almost always 100 °C higher than the outdoor temperature. This demonstrates a strong correlation between the outdoor temperature and the temperature of the raw gas.

The data set containing the temperature data includes almost 80 000 point measurements and to be able to use the data for simulation purposes, the data had to be processed. First, the year was divided into a summer scenario including the data from April 16th to October 15th and a winter scenario including data from October 16th to April 15th. Then, average, maximum and minimum values for both scenarios were found. The main discoveries from processing the temperature data are displayed in Table 3.3.

---

[1] The outdoor temperatures are gathered from the closest weather station in Lærdal owned by the Norwegian Meteorological Institute (Norwegian Meteorological Institute, 2009).

Table 3.3: Temperature characteristics of the Ål raw gas

Temperature	Winter scenario	Summer scenario
Average	98 °C	111 °C
Maximum	113 °C	124 °C
Minimum	87 °C	101 °C

From the result one can deduce that a reasonable winter scenario temperature estimate would be 100 °C ± 10°C. Similarly for the summer scenario a reasonable temperature estimate would be 110 °C ± 10°C.

Acid Dew Point

The raw gas contains SOx gases that originate from the carbon anodes used in the electrolysis process to produce aluminium. The majority of the SOx gas is SO_2, which does not pose a problem when the raw gas is cooled down in a heat exchanger. However, the gas also contains small amounts of SO_3 and H_2SO_4, which will condense when the gas reaches its dew point temperature. The dew point temperature is mainly dependent on the SO_3, H_2SO_4 and water vapor concentration, but is hard to estimate because of the complex chemical composition of the raw gas.

Exact dew point measurements does not exist, but in 2001 Kolderup and Juliussen used an acid dew point meter in the raw gas at Hydro Sunndalsøra. The results indicated that the dew point is lower than 40 °C. As no exact value is found, it is assumed that as long as the temperature of the raw gas and the heat exchanger walls is above 40 °C, SO_3 and H_2SO_4 condensation is avoided.

3.1.2 The Heat Sink

The heat sink for the system is water arriving from the Tya power station after being fed to the turbines to produce electricity. At the moment, some of this water is used at Tya casthouse to cool down the sheet ingots in the casting process. The water supplied to Tya cast house is on average 12°C in the summer time and 2°C in the winter time. These data are not exact values, but based on observations done by the Tya cast house operators who monitor the waters momentary temperature at all times. The uncertainty that accompanies the heat sink temperature is thereby substantial and has to be investigated in further detail before an investment decision can be taken. When it comes to availability no exact data of the quantity available exists, the water is therefore assumed to be an unlimited resource in this simulation.

3.1.3 Direct and Indirect System Design

Figure 3.3 is a principle sketch of the difference between a direct (a) and an indirect (b) supply system. The difference between the two is the closed loop heat supply in the indirect system that transports the heat from the raw gas to the working fluid in the ORC. In the illustration, and in the simulation that follows, water is used as heat supply fluid in the indirect system, but different oils and water glycol mixtures can also be used.
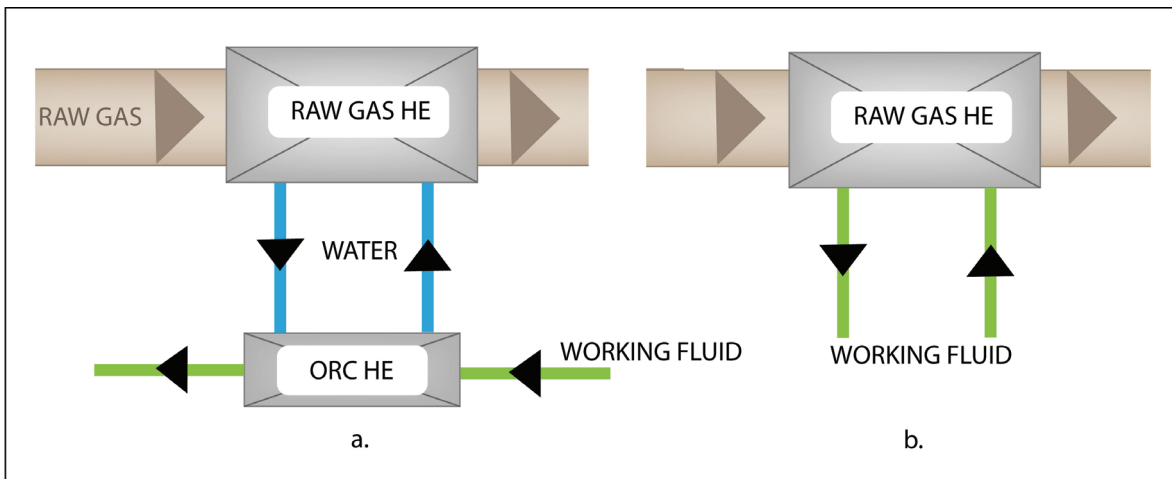
Figure 3.3: Indirect (a) and direct (b) system

The two designs each have their advantages:

The indirect system is easier to use if there are several raw gas heat exchangers delivering heat to the same ORC unit, or if the ORC unit is not in the immediate vicinity of the raw gas heat exchanger. This because water is easier and less expensive to transport than a pressurized working fluid. The indirect system also offers flexibility for future applications of the flue gas heat and the possibility to combine different waste heat sources (such as waste heat extracted from the cathode shell and raw gas combined). For new technologies that have to be tested before they are used in large scale, like the ORC for low temperature waste heat applications, the indirect system seems to be an attractive choice.

Another positive property of the indirect system is that it makes the ORC not directly affected by the dew point temperature limitation. As already stated, the raw gas dew point limits the inflow temperature of the heat exchanging fluid (water for indirect system and working fluid for direct system) to 40 °C. This limits the total amount of energy that can be extracted by the raw gas heat exchanger, both for the direct and the indirect system. In the direct system it also affects the system efficiency by restricting the return temperature of the working fluid to 40 °C. In the indirect system, however, the working fluid has no lower temperature limitation and can utilize a greater share of the theoretical Carnot efficiency.

The direct system also has got advantages. By direct heat exchange with the raw gas, installation and operation costs of a second heat exchanger are prevented. In addition, the

irreversibility provided by the temperature difference between the water and the working fluid in the second heat exchanger is not present. The maximum achievable temperature for the working fluid is therefore higher in a direct than an indirect system. As such, the system might be less expensive and have a better efficiency than the indirect design.

Because of the desirable properties of both systems, the working fluid simulation will have two base case scenarios: one direct and one indirect design.

3.1.4 Thermal Efficiency

The thermal efficiency is made up of the Carnot efficiency together with irreversibilities or losses in the ORC process. It is defined as the ratio of power output to power input. In this case the net power output is the electrical power produced by the generator, $P_{generator}$, minus the electrical power used by the pump, P_{pump}, and the power input is represented by heat from the heat source, $\dot{Q}_h$:

$$\eta_{th} = \frac{P_{generator} - P_{pump}}{\dot{Q}_h}$$
(3.1)

Carnot Efficiency

The Carnot efficiency for a cycle with gliding heat source temperature is expressed by equation (2.3). For the summer scenario with a heat source temperature of 110 °C and a heat sink temperature of 17°C the Carnot efficiency becomes 14.0%. For the winter scenario with a heat source temperature of 100 °C and a heat sink temperature of 7°C the Carnot efficiency becomes 14.5%. It is higher in the winter as a heat sink temperature decrease is more favorable to the efficiency than a heat source temperature increase. For more details on this subject, see Chapter 2.1.2. Carnot Cycle Efficiency.

Heat Exchanger Pinch Point

The heat transferred from the hot to the cold fluid per unit area in the heat exchanger, $\dot{Q}$, can be expressed as

$$\dot{Q}\left[W/m^2\right] = U\left[W/m^2 K\right] \cdot \Delta T\left[K\right]$$
(3.2)

Where U is the heat transfer coefficient and ΔT is the temperature difference between the hot and the cold fluid. There is usually a lower limit to the minimum heat transfer per unit area because of the costs associated with increased heat exchanger area. As the heat transfer coefficient is fairly constant, this constraint is applied to ΔT. The minimum temperature difference in a heat exchanger is called the pinch point and is an important parameter in heat exchanger design.

In the two systems undergoing simulation there are two different types of heat exchangers; a liquid-to-liquid heat exchanger and a gas-to-liquid heat exchanger. The liquid-to-liquid heat exchanger is in the simulations set to have a pinch point of 5°C. This is a general value found in standard liquid-to-liquid heat exchangers (Næss, 2009). The air-to-liquid heat exchanger is the raw gas heat exchanger. The pinch point in the raw gas heat exchanger is somewhat higher than in a pure liquid-to-liquid heat exchanger. This is a consequence of the demanding operating environment and the inferior heat transfer coefficient of air compared to fluids in general. In the simulations the minimum temperature difference is thus set to 15 °C (Næss, 2009).

As heat exchanger design optimization is beyond the scope of this assignment the pinch points given are only rough estimates. However, they reflect the difference between an air-to-liquid and a liquid-to-liquid heat exchanger well.

Mechanical Efficiencies

Because of irreversibilities in the real ORC unit, the thermal efficiency is usually only 50% of the Carnot efficiency. The irreversibilities in the heat exchanger is represented by the exergy losses between heat source and heat sink and is already been defined by the HE pinch point. In addition to the minimum temperature difference in the heat exchangers, the mechanical efficiency of the pump, the turbine and the generator in the ORC is included in the simulation. The mechanical efficiency is set to be 0.7 for the pump and 0.8 in all for the turbine and the generator, which are common efficiency values for ORC units (Ladam, 2009).

3.1.5   Method and Framework

Software Used

All data used in the simulations is retrieved from the REFPROP database, version 8.0. Microsoft Excel 2003 is used to carry out the simulations.

REFPROP is an acronym for REFerence fluid PROPerties and is developed by the National Institute of Standards and Technology (NIST). It provides tables and plots of the thermodynamic and transport properties of industrially important fluids and their mixtures with an emphasis on refrigerants and hydrocarbons. REFPROP provides some of the most accurate pure fluid and mixture models currently available.

Framework

On the background of the information found earlier in this section, the following parameters are dimensioning for the ORC unit:

Raw gas temperature, summer	110	°C
Raw gas temperature, winter	100	°C
Cooling water temperature, summer	12	°C
Cooling water temperature, winter	2	°C
Min. temperature difference in raw gas heat exchanger	15	°C
Min. temperature difference in pure fluid heat exchangers	5	°C
Min. temperature of working fluid in raw gas heat exchanger	40	°C
Raw gas mass flow rate	522.54	kg/s
Cooling water mass flow rate	∞	kg/s
Carnot efficiency, summer	14.0	%
Carnot efficiency, winter	14.5	%
Turbine efficiency	80	%
Pump efficiency	70	%

3.1.6 Working Fluid Selection

Ideal Working Fluid Properties

For the design and performance of most PPU the working fluid properties have a decisive influence. The optimal working fluid satisfies all system requirements while maximizing power output and minimizing costs. When selecting a suitable working fluid for a given cycle the following factors are important (Hornnes and Bolland, 1991 and Badr et al., 1985):

I.   The temperature - pressure curve

The temperature – pressure curve of a given fluid gives the melting- and boiling point for a working fluid. In addition, the critical temperature and pressure is given by this curve. The condensation and evaporation temperatures in a Rankine cycle are often decided by the heat source and heat sink temperatures. For an ideal fluid the condensation pressure should not be much inferior to the atmospheric pressure in order to avoid infiltration of atmospheric air into the system. When it comes to the evaporator pressure, it should be considerably higher than the condensation pressure for optimal turbine operation. On the other hand, it is important that the evaporator pressure is not excessive, as it can lead to mechanical stress problems and require expensive components. Another criterion is obviously that the melting point of the fluid should be below ambient temperature as solidification in the system will cause problems.

II. The temperature – entropy curve

The shape of the T-s curve is important both for the vapor and liquid saturation lines. In both cases the wanted shape is a vertical line (ds/dT = 0). After the working fluid exits the compressor in a sub-cooled state, a nearly vertical liquid saturation line reduces the amount of heat

required to rise the temperature of the liquid to the evaporation temperature in the evaporator. A high ratio of the latent heat of vaporization to the liquids specific heat is also favorable in this context.
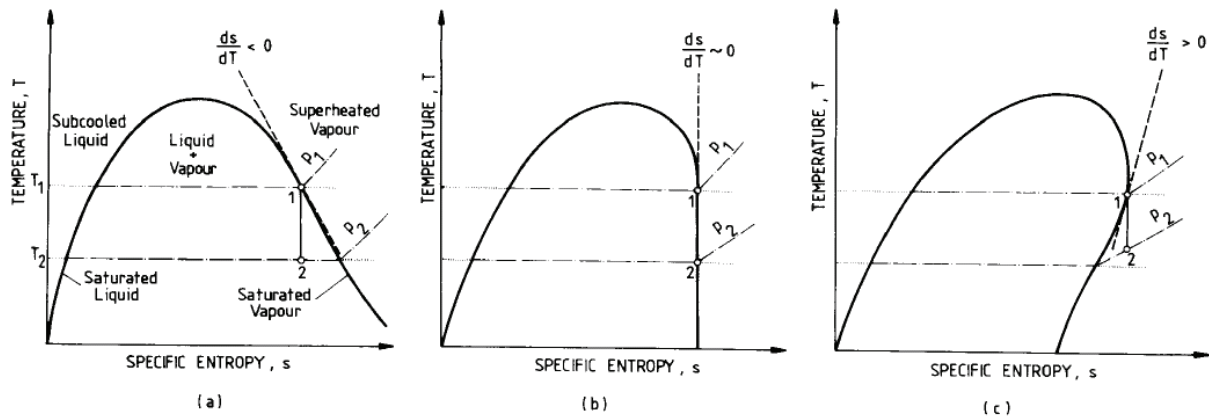
Figure 3.4: T-s diagram of three different fluids with isentropic turbine expansion. a) negative ds/dT curve b) ds/dT = 0 c) positive ds/dT curve (Badr et al., 1985)

The shape of the vapor saturation line affects the state of the working fluid exiting the turbine. Figure 3.4 displays three different scenarios. Fluid a) has a negative ds/dT curve and, as such, moisture is produced in the turbine. This can be prevented by superheating the steam at the turbine inlet, but this requires excess heat and heat transfer area in the evaporator. Fluid c) is retrograde (has a positive ds/dT curve) and the fluid is superheated at the turbine outlet. In this case, not all the superheated vapor is transformed to work in the turbine which reduces the cycle power output. The superheated vapor has to be cooled down in the condenser, which means that the average temperature in the condenser increases, reducing cycle efficiency and increasing condenser heat transfer area. For retrograde fluids it is common to place an internal heat exchanger between the turbine outlet and the evaporator inlet to increase cycle efficiency (see Chapter 2.3.5). Fluid b) does not have any of the above problems and has, in most cases, the most sought-after saturation curve.

The complexity of the molecule is a good indication of the shape of the T-s curve. A molecule with four to six atoms has an almost straight vapor saturation line while molecules with larger numbers of atoms are retrograde and molecules with less have a negative ds/dT curve (Lakew, 2009).
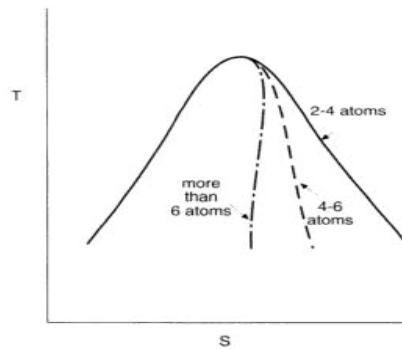
Figure 3.5: Effect of molecular complexity on the vapor saturation line (Lakew, 2009)

III. Molecular weight

There are several physical properties of the working fluids that depend on their molecular weight. An increase in molecular weight leads to:

- Higher mass flow for same power output.
- Lower speed of sound, which is important in turbine dimensioning.
- Decrease in turbine stages because of lower enthalpy difference for a given capacity (See Figure 3.6).
- Lower heat transfer.
- Increased viscosity, which leads to higher friction.

The greater part of the organic working fluids have a molecular weight above 100 kg/kmol, which is high compared to water with a molecular weight of 18 kg/kmol.
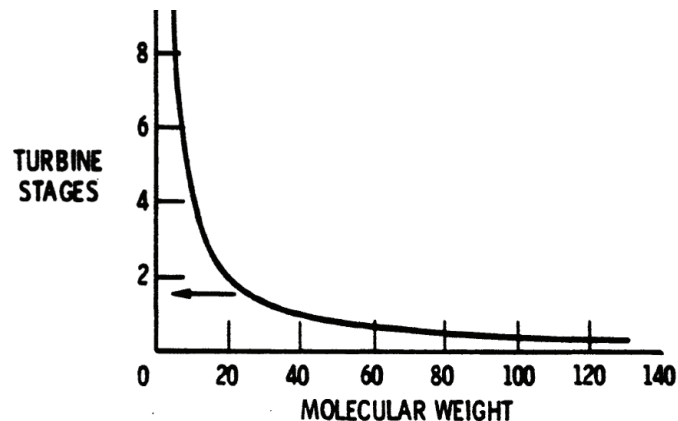
Figure 3.6: Molecular weight influence on the number of turbine stages (Lakew, 2009)

IV. Heat transfer properties

Good heat transfer properties reduce the size, and therefore the cost, of the heat exchangers. To obtain a good heat transfer coefficient the fluid should have high thermal conductivity, low viscosity and a high density.

V. Specific volume

For both the liquid and vapor phase it is desirable with high densities. High liquid density leads to low pump work while low vapor volume reduces component sizes and contributes to more efficient turbines.

VI. Thermal stability

Most fluids tend to dissociate at a given temperature, certain lubricants and container materials can also cause a fluid to dissociate. When dissociation occurs, the fluid can produce unwanted gases and compounds that lower the heat transfer rate and have corrosive effects on system

materials. It is therefore important that the fluid chosen does not dissociate in the system temperature range and is compatible with the materials and lubricants chosen.

VII.   Commercial availability and cost

It is desirable that the compound chosen is cheap and is readily available in great quantities.

VIII.   Safety

For obvious reasons the optimal working fluid should not be flammable, toxic, explosive and radioactive. In instances where working fluids that possess one or more of these properties extra safety measures should be implemented. Toxicity is usually identified by a threshold limit value (TLV) and flammability is generally identified by the fluid's lower flammability limit (LFL). Both properties are available from the fluid's MSDS (material safety data sheet). The ASHRAE standard 34 classifies refrigerants into two classes of toxicity (A = no toxicity identified at concentrations less than or equal to 400ppm and B = evidence of toxicity at concentrations below 400 ppm), and three groups of flammability characteristics (1 = no flame propagation in air at 21 °C and 101 kPa, 2 = LFL more than 0.10 kg/m^3 and 3 = highly flammable substance with a LFL less than or equal to 0.10 kg/m^3) (International Institute of Refrigeration, 2006).

IX.   Environmental impact

Environmental impact measures, such as the global warming potential (GWP) and the ozone depletion potential (ODP) are more in focus now than ever before as global warming is put on the agenda. Environmental regulations, such as the Montreal and the Kyoto protocol, have removed many working fluids from the market. In addition, companies are becoming more conscious of the environmental footprint they leave behind. As such, the optimal working fluid should not be poisonous and have low GWP and ODP.

Potential Working Fluids

The perfect fluid does not exist, but for a given system there is always one fluid that has certain favorable characteristics compared to all other working fluids. One way to find good candidates that are suitable for low temperature heat source applications is to perform a working fluid screening. The fluids used for the screening originates from the REFPROP 8.0 database. The thermophysical properties of the fluids were also gathered from the database. The original database contains 84 different pure components. By applying some general system requirements the number of fluids relevant for the low temperature ORC cycle was reduced to 27. The requirements are:

- Condenser saturation pressure should be above 0.5 bar. This to provide enough suction head to prevent cavitation to occur at the pump and to prevent atmospheric air from entering the system. (Badr et al., 1985).
- Critical temperature of the working fluid should be above 20 °C. This to ensure that the working fluid always is in the subcritical region when giving off heat to the heat sink in the condenser.
- Transcritical systems will not be considered as the excel model is unable to handle the extra set of variables associated with transcritical cycles. Although transcritical cycles experience better temperature fit with the heat source, they also have large pump work, operate under high pressures and can be challenging to regulate. This is some of the reasons none of the leading ORC companies have specialized in transcritical system technology.
- Working fluids restricted by the Montreal Protocol (1987) will not be considered. In the Copenhagen Amendment (1992) it was decided to phase out all CFC's by 1995. The Beijing Amendment (1999) instructs the developed countries to freeze production of HCFC's by 2003. Neither CFC's nor HCFC's will therefore be considered in this report.
- When there are several isomers within the same functional group only one of the isomers will be considered: butane and iso-butane; butene, iso-butene, trans-butene and cis-butene; R236ea and R236fa. In this case butane, butene, trans-butene, cis-butene and R236ea will be removed from the list.

In addition, nitrous oxide (N_2O) and hydrogen sulfide (H_2S) are removed. The first because of its strong oxidizing nature (Air Products, 2008) and hydrogen sulfide because it is very toxic, extremely flammable and dangerous for the environment (Air Liquide, 2005). The resulting list of working fluids that satisfy the requirements is shown on the next page. This list is further used for the direct and indirect working fluid screening.

Table 3.4: Possible working fluids for the ORC unit

Name	Chemical formula	# atoms	Molar weight (kg/kmol)	Critical temperature (°C)	Saturation pressure in MPa		Saturated liquid properties at 7 °C				Latent heat of vap. 60 °C (kJ/kg)	Slope of sat. vapor line
					7 °C	60 °C	Density (kg/m3)	Cp (J/kgK)	Viscosity (uPa-s)	Th.C. (W/mK)		
Ammonia	NH3	4	17	132	0.554	2.616	629	4.657	158	538.06	997	<< 0
Ethane	C2H6	8	30	32	2.817	x	382	3.537	10	26.39	x	<< 0
Propane	C3H8	11	44	97	0.584	2.117	519	2.548	117	102.42	259	< 0
Cyclopropane	CH2-CH2-CH2	9	42	125	0.431	1.682	646	2.421	u	u	343	<< 0
Propylene	C3H6	9	42	91	0.716	2.528	536	2.489	114	122.49	250	< 0
Propyne	C3H4	7	40	129	0.335	1.443	640	2.187	u	u	406	<< 0
Iso-butane	C4H10	14	58	135	0.200	0.869	572	2.321	184	95.93	285	≥ 0
Iso-butene	C4H8	12	56	145	0.170	0.781	610	2.286	185	108.51	315	≥ 0
Carbon dioxide	CO2	3	44	31	4.177	x	883	2.822	87	101.84	x	<< 0
Carbonyl sulfide	COS	3	60	106	0.796	2.790	1040	1.298	u	u	197	<< 0
Neopentane	(CH3)4C	17	72	161	0.092	0.461	604	2.205	303	99.58	272	> 0
Dimethylether	C2H6O	9	46	127	0.338	1.447	690	2.331	147	157.09	336	< 0
Perfluorobutane	C4F10	14	238	113	0.144	0.725	1561	1.047	u	u	72	> 0
Sulfur dioxide	SO2	3	64	157	0.205	1.102	1417	1.376	u	u	316	<< 0
Sulfur hexafluoride	SF6	7	146	46	1.512	x	1506	1.089	u	u	x	≤ 0
Trifluoroiodomethane	CF3I	5	196	123	0.287	1.180	2121	0.533	321	57.92	77	< 0
R32	CH2F2	5	52	78	1.012	3.933	1031	1.329	12	12.45	176	<< 0
R41	CH3F	5	34	44	2.461	x	653	2.783	105	139.36	x	<< 0
R125	CHF2CF3	8	120	66	0.832	3.170	1286	1.287	184	66.88	52	≤ 0
R134a	CH2FCF3	8	102	101	0.375	1.682	1271	1.361	244	88.93	139	< 0
R143a	CH3CF3	8	84	73	0.766	2.874	1000	1.167	10	14.00	94	< 0
R152a	CH3CHF2	8	66	113	0.337	1.501	943	1.723	201	105.80	229	< 0
R218	CF3CF2CF3	11	188	72	0.517	2.031	1421	1.097	220	49.72	44	> 0
R227ea	CF3CHFCF3	11	170	102	0.252	1.176	1460	1.131	306	65.43	88	> 0
R236fa	CF3CH2FCF3	11	152	125	0.142	0.765	1418	0.832	10	11.33	123	> 0
R245fa	CHF2CH2CF3	11	134	154	0.072	0.463	1386	0.891	10	11.73	168	> 0
RC318	CF2-CF2-CF2-CF2	12	200	115	0.168	0.839	1568	1.070	475	69.53	86	> 0

3.2 Cycle Simulation Results and Discussion

3.2.1 Direct System Design

For the direct system design, the main challenge is the 40 °C temperature limitation on the working fluid in the evaporator. The problem is not the restriction on how far down the raw gas can be cooled, it is rather the pre-set condensation temperature. Because of the 40 °C temperature limit, the condensation temperature in a standard ORC unit would be close to 40 °C, as the pressure increase over the pump rises the temperature of the working fluid marginally. The high condensation temperature has two consequences:

- The temperature difference (and therefore also the pressure difference) between the evaporator and the condenser will become small. This leads to bad turbine efficiencies.
- Bad cooling water utilization, which leads to low thermal efficiency.

To avoid the temperature limitation it is possible to use an internal heat exchanger (as described in Chapter 2.3.5). For traditional applications the IHE is used with retrograde fluids to recuperate the superheated steam not used to produce work in the turbine. In this case, however, the recuperator is used to lower the condensation temperature and preheat the high pressure fluid going into the evaporator. How this leads to a greater power output is demonstrated in Figure 3.7.
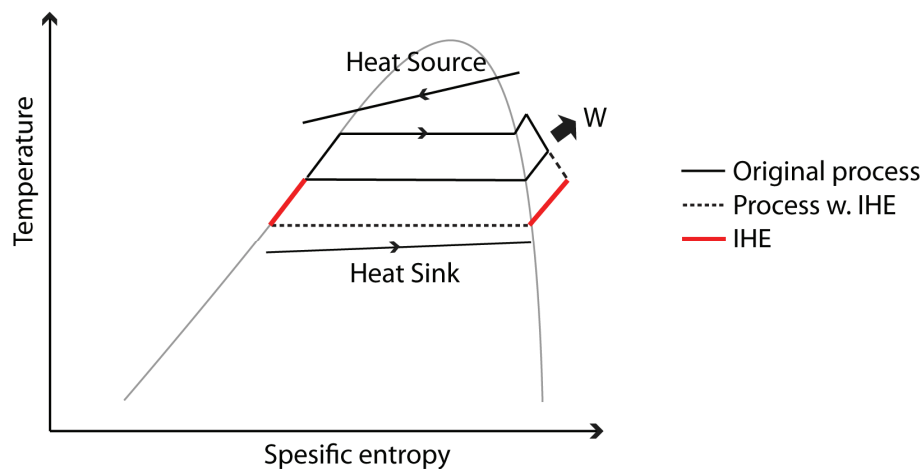
Figure 3.7: ORC process with and without recuperator

For the direct system design it is therefore chosen to only look at systems with IHE. The direct system design is shown in Figure 3.8 together with the nomenclature used when referring to the different process steps.
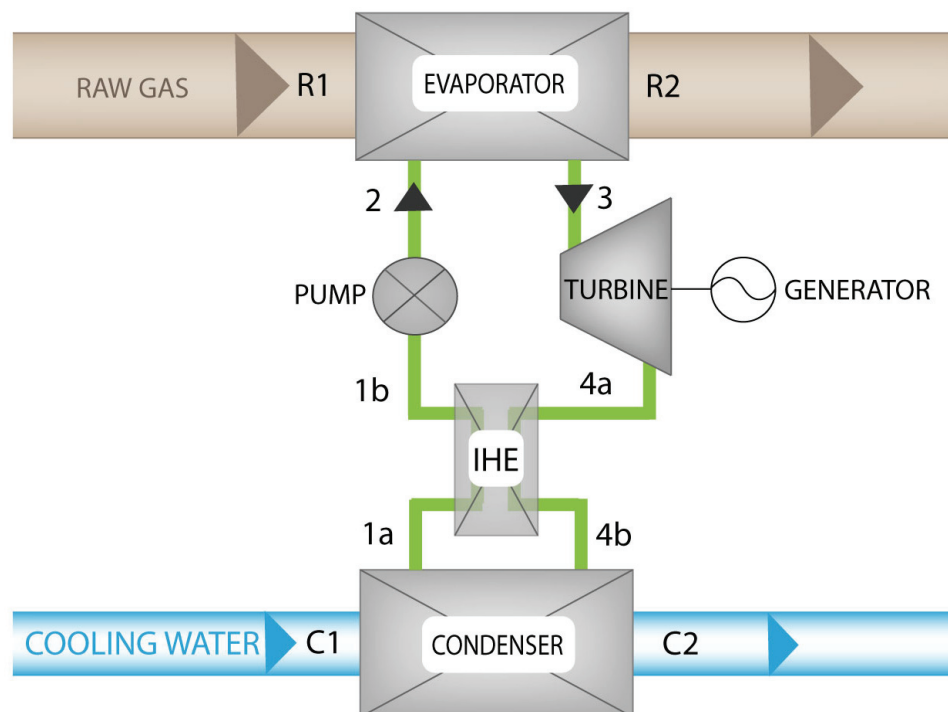
Figure 3.8: Direct system sketch with nomenclature

Working Fluid Screening

The evaporation of the working fluid should not occur too close to its critical point, as standard regulation strategies could not be applied. For the winter scenario, the raw gas temperature is 100°C. To avoid complications, fluids with a critical temperature below 90 °C (10 °C lower than the raw gas temperature) are removed from the list. This eliminates ethane, CO_2, SF_6, R32, R41, R125, R143a and R218 as potential working fluids.

Working fluids with very negative slope of the saturation vapor line are not suited for systems with IHE (see Chapter 2.3.5). This eliminates NH_3, cyclopropane, propyne, carbonyl sulfide and SO_2 from the list.

The remaining working fluids are propane, propylene, isobutane, isobutene, neopentane, dimethylether (dme), perfluorobutane (C_4F_{10}), trifluoroiodomethane (CF_3I), R134a, R152a, R227ea, R236fa, R245fa and R318. The 14 working fluids are all qualified as possible working fluid for the direct system and will be simulated according to the direct system requirements.

Simulation Results

Table 3.5: Simulation results for a direct system design, summer scenario (110°C/12°C)

Working fluid	P_{net} (kW)	$\dot{m}$ (kg/s)	LP (MPa)	HP (MPa)	T_c (°C)	T_e (°C)	T_3 (°C)	T_{4a} (°C)	T_{R2} (°C)	η_{th}
Propane	2277	58.91	0.77	2.01	17	57.57	90.23	54.28	66.78	0.10
Propylene	2305	59.44	0.94	2.37	17	56.89	95	55.30	66.33	0.10
Isobutane	2225	60.97	0.28	0.81	17	57.06	80.94	53.12	67.09	0.10
Isobutene	2224	55.96	0.24	0.72	17	56.51	84.01	53.69	67.24	0.10
Neopentane	2216	66.20	0.13	0.43	17	57.42	74.99	52.01	67.21	0.10
Dme	2263	50.38	0.47	1.32	17	56.07	94.97	55.03	67.26	0.10
Perfluorobutane	2311	228.89	0.21	0.75	17	61.22	70.96	51.43	65.94	0.10
Trifluoroiodomethane	2258	223.00	0.39	1.07	17	55.47	95	55.55	66.69	0.10
R134a	2296	111.32	0.52	1.58	17	57.37	92.22	56.12	66.86	0.10
R152a	2278	75.90	0.47	1.27	17	53.21	95	56.86	64.66	0.09
R227ea	2285	178.22	0.35	1.16	17	59.41	78.85	53.14	66.29	0.10
R236fa	2251	137.12	0.21	0.72	17	57.83	81.22	55.16	66.84	0.10
R245fa	2230	105.52	0.11	0.42	17	56.68	82.87	54.70	67.22	0.10
R318	2270	191.79	0.24	0.83	17	59.54	74.93	53.10	66.39	0.10

Table 3.6: Simulation results for a direct system design, winter scenario (100°C /2°C)

Working fluid	P_{net} (kW)	$\dot{m}$ (kg/s)	LP (MPa)	HP (MPa)	T_c (°C)	T_e (°C)	T_3 (°C)	T_{4a} (°C)	T_{R2} (°C)	η_{th}
Propane	2036	60.58	0.63	1.37	9.81	40	85	58.38	55	0.08
Propylene	1823	61.85	0.85	1.65	13.13	40	85	58.20	55	0.07
Isobutane	2244	55.21	0.20	0.63	7	46.41	84.80	57.12	59.75	0.10
Isobutene	2225	56.66	0.17	0.48	7	40.96	85	58.10	55.71	0.09
Neopentane	2185	57.09	0.09	0.33	7	47.54	85	61.43	61.82	0.11
Dme	1803	53.85	0.42	0.89	13.46	40	85	57.20	55	0.07
Perfluorobutane	2201	196.39	0.14	0.55	7	49.45	72.84	54.62	60.58	0.10
Trifluoroiodomethane	1779	235.37	0.35	0.73	13.69	40	85	57.56	55	0.07
R134a	1916	116.18	0.44	1.02	11.71	40	85	59.66	55	0.08
R152a	1702	76.71	0.44	0.91	15.04	40	85	58.32	55	0.07
R227ea	2239	154.80	0.25	0.87	7	48.08	81.63	57.44	60.20	0.10
R236fa	2243	125.80	0.14	0.52	7	45.55	85	60.11	58.86	0.10
R245fa	2224	106.14	0.07	0.26	7	41.27	85	59.63	55.94	0.09
R318	2212	167.40	0.17	0.62	7	48.28	77.94	56.95	60.31	0.10

Analysis of results

The trend is a slightly higher power output in the summer than in the winter even though the Carnot efficiency is higher in the winter scenario. The reason is that the summer scenario has a higher condenser temperature, and as such the recuperated heat required is less than in the winter time.

The working fluid that obtained the highest power output overall was R227ea with a power output of 2285 kW for the summer scenario and 2239 kW for the winter scenario. However, from the results from the summer scenario in Table 3.5 it can be seen that the different working fluids obtained approximately the same net power output for the given raw gas and cooling water temperature. The results only varied 2-3% between the best and the worst performer. While the pressure levels and mass flow rates changed depending on medium, the power output remained the same. The reason could be the many limitations applied to the cycle which makes the optimal operating conditions for all fluid almost identical.

For the winter scenario the results are more diverse. Every fluid with negative sloped saturated vapor line, that is propane, propylene, dme, trifluoroiodomethane, R134a and R152a, did not manage to supply the required recuperated heat, $\dot{Q}_{IHE}$, to operate at 7°C condensation temperature in the winter scenario. Because all the fluids mentioned have negative sloped vapor saturation lines they need to provide more superheat than the other fluids before entering the turbine to have sufficient overheating at the turbine outlet to supply the required $\dot{Q}_{IHE}$. It can be seen from Table 3.6 that T_3 is at its maximum value for all the fluids mentioned, but still the overheating at the turbine outlet is not enough, which results in the higher condensation temperature. The alternative would be to lower the evaporation temperature, but because of the increased risk of sulfuric acid formation under 40 °C, this is not a viable option. Figure 3.9 displays this problem with dme as working fluid.
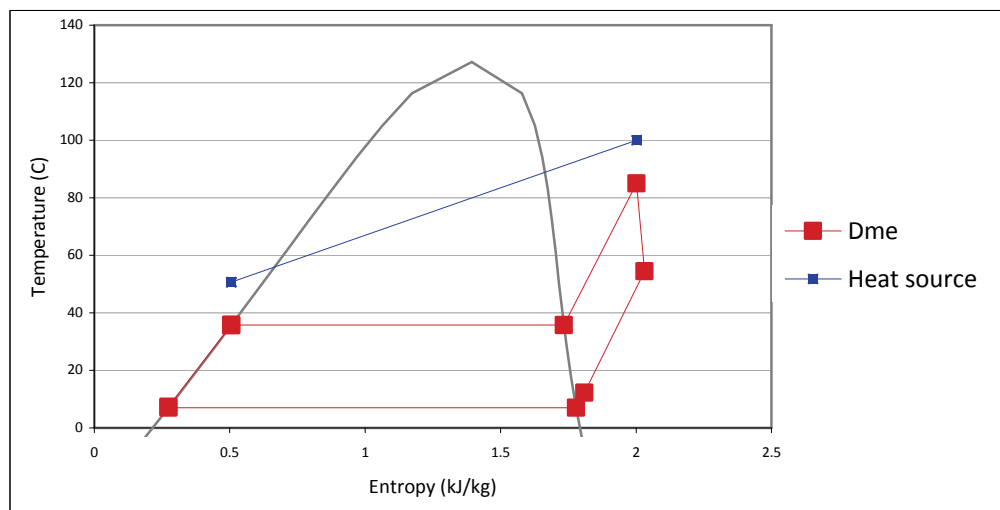
Figure 3.9: Dme, winter scenario. Evaporation temperature under 40 °C

The increased condensation temperature gives a lower thermal efficiency and thus a lower power output. On average, the fluids with negative vapor saturation line has on average an 18% lower power output than isobutane, which has the highest power output in the winter scenario (2244 kW). Based on this observation, propane, dme, trifluoroiodomethane, R134a and R152a are removed from the list of potential working fluids for the direct system design.

Sensitivity Analysis

The raw gas experiences temperature fluctuations, and a direct system design is more vulnerable to these temperature changes than an indirect design. The next step is therefore to perform a sensitivity analysis of the remaining fluids to see if they can handle the temperature fluctuations. From Chapter 3.1.1, the fluctuations were calculated to be ± 10 °C both in the summer and the winter scenario. From the results above one can deduce that the most demanding operating temperatures for the working fluid will be the winter scenario with 90°C raw gas temperature. In Table 3.7 the eight remaining working fluids, isobutane, isobutene, neopentane, C_4F_{10}, R227ea, R236fa, R245fa and R318, are tested for this scenario.

Table 3.7: Sensitivity analysis of the direct system design, winter scenario (90°C/2°C)

Working fluid	P_{net} (kW)	$\dot{m}$ (kg/s)	LP (MPa)	HP (MPa)	T_c (°C)	T_e (°C)	T_3 (°C)	T_{4a} (°C)	T_{R2} (°C)	η_{th} (%)
Isobutane	1429	50.15	0.24	0.53	11.99	40	75	55.19	55	7.50
Isobutene	1310	46.83	0.22	0.47	14.43	40	75	54.88	55	6.88
Neopentane	1676	53.05	0.09	0.27	7	40.22	75.00	55.32	55.17	8.83
Perfluorobutane	1636	166.02	0.14	0.46	7	43.20	70.18	54.66	57.10	9.13
R227ea	1566	140.48	0.27	0.70	8.99	40	75	56.70	55	8.22
R236fa	1385	112.40	0.18	0.44	12.71	40	75	57.36	55	7.27
R245fa	1321	88.15	0.10	0.25	14.19	40	75	56.10	55	6.93
R318	1657	142.64	0.17	0.52	7	42.30	75.00	57.00	56.61	9.11

The results from the sensitivity analysis show that Neopentane, C_4F_{10} and R318 seem to be the working fluids best suited for the direct system design as they can operate over the entire temperature range, while maximizing power output. All three fluids are retrograde and thereby require a smaller superheat than the other fluids, which makes them able to stay within the set boundaries for all operating conditions. Both C_4F_{10} and R318 are categorized by being retrograde fluids and having a small latent heat of vaporization. The modest latent heat of vaporization leads to a high evaporation temperature, which is why C_4F_{10} and R318 have a higher thermal efficiency than neopentane. In addition, the two fluids have a nearly vertical liquid saturation line, which reduces the amount of heat required to rise the working fluid temperature to 40 °C after the pump.

Despite the positive fluid characteristics of C_4F_{10} and R318, Neopentane has the highest power output of 1676 kW. This is a result of neopentane's high heat source exploitation. Even though neopentane's thermal efficiency is inferior to both C_4F_{10} and R318, the higher energy supply from the raw gas proves to be sufficient for it to be the best power producer in the sensitivity analysis.

Figure 3.10 displays the difference between the optimal cycle configurations of C_4F_{10}, neopentane and R134a for a 90°C/2°C direct system design. R134a is included as it is one of the most common working fluids used in ORC applications today. R134a satisfies all constraints in the 85 °C/2 °C system with a condensation temperature of 18.5 °C. However, because of the augmented condensation temperature, the net work output is only 1 111 kW, 33.7 % less than neopentane.
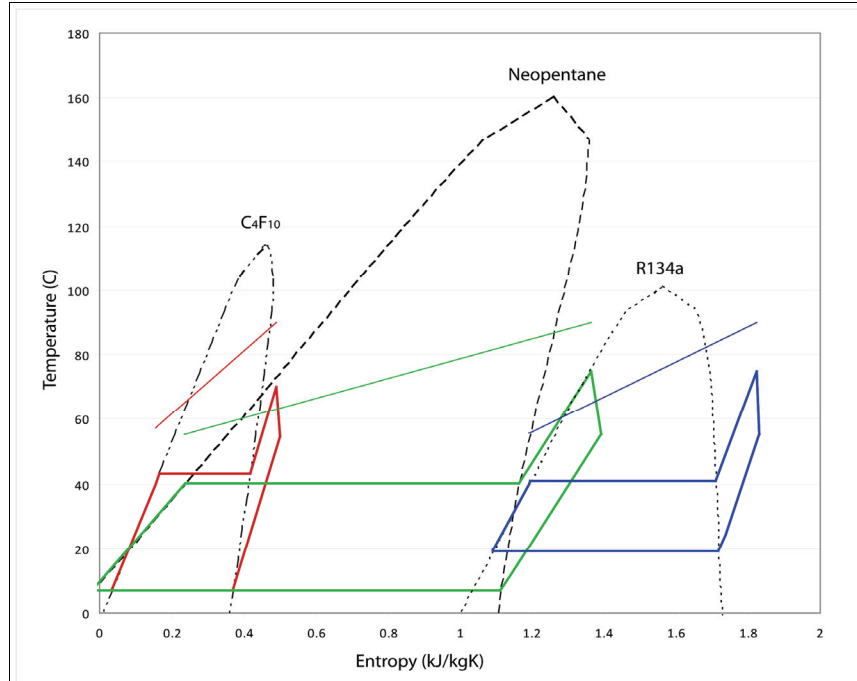
Figure 3.10: Cycle optimization for C4F10, neopentane and R134a for a 90°C/2°C direct system design

Optimal Working Fluid for a Direct System Design

From the simulation results four fluids have distinguished themselves. R227ea has, on average, the highest power output for the summer and winter scenario while C_4F_{10}, neopentane and R318 outperformed the other fluids in the sensitivity analysis. Table 3.8 displays the net power output for all four fluids.

Table 3.8: Net power output for potential working fluids. Winter scenario (100°C/2°C), summer scenario (110°C/12°C) and sensitivity analysis (90°C/2°C)

Working fluid	Net power output (kW)		
	Winter scenario	Summer scenario	Sensitivity analysis
Neopentane	1676	2185	2216
C_4F_{10}	1636	2201	2311
R227ea	1566	2239	2285
R318	1657	2212	2270

By looking at the simulation results it is clear that neopentane is not an ideal fluid after all, as it has the lowest power output both for the summer and the winter scenario. Furthermore, C_4F_{10} and R318 are both perfluorocarbons with four carbon atoms, which makes their fluid characteristics very similar. As R318 has a more even power output performance than C_4F_{10}, it

can be said to be a more suitable candidate than C_4F_{10}. Neopentane and C_4F_{10} are therefore removed from the list of ideal working fluids and only R227ea and R318 remain.

Table 3.9: Working fluid properties for a direct system, winter scenario

Working fluid	P_{net} (kW)	H_{vap} [1] (kJ/kg)	$\dot{V}_4$ (m^3/kg)	$\dot{m}$ (kg/s)	HP – LP (kPa)	Slope of sat. vapor line	Safety class. [2,5]	ODP[3,5]	GWP[4,5]
R227ea	2239	97	0.06	155	0.62	> 0	A1	0	3220
R318	2212	93	0.08	167	0.45	> 0	A1	0	10250

1) Latent heat of vaporization at T_e
2) Safety classification in accordance with ASHRAE Standard 34
3) Ozone Depletion Potential relative to CFC-11
4) Global Warming Potential relative to CO_2 for 100-year integration
5) From RTOC, 2006
n.a. = not accessible

As seen from Table 3.9 the two remaining fluids, R227ea and R318 have very similar fluid properties. Compared to other working fluids, both have a small H_{vap}, a small specific volume at the turbine outlet, a large mass flow rate and a small pressure difference in the turbine. However, compared to each other, R227ea has more favorable properties than R318, especially when it comes to the pressure difference in the turbine and the GWP. It therefore seems like R227ea is the optimal working fluid for the direct system design. It should be noted, however, that several important factors in choosing the optimal working fluid are not accounted for in this simulation. These include costs of components and practical feasibility of the system configuration. R227ea can therefore be said to be the optimal working fluid from a thermodynamic point of view, but to determine if this also account for real life applications are beyond the scope of this thesis to decide.

3.2.2 Indirect System Design

The indirect system model does not have any temperature restrictions directly connected to the ORC. The primary system design does therefore not include an IHE as the direct system design. The system design and the nomenclature used in the simulations are shown in Figure 3.11.
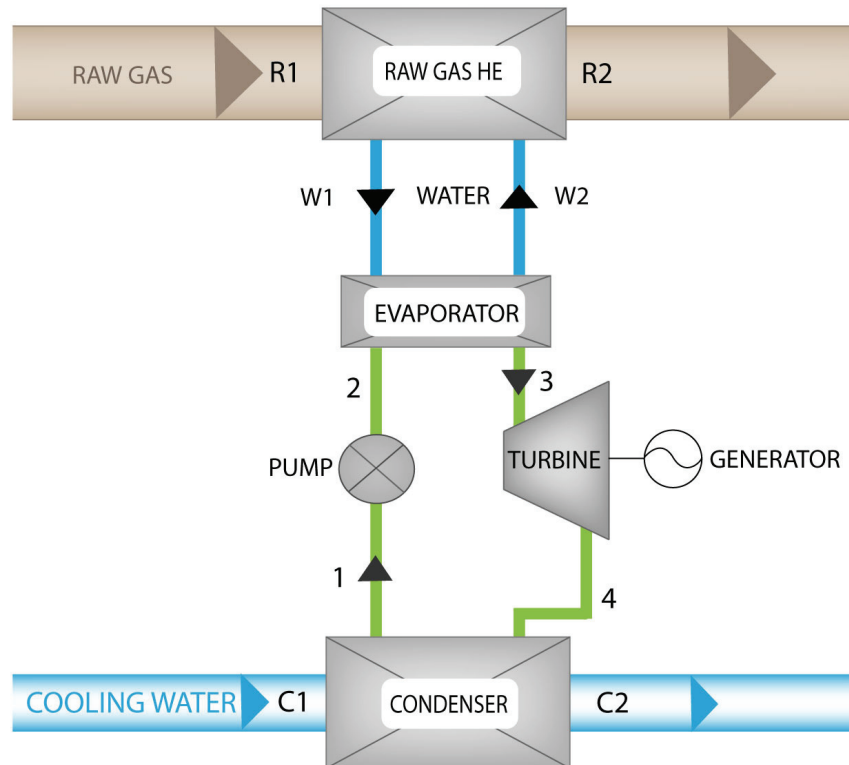
Figure 3.11: Indirect system sketch with nomenclature

The heat supply circuit has a 40 °C minimum temperature restriction at W2, because of the risk of sulfuric acid formation in the raw gas heat exchanger.

For simplicity, the temperature drop of the raw gas is assumed to be equal to the temperature rise of the water in the raw gas heat exchanger. The water mass flow will thereby be constant and can be calculated from the relationship:

$$\left[\dot{m} \cdot C_P \cdot \Delta T \right]_{rawgas} = \left[\dot{m} \cdot C_P \cdot \Delta T \right]_{water}$$

$$\Delta T_{rawgas} = \Delta T_{water} \rightarrow \left[\dot{m} \cdot C_P \right]_{rawgas} = \left[\dot{m} \cdot C_P \right]_{water}$$

$$\dot{m}_{water} = \frac{\left[\dot{m} \cdot C_P \right]_{rawgas}}{C_{P\_water}} \tag{3.3}$$

With the following values applied (Incompera et al., 2007):

$C_{P\_rawgas} \approx C_{P\_nitrogen}$ (100°C) = 1.043 kJ/kgK

C_{P_water} (80°C) = 4.197 kJ/kgK

$\dot{m}_{rawgas}$ = 522.54 kg/s

Using equation (3.3) the water mass flow becomes:

$$\dot{m}_{water} = \frac{[\dot{m} \cdot C_P]_{rawgas}}{C_{P\_water}} = 129.86 \text{ kg/s}$$

Working Fluid Screening

Because the indirect system design does not have an internal heat exchanger, or any temperature restrictions on the working fluid, there are few criteria the working fluid has to fulfill which are not already mentioned in Chapter 3.1.6. However, as for the direct system design, the evaporation of the working fluid should not take place too close to the fluids critical point. For the winter scenario, the water supply temperature is 85 °C. To avoid complications, fluids with a critical temperature below 75 °C (10 °C lower than the raw gas temperature) are removed from the list. This eliminates ethane, CO_2, SF_6, R41, R125, R143a and R218 as potential working fluids.

The 20 remaining working fluids meet the indirect system requirements and will be simulated in accordance with the indirect system performance criteria.

Results

Table 3.10: Simulation results for an indirect system design, summer scenario (95°C/12°C)

Working fluid	P_{net} (kW)	$\dot{m}$ (kg/s)	LP (MPa)	HP (MPa)	T_e (°C)	T_3 (°C)	T_4 (°C)	T_{W2} (°C)	η_{th} (%)
Ammonia	1978	18.09	0.78	2.09	51.07	90	26.70	50.63	8.19
Propane	2046	68.83	0.77	1.94	55.85	55.85	17	47.17	7.86
Cyclopropane	1977	46.83	0.58	1.45	53.30	90	51.46	51.08	8.27
Propylene	2027	63.47	0.94	2.30	55.35	68.81	27.84	48.20	7.96
Propyne	1967	40.50	0.46	1.23	53.15	90	50.25	51.71	8.35
Isobutane	2031	65.90	0.28	0.77	54.62	54.62	27.00	48.30	7.99
Isobutene	2007	60.26	0.24	0.68	54.27	54.27	24.25	49.27	8.06
Carbonyl sulfide	2004	82.59	1.05	2.39	52.49	90	38.35	50.09	8.20
Neopentane	2032	70.06	0.13	0.40	54.36	54.36	32.40	47.97	7.94
Dimethylether	1984	49.35	0.47	1.25	53.69	80.12	42.09	50.56	8.20
Perfluorobutane	2161	250.92	0.21	0.66	56.14	56.14	38.24	41.17	7.38
SO_2	1965	58.89	0.30	0.87	51.26	90	29.42	51.06	8.21
Trifluoroiodomethane	1980	216.95	0.39	1.02	53.80	78.48	40.63	50.49	8.17
R32	2108	75.22	1.36	3.41	53.64	90	33.19	48.60	8.34
R134a	2065	129.30	0.52	1.51	55.61	55.61	17.08	47.28	7.95
R152a	2007	69.00	0.47	1.30	53.89	85.51	46.19	50.33	8.25
R227ea	2157	201.04	0.35	1.08	56.56	56.56	30.53	43.88	7.75
R236fa	2085	150.29	0.21	0.67	55.18	55.18	29.63	46.61	7.92
R245fa	2027	113.69	0.11	0.39	54.14	54.14	26.56	48.71	8.04
R318	2130	210.58	0.24	0.75	55.79	55.79	35.09	43.74	7.64

Table 3.11: Simulation results for an indirect system design, winter scenario (85°C/2°C)

Working fluid	P_{net} (kW)	$\dot{m}$ (kg/s)	LP (MPa)	HP (MPa)	T_e (°C)	T_3 (°C)	T_4 (°C)	T_{W2} (°C)	η_{th} (%)
Ammonia	2029	17.45	0.55	1.60	41.05	80	14.95	40.87	8.46
Propane	2080	61.30	0.58	1.61	47.16	47.16	7.26	40	8.50
Cyclopropane	2043	45.72	0.43	1.14	42.89	80	40.25	40.94	8.53
Propylene	2070	56.16	0.72	1.86	45.32	65.76	25.70	40	8.46
Propyne	2024	39.58	0.34	0.95	42.80	80	39.76	41.82	8.62
Isobutane	2079	61.49	0.20	0.61	45.58	45.58	16.82	40	8.50
Isobutene	2059	57.64	0.17	0.53	44.40	44.40	13.64	40	8.41
Carbonyl sulfide	2058	79.19	0.80	1.92	42.14	80	28.09	40.32	8.47
Neopentane	2082	65.28	0.09	0.32	45.77	45.77	22.26	40	8.51
Dimethylether	2044	45.83	0.34	0.97	43.29	80	41.69	40.97	8.54
Perfluorobutane	2112	195.30	0.14	0.61	53.06	53.06	32.19	40	8.63
SO_2	2019	57.30	0.21	0.65	41.14	80	17.55	41.15	8.47
Trifluoroiodomethane	2037	199.85	0.29	0.80	43.40	80	42.07	41.01	8.51
R32	2135	69.22	1.01	2.72	43.80	80	22.26	40	8.72
R134a	2099	115.47	0.37	1.22	47.05	47.05	7.61	40	8.58
R152a	2064	65.26	0.34	1.00	43.47	80	40.53	40.66	8.56
R227ea	2148	166.51	0.25	0.94	50.95	50.95	22.57	40	8.78
R236fa	2120	133.74	0.14	0.55	47.66	47.66	20.34	40	8.66
R245fa	2069	102.66	0.07	0.31	46.63	46.63	16.54	41.71	8.79
R318	2128	174.58	0.17	0.66	50.66	50.66	27.50	40	8.70

Analysis of Results

As a consequence of the lenient system requirements (compared to those for the direct system), all working fluids managed to fulfill the system requirements for both scenarios. As a result of the more numerous potential cycle configurations the net power output (P_{net}) of the different working fluids varied to a greater extent than for the direct system. For both scenarios, the net power output for the different working fluids stayed within a 10 % range.

All fluids experienced a greater thermal efficiency during the winter. This coincides with the power output, which was greater in the winter than in the summer for all working fluids except C_4F_{10}, R227ea and R318. These fluids had a very low T_{W2} in the summer time, which corresponds to good heat transfer between the hot water and the working fluid. In the winter time the fluids' T_{W2} was approximately the same, but T_{W1} was 10 °C less, which lead to a smaller heat transfer from the hot water and an inferior power output.

The working fluid that obtained the highest work output overall was R227ea with a power output of 2157 kW for the summer scenario and 2148 kW for the winter scenario.

Fluids with a high temperature at point 4, such as cyclopropane, dimethylether and R152a, are strong candidates for getting an IHE installed. However, in this case, the effect of having an IHE installed would be minimal. An IHE increases the thermal efficiency by increasing the average heat intake temperature and decreasing the average condenser temperature. This normally leads to a greater power output. But as the IHE transfers heat internally to the working fluid before the evaporator it replaces some of the heat demand normally supplied by the heat source. As such, it reduces the amount of heat transferred from the heat source, reducing the source utilization factor. The increase in thermal efficiency is thereby neutralized by the decrease in heat supplied to the cycle. If a higher temperature limitation was set on the water at W2 an IHE could again become relevant.

Optimal Working Fluid for an Indirect System Design

In theory there are 20 fluids that potentially can be used in the ORC if an indirect system design is chosen. However, the goal of this chapter was not to find potential working fluids, but the optimal working fluid. Hence it is reasonable to eliminate the ten fluids with the lowest net power output. These fluids are ammonia, cyclopropane, propylene, propyne, isobutene, carbonyl sulfide, dme, SO_2, CF_3I and R152a.

The remaining fluids are displayed in Table 3.12, sorted by descending net power output, together with some of their dimensioning properties, including their latent heat of vaporization (H_{vap}), Volume flow rate at the turbine outlet ($\dot{V}_4$), safety classification and global warming potential.

Table 3.12: Working fluid properties for an indirect system, winter scenario

Working fluid	P_{net} (kW)	H_{vap}[1] (kJ/kg)	$\dot{V}_4$ (m³/kg)	$\dot{m}$ (kg/s)	HP − LP (kPa)	Slope of sat. vapor line	Safety class.[2,5]	ODP[3,5]	GWP[4,5]
R227ea	2153	95	9	167	0.69	> 0	A1	0	3220
C4F10	2136	75	14	195	0.46	> 0	n.a.	n.a.	n.a.
RC318	2129	91	12	175	0.49	> 0	A1	0	10250
R32	2121	227	3	69	1.70	<< 0	A2	0	675
R236fa	2103	132	14	134	0.40	> 0	A1	0	9810
R134a	2082	155	6	115	0.85	< 0	A1	0	1430
Propane	2063	291	5	61	1.03	< 0	A3	0	20
Neopentane	2057	285	23	65	0.22	> 0	n.a.	n.a.	n.a.
Isobutane	2055	305	12	61	0.41	≥ 0	A3	0	20
R245fa	2048	177	25	103	0.24	> 0	B1	0	1030

1) Latent heat of vaporization at T_e
2) Safety classification in accordance with ASHRAE Standard 34
3) Ozone Depletion Potential relative to CFC-11
4) Global Warming Potential relative to CO_2 for 100-year integration
5) From UNEP, 2006
n.a. = not accessible

As seen from Table 3.12, the three top performance working fluids all have similar properties. However, the fourth, R32, have a very different characteristic than the top three. Figure 3.12 displays the difference between the optimal cycle configurations of R227ea and R32 for an 85°C / 2°C indirect system design.
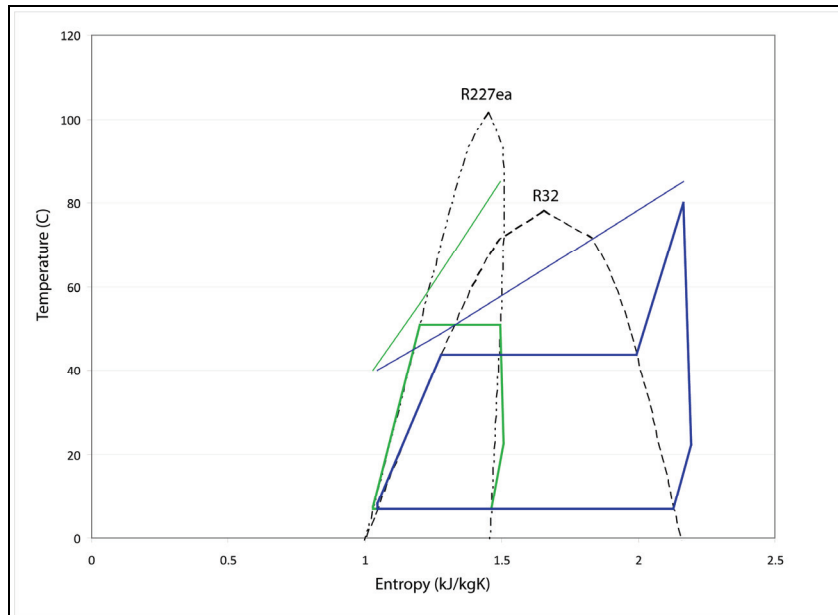
Figure 3.12: Cycle optimization for R227ea and R32 for an 85°C/2°C indirect system design

As seen from the figure, R32 has a larger heat of vaporization than R227ea, and has a bell shaped phase-equilibrium curve. The optimal cycle configuration therefore includes

overheating before the turbine inlet to prevent droplet formation in the turbine. The overheating contributes to a better temperature fit between the heat source and the working fluid. On the down side, the vapor also has inferior heat transfer properties in the superheated region compared to that in the two-phase region. This corresponds to additional heat exchanger area, and thereby greater investment costs and heat exchanger dimensions, when the fluid is in the superheated region.

The operating pressures of R227ea and R32 are also very different. While R32 has an evaporation pressure of 34.1 bar in the summer scenario, R227ea has an evaporation pressure of only 10.8 bar. Components to be used in a pressurized system, such as pipes, flanges and compression fittings, are chosen as to which pressure rating the system belongs to. In the case of R227ea, components have to satisfy the PN 16 standard, whereas components in the R32 system have to comply with the PN 40 standard. Because of the high pressure rating of R32 the system will involve additional investment costs compared to the R227ea system.

Because of the high pressure rating and the superheating, R32 might not be an ideal working fluid. Another interesting fluid is R134a which works with higher pressures than R227ea, but has almost the same critical temperature. In the simulations, R134a has on average only 3.3 % lower power output than R227ea. It also has no superheating, both at the evaporator and the condenser (Figure 3.13). This lead to efficient heat transfer as phase change has a superior heat transfer coefficient than pure heating of a fluid.
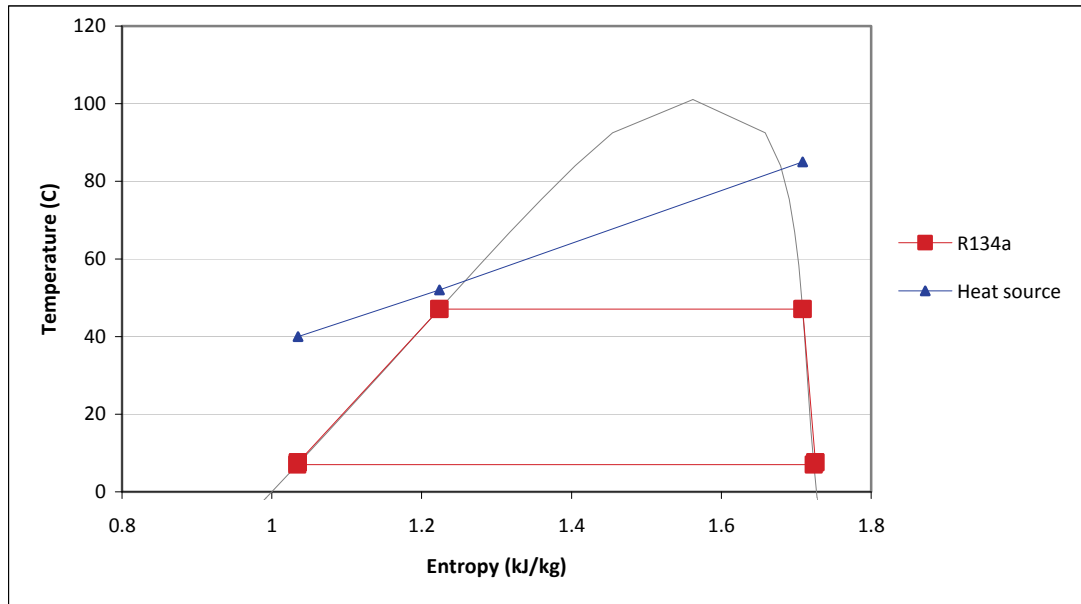
Figure 3.13: Cycle optimization for R134a for an 85°C/2°C indirect system design

All in all, to pronounce the optimal working fluid for the indirect system is not appropriate, as several fluids possess good qualities that are favorable for an indirect system. In real systems the component sizes and costs related to the different working fluids are important decisive factors, and in this simulation they have not been taken into account.

3.3 Summary

The heat source for the ORC unit is raw gas from the production of aluminium. The raw gas has a mass flow rate of 1456000 Nm^3/h and has an average temperature of 110°C in the summer and 100°C in the winter. The heat sink is water originating from the Tya power station and is estimated to have an average temperature of 12°C in the summer and 2°C in the winter. The heat sink is considered to be an unlimited source as no data concerning this issue has been obtained.

For a direct design solution it is necessary to install an IHE for optimal cycle performance. R227ea proved to be the best performer for the direct system with an average power output of 2262 kW.

The indirect system solution has a broader selection of relevant working fluids than the direct design because of the absence of the IHE. The simulation results showed that the power output does not vary much between the working fluids, even though they display a wide variety of thermophysical properties. Again, R227es achieved the highest performance with an average power output of 2153 kW, 5% lower than for the direct system design.

In both the direct and indirect system, to point out one ideal working fluid is impossible as not all parameters relevant in working fluid selection are taken into consideration. The final decision would involve an optimization between investment costs and power output of each working fluid, which is beyond the scope of this thesis.

4 Final System Design

Whereas Chapter 3 had a theoretical approach to find the optimal organic Rankine cycle power production unit, this chapter has focused more on the practical solutions that can make the installation of an ORC power production unit possible in Årdal. The outline of the power production unit was found by looking at the local conditions and the layout of the future ÅI FTP. The net power output from the power production unit was found by adding additional system restrictions to the ORC simulation model in Chapter 3, and including power consumption from all auxiliary system components. Furthermore, several system solutions received from ORC manufacturers were compared based on system performance and financial viability.

4.1 PPU Layout

4.1.1 Heat Source Connection Layout

In Chapter 3 it was established that the raw gas heat exchanger was to be placed in front of the dry scrubber in the FTP. In order to do this, the layout of the gas ducts going from the pot rooms and into the FTP has to be mapped. In ÅI, the exhaust gas ducts from the cells run through the basement of the pot rooms before they emerge between the two pot room sections A and B, as illustrated in Figure 4.1. The gas ducts have eight entry points to the FTP, each entering a separate filter. The FTP is divided into two dry scrubber units, Å0025 and Å0026, each containing four filters and eight wet scrubbers treating the gas exiting the individual dry scrubber filters.

GASSFØRINGER ÅI
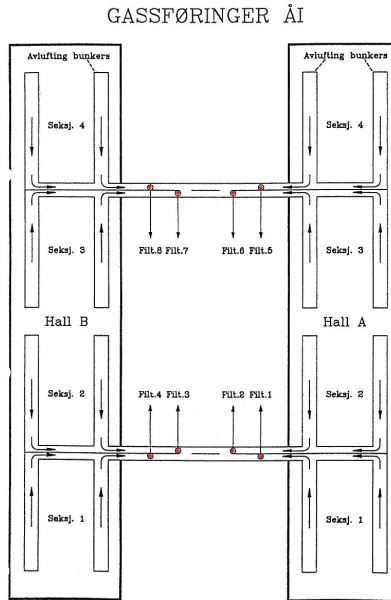
Figure 4.1: ÅI gas duct layout
Per Gunnar Søvik, Internt HBS Dokument Hydro Aluminium Årdal 10.07.2003

The current layout of the FTP unit is roughly sketched in Figure 4.2. It is placed in the center between the two pot room sections and the gas duct exiting points. As stated in the introduction, the current FTP is old and ready for replacement. It is therefore highly unlikely that a PPU will be installed before the FTP is modernized.
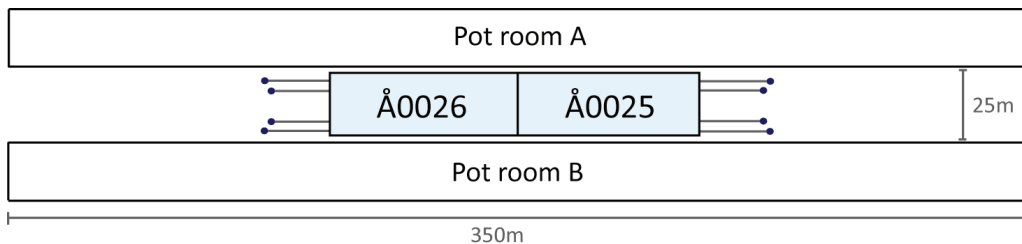
Figure 4.2: Current FTP layout

All raw gas exiting the pot rooms has to be treated for pollutants before entering the atmosphere. As aluminium production is a continuous process, the FTP also has to work continuously. This implies that a new FTP has to be built while the old FTP is still running. The placement of the new FTP is a challenge, as the space between the two pot rooms is limited. A solution presented by Alstom, is to build the new FTP in two stages. The first stage would include the construction of an FTP unit to replace Å0025 next to the existing Å0025. The second stage would encompass the demolition of the old Å0025 unit and the erection of a new unit to replace Å0026. Instead of eight entrances to the FTP, the new design would only have four entrances, two to each FTP unit. The new design is illustrated in Figure 4.3.
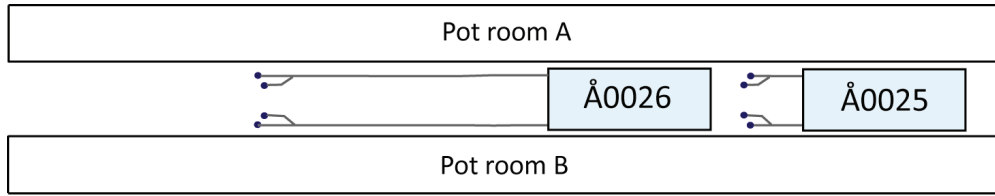
Figure 4.3: New FTP layout presented by Alstom

Connection Point

Because the raw gas is treated in four separate units in the new design, four individual heat exchangers are required to extract heat from the raw gas to the working fluid. This implies that the ORC should use an indirect supply system, as transporting a pressurized fluid for long distances is expensive, both because of the required system components and because of the large amount of working fluid needed. An indirect system also has additional advantages, such as larger freedom in selecting working fluid and heat source flexibility. A disadvantage is a lower max operating temperature of the working fluid, however, the simulation done in Chapter 3 suggests that there is only a 5 % difference in power output between the direct and the indirect system design.

The heat exchangers could either be placed next to the gas duct entry points (configuration A) or close to the entrances of the dry scrubber (configuration B). Figure 4.4 shows the two possible solutions together with the working fluid transportation circuit indicated by the red lines. In the figure the ORC is assumed to have the dimension 20 m x 10 m, which is an over estimate based on the proposed solutions discussed later in this chapter. Compared to the dimensions of the FTP, the ORC seems to take up little space between the two pot room sections. The module is placed close to pot room A, instead of in the center of the alley way, for better access to Å0026 if needed.
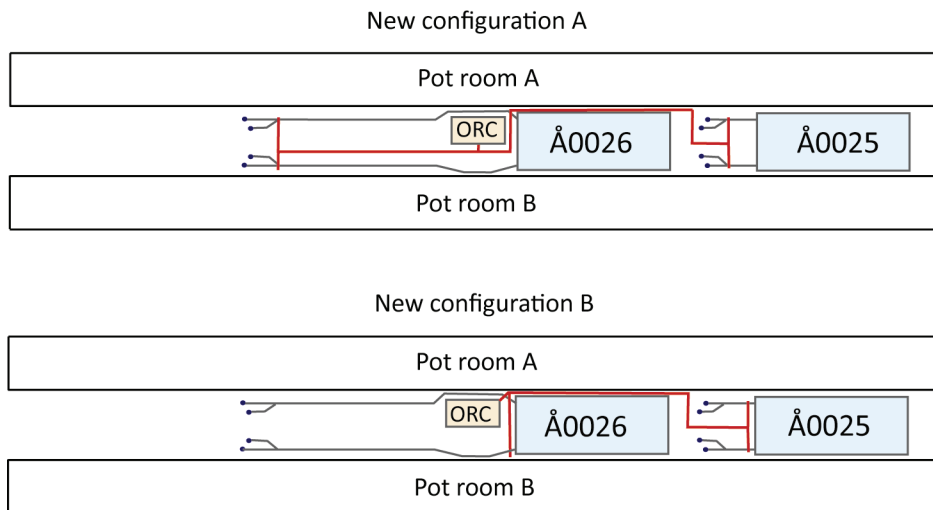
Figure 4.4: Two possible heat exchanger placements; (A) near the gas duct entry points, (B) near the dry scrubber entrances

Configuration A requires approximately 470 m transportation piping, whereas configuration B requires about 300 m.

Because of the long distances, all pipes transferring heat to the ORC unit should be insulated (Heat loss from the pipes is discussed later in this chapter). This represents an additional cost of about 1000 NOK per m^2 that needs to be insulated (Næss, 2009). The total surface area of piping transferring heat to the ORC unit should therefore be minimized. Table 4.1 displays the parameters used to calculate the total surface area that require insulation for configuration A. With a water mass flow rate of 65 kg/s (130 kg/s divided in two, since there are two main supply pipes) and a velocity of 1m/s, the water pipes would have a radius of 14 cm, which corresponds to a surface area of 425 m^2 that needs to be insulated.

Table 4.1: Required insulated surface area, configuration A

Volumetric flow rate	0.065	Nm^3/s
Velocity	1	m/s
Pipe length	470	m
Surface area	425	m^2

Configuration B requires insulation of approximately 200 m gas ducts in addition to 300 m water pipes. Table 4.2 displays the parameters used to calculate the total surface area that require insulation for configuration B. The raw gas occupies a larger volume than the hot water and each gas duct has a volumetric flow rate of 101 Nm^3/s (1 456 000 Nm^3/h in total divided on the four gas ducts). This results in large duct dimensions and duct surface areas. With a velocity of 15 m/s the raw gas duct surface area that needs to be insulated is 1841 m^2. This result in a total of 2112 m^2 insulation needed for configuration B.

Table 4.2: Required insulated surface area, configuration B

Hot water		
Volumetric flow rate	0.065	Nm^3/s
Velocity	1	m/s
Pipe length	300	m
Surface area	271	m^2
Raw gas		
Volumetric flow rate	101	Nm^3/s
Velocity	15	m/s
Pipe length	2x100	m
Surface area	1841	m^2

The above numbers are only estimates, but clearly illustrate the difference in insulating the gas ducts to the water pipes. Configuration A has an extra investment cost because of the additional 170 m of water piping needed in comparison to configuration B. However, configuration B requires 1687 m^2 extra insulation and with a price tag of 1000 NOK/m^2 the additional insulation would cost about 1.7 MNOK. 170 m water piping is usually much less expensive than this. Moreover, the raw gas ducts have shorter lifetimes than the water supply pipes because of the abrasive nature of the raw gas. The detection and repair of leakages would be more

troublesome if the pipes were insulated. In light of this, configuration A seems to be the best choice for supplying heat to the ORC module.

Series versus Parallel Hot Water Connection

The actual connection between the ORC and the raw gas heat exchangers can be done in series or parallel. If connected in series the raw gas heat exchangers will all have different designs because they will have dissimilar water inlet temperatures. The first heat exchanger after the ORC will have a large temperature difference between the water and the raw gas, which requires a small heat exchange surface area. The last heat exchanger before the water re-enters the ORC, however, will have a too high inlet temperature to extract the same amount of heat from the raw gas as the first heat exchanger. In addition, the last heat exchanger will have to have a large surface area to compensate for the smaller temperature difference. The different heat exchanger designs lead to a disproportioned system which can be difficult to control.
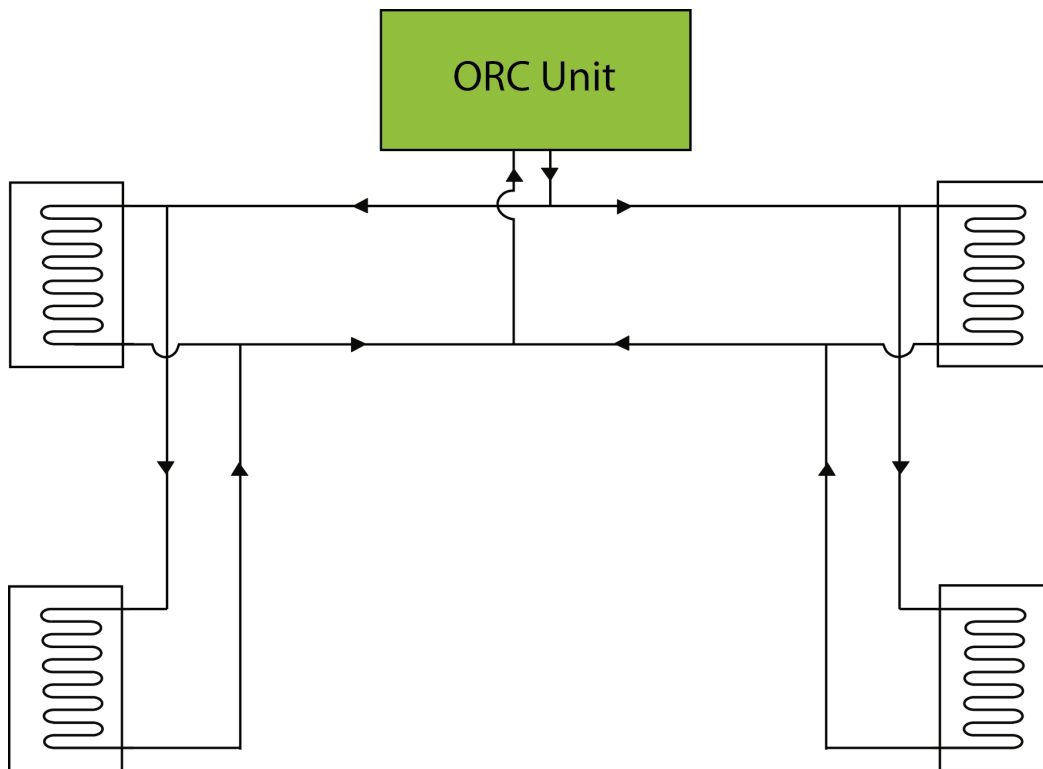
Figure 4.5: Parallel heat exchanger connection

Figure 4.5 is a rough sketch of the heat exchangers in parallel connection. In a parallel connection, all heat exchangers have the same inlet temperature and design. This leads to a more stable system. Moreover, in a parallel system you only need one spare heat exchanger in case of a heat exchanger break down as they all have the same configuration. Because of the obvious advantages of a parallel connection, such as maximum heat source exploitation and symmetrical design, it is chosen as the optimum supply system for the ORC unit at Årdal.

Redundancy

The raw gas heat exchangers are positioned upstream the FTP. If the ORC unit is not operating or one of the heat exchangers breaks down, the raw gas still must be passed to the FTP for cleaning. This can be solved by adding a bypass to the raw gas ducts as illustrated in Figure 4.6. If the heat exchanger cannot be used, the raw gas bypasses it and goes directly to the FTP.
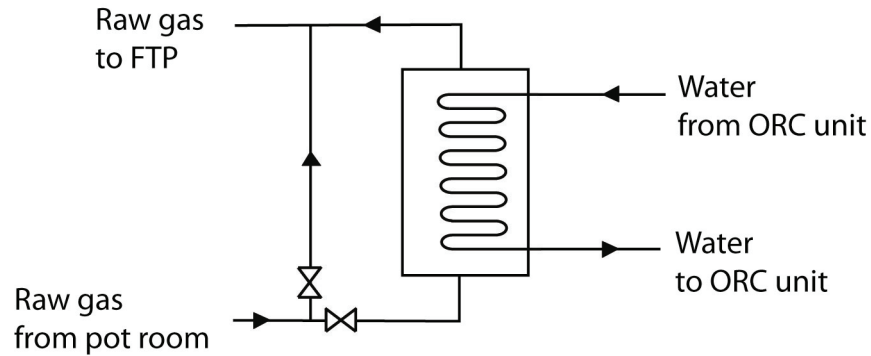
Figure 4.6: Raw gas bypass connection

One thing to take into consideration when the bypass system is used is the higher entry temperature of the gas to the FTP. The current FTP at ÅI is dimensioned for gas at 90 °C – 110 °C, but the new FTP will be handling much lower temperatures (55 °C – 70 °C) and will perhaps not be able to process gas at 110°C. One solution is to inject water into the raw gas to cool it down. The subject of water injection to cool down raw gas is treated in Hanne Mari Karlsen's master thesis "Cooling of Raw Gas from Aluminium Electrolysis Cells", spring 2009.

If the raw gas heat exchangers have to be changed or cleaned often, it can be favorable to install two additional heat exchangers that can be employed when one or two of the heat exchangers are put out of operation. This solution is displayed in Figure 4.7. The extra heat exchanger ensures that the ORC receives maximum load at all times. This solution should, however, only be used if the heat exchangers have a short lifetime or frequently require maintenance, as the added investment cost of installing two extra heat exchangers has to be paid pack by the extra power output provided by them during their limited operation time.
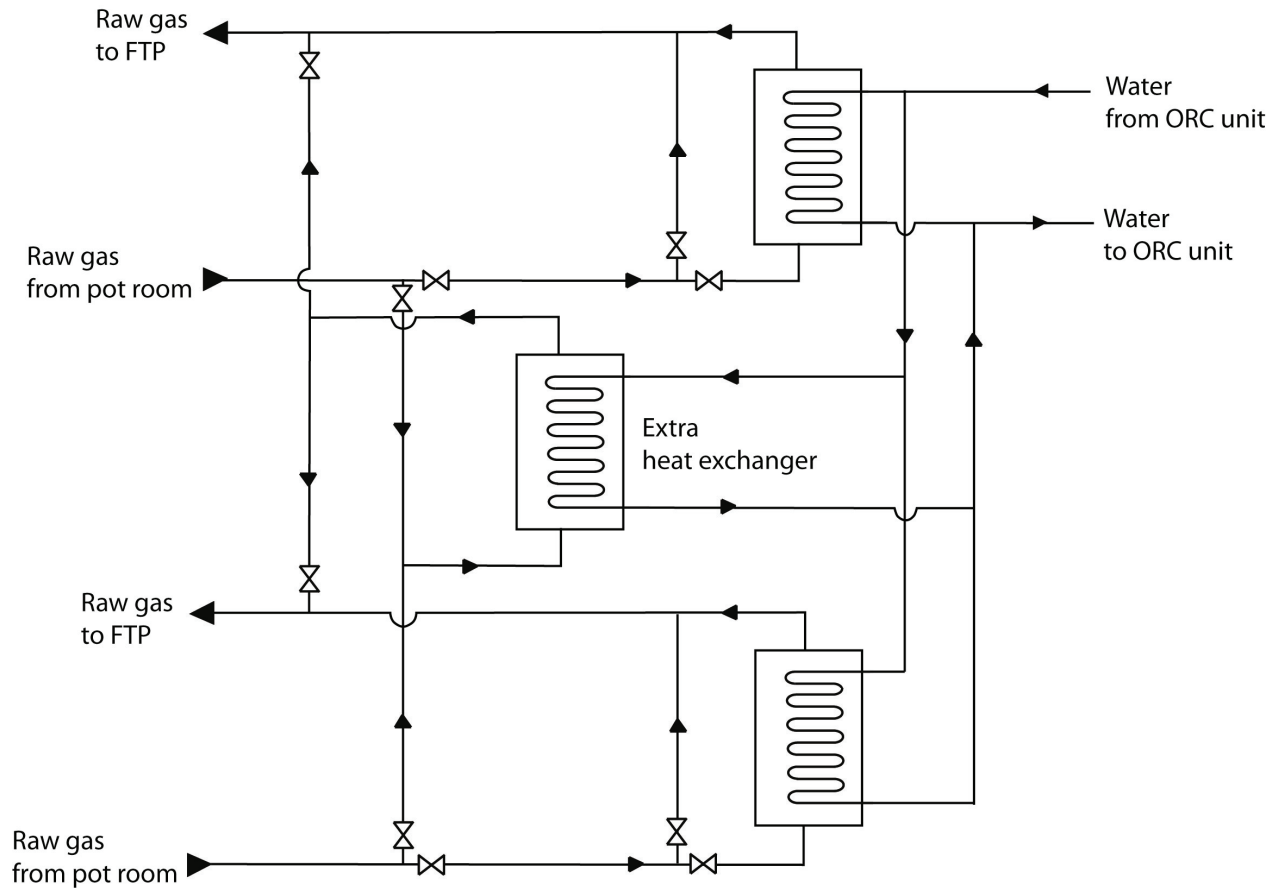
Figure 4.7: Implementation of an extra heat exchanger to the raw gas supply system

Heat Loss in the Hot Water Supply System

The pipes transporting hot water to and from the ORC unit are placed outside, always exposed to the local weather conditions in Årdal. The temperature within the pipes that run from the raw gas heat exchanger to the ORC unit starts at 95 °C on average in the summer and 85°C in the winter. It is desirable that the water maintains its high temperature until it reaches the ORC unit for maximum system efficiency. Moreover, it is required that the water inlet temperature to the raw gas heat exchanger do not fall below 40 °C because of the risk of acid formation. As such, it is important to know the magnitude of the temperature drop in the water pipes.

To establish the influence of ambient air temperature on heat loss from the hot water transportation pipes a worst case scenario is picked, with an ambient temperature of − 10 °C and an initial water temperature of 95 °C, to be sure all operating conditions are covered. Furthermore, the pipe is assumed to be 100 m long and carry half of the water supply to the ORC unit, 65 kg/s. This is similar to one of the water pipe branches transporting hot water from two of the heat exchangers to the ORC module (See Figure 4.4, configuration A). For simplicity, the water speed is set to be 1 m/s, with a water density of 1000 kg/m^3, this result in an inner pipe diameter of 28.77 cm.
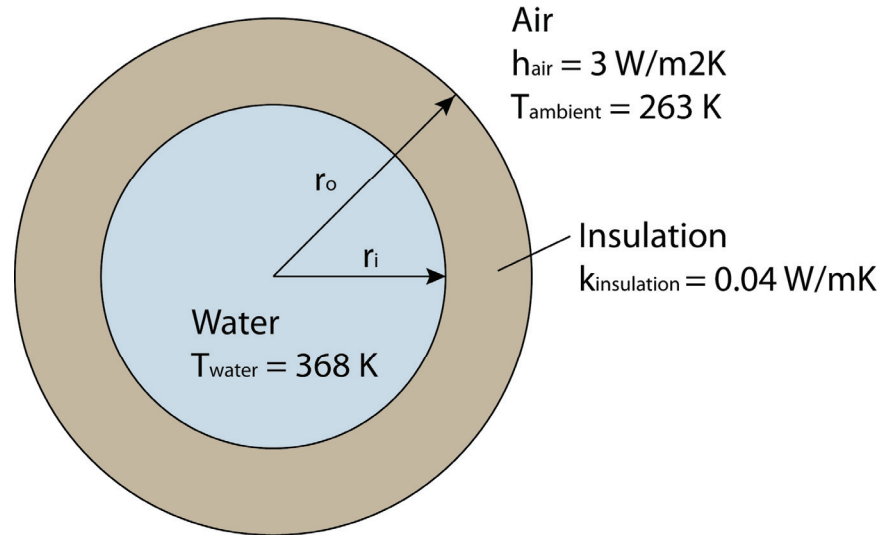
Figure 4.8: Water pipe cross-section with thermophysical properties

Figure 4.8 is an illustration of the cross sectional area of the water pipe including nomenclature and thermophysical properties used in calculating the heat loss. The thermal conductivity coefficient of Glava pipe insulation, $k_{insulation}$, is set to 0.04 W/mK (Glava, 2008). The convective heat transfer coefficient of air, h_{air}, is hard to establish as it depends on the speed and temperature of the air, however, in this calculation it is approximated to be 3 W/m²K. The thermal resistance in the water and the steel pipe is negligible compared to the resistance in the insulation and air and are therefore not included in the calculation.

The heat loss in a pipe can be expressed as the temperature difference between the inside and the outside of the pipe divided by the total thermal resistance, R_{total}, of the pipe. In the case of the hot water pipe the heat loss becomes:

$$\dot{Q}_{loss} = \frac{(T_{ambient} - T_{water})}{R_{total}}$$ (4.1)

The thermal resistance is divided into terms of resistance for convection and resistance for conduction. In the case of the water pipe, the heat is transferred by conduction through the insulation and by convection from the insulation to the air. For radial systems the total resistance can then be expressed as (Incompera et al., 2007):

$$R_{total} = \frac{\ln(r_o/r_i)}{2\pi k_{insulation}L} + \frac{1}{2\pi r_o h_{air}L}$$ (4.2)

Where L is the length of the pipe.

The heat loss is best visualized as the temperature difference between the beginning and the end of the pipe, which can be expressed as:

$$\Delta T_{loss} = \frac{\dot{Q}_{loss}}{\dot{m}_{water} \cdot C_{P\_water}}$$ (4.3)

The calculation was performed for a hot water pipe with 0 cm, 5 cm and 10 cm insulation. The results are displayed in Table 4.3.

Table 4.3: Calculation results for heat loss from a 100m long hot water pipe

Isolation thickness (cm)	0	5	10
$\dot{Q}$ (kW)	-28.47	-7.19	-4.53
ΔT_{loss} (°C)	-0.104	-0.026	-0.017

As seen from the table, a pipe without insulation does not experience a larger heat loss than 0.1 °C, even though the ambient temperature is -10 °C. The heat loss is low because of the large amount of water that is transported in the pipes. The pipes should be insulated, however, as other weather conditions, such as rain and snow, can increase the heat loss from the pipes, and a thin layer of insulation (e.g. 5 cm) can diminish this effect.

4.1.2 Heat Sink Properties and Layout

In the simulations in Chapter 3 the heat sink, which is cold fresh water, was assumed to be infinite. In real life this is not possible, hence the condensation temperature in the ORC will be higher than in the simulations. The increase in condensation temperature decreases the cycle efficiency as the temperature difference between the condenser and evaporator decreases. To illustrate the relationship between cold water supply and power output a simulation using R134a as working fluid was performed. While the evaporation temperature was held constant at 85°C, the condensation temperature was varied between 7 °C and 23°C.

The heat transferred to the cold water in the condenser, $\dot{Q}_C$, is proportional to the cold water's mass flow, $\dot{m}_{water}$, and its required temperature rise, ΔT_R:

$$\dot{Q}_C\left[kW\right]=\dot{m}_{water}\left[kg/s\right]\cdot C_{P\_water}\left[kJ/kgK\right]\cdot\Delta T_R\left[K\right] \qquad (\,4.4)$$

The simulation results are displayed in Table 4.4 and are visualized in Figure 4.9.

Table 4.4: Influence of cold water temperature rise on required water mass flow and power output

ΔT_R	P_{net} (kW)	$\dot{Q}_C$ (kW)	$\dot{m}_{water}$ (kg/s)	Diameter (m)	η_{th}
0	2099	22370	∞	∞	8.58
2	1976	22180	2645	1.84	8.18
4	1855	21987	1311	1.29	7.78
6	1736	21791	866	1.05	7.38
8	1619	21592	644	0.91	6.98
10	1504	21389	510	0.81	6.57
12	1390	21184	421	0.73	6.16
14	1279	20975	357	0.67	5.75
16	1169	20762	309	0.63	5.33

As seen from Figure 4.9, for water mass flow rates below 2000 m^3/h, a small change in water supply has a substantial influence on the ORC power output. This is an important discovery as it is very likely that the actual water supply available will be under 2000 m^3/h (2000 m^3/h is a substantial amount of water to retrieve). It shows that for small and moderate water mass flows available it is favorable to use the entire water source. For larger mass flows, the extra power output will not be as lucrative because of the large volume flow needed to increase the efficiency which will require extra space and investment costs.
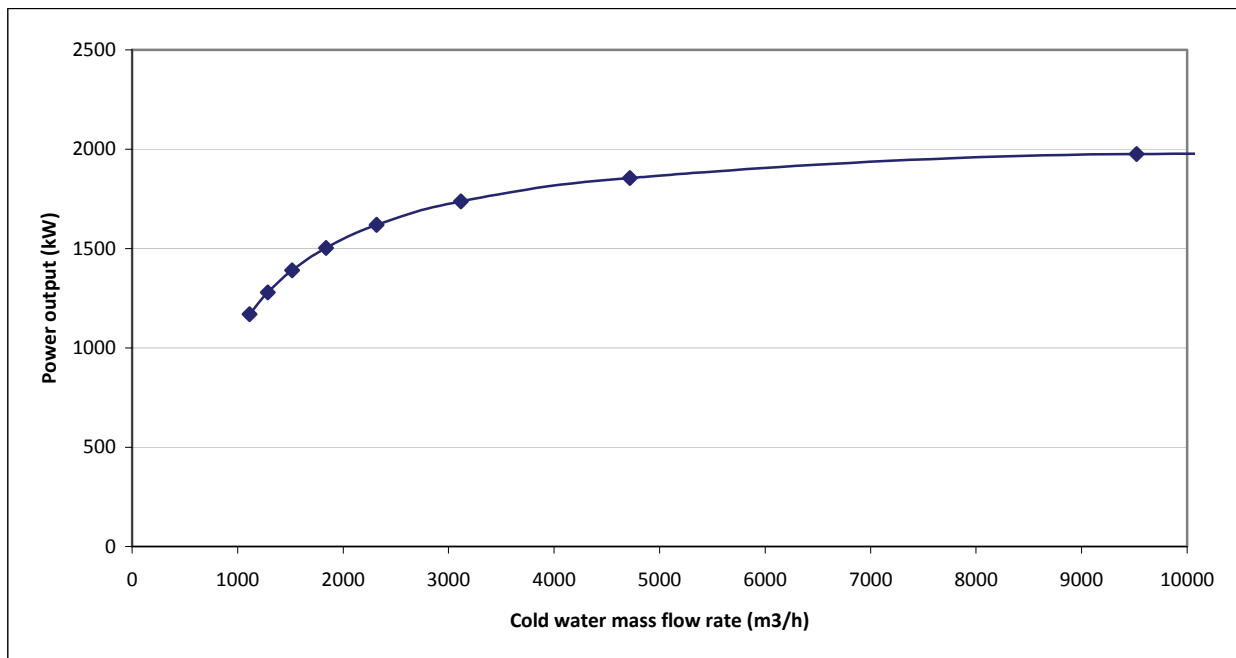
Figure 4.9: Cold water mass flow rate influence on power output

Because the amount of cold water available in Årdal has not been established yet, a volume flow rate has to be chosen for the ORC performance estimate in the next section. For simplicity this flow rate is chosen to be 500 kg/s throughout the year. However, before a final decision is

made concerning an ORC installation in Årdal, the location and size of the best heat sink available has to be established.

At the moment, fresh water originating from Tyin hydro power station seems like the most promising heat sink. In the ORC simulations done in Chapter 3 the Tyin water temperature was approximated to 12 °C in the summer time (April 16th to October 15th) and 2 °C in the winter time (October 16th to April 15th) based on observations done by the Tya cast house operators. These temperatures will also be used in the final system performance estimate. Power consumption of a pump in the cooling water supply pipe is not included in the analysis. As the cooling water originates from the Tyin power station, the height difference between the power station and the ORC unit is assumed to produce a sufficient suction pressure to supply the cooling water to the ORC unit.

A graph displaying the cooling water temperature originating from Tyin power station was received July 4th 2009 and is appended to this report as Appendix B. The graph confirms that the temperature of the water stays fairly constant at 2 °C during the winter months, but in the summer months the temperature seems to vary between 3 °C and 13 °C. An average summer temperature of 12 °C is therefore an overestimate, as the real value is closer to 7 °C. Because of the late arrival of the graph, it is not accounted for in this thesis, but could be valuable for further investigations. On a final note, to find the exact temperature of the cooling water looses its significance when the available volume flow rate cannot be established, as the minimum condensation temperature in the ORC depends on both the cooling water temperature and mass flow rate.

4.1.3 ORC System Components and Design

The power production unit is composed of the ORC unit, heat supply and heat discharge system and a power generator. The design of the heat supply system is already established in the sections above as an indirect system with four raw gas heat exchangers connected in parallel to a water circuit supplying hot water to the ORC. The heat discharge system has a simpler design, as the cold fresh water is removing heat directly from the condenser of the ORC unit. The actual ORC unit itself has a general design as illustrated in Figure 3.11 in Chapter 3.2.2. There are, however certain adjustments to the design that has to be made in order for the ORC unit operation to run smoothly. In this context there are mainly two design features that should be mentioned.

The first design feature is the evaporator. The evaporator preheats, evaporates and, in most cases, superheats the working fluid before it enters the turbine. As the working fluid goes through the different stages, it changes its thermodynamic properties. A consequence is that the evaporator has to be divided into three compartments, each optimized for one of the stages. The heat exchanger does not have to physically be three different heat exchangers, but the evaporator needs to be divided into three compartments. One solution that is often used is to separate the units into one preheater and one evaporator. Most evaporators are designed to

handle a little superheating in the end and a separate superheat heat exchanger is seldom necessary. For fluids, like R134a, that have a negatively sloped liquid saturation line, the fluid should be superheated a few degrees to prevent droplet formation in the turbine. Whereas for retrograde fluids this is not necessary (see Chapter 2.3.5).

The second design feature is the receiver that acts as a working fluid reservoir. If the operation conditions of the ORC module changes, whether it is the heat source or heat sink temperature or mass flow rate that goes up or down, the ORC module has to adapt so that the system always is in equilibrium. This is done by regulating the mass flow and quantity of working fluid in the different parts of the system. As an example, if the heat source temperature increases the evaporation pressure or mass flow rate of the working fluid has to be increased in order to maintain optimal operating conditions. In both cases more working fluid has to circulate in the cycle and the needed working fluid is taken from the receiver. The receiver does not need to be a separate unit, but can be a working fluid recervoir at the bottom of the condenser. In that case the receiver is called the hotwell. A simple illustration of this design is displayed in Figure 4.10.
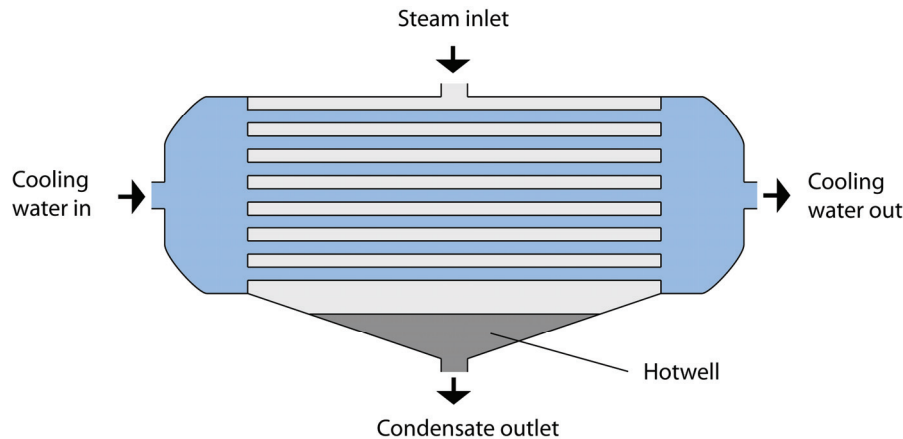
Figure 4.10: Simple condenser sketch with hotwell

The liquid that enters the pump after the receiver should always be subcooled a few degrees to prevent cavitation in the pump. This can either be done by subcooling the liquid in the receiver or hotwell (condensate depression), or by increasing the pressure between the condenser and the pump by installing the pump a few meters below the condenser. Condensate depression is easy to accomplish in the receiver or the hotwell and can be controlled by regulating the cooling water mass flow. Excessive depression is not desirable as it decreases system efficiency because the fluid has to be reheated in the evaporator afterwards.

The final system design is shown in Figure 4.11 on the next page. It includes four raw gas heat exchangers in parallel connection to a hot water supply circuit. The hot water is circulated in the circuit by the use of two pumps. The two pumps are not simultaneously in operation, but interchange to always ensure a continuous supply of hot water to the ORC unit. The main components of the ORC unit are the preheater, the evaporator, the turbine, the condenser the receiver and the pump. A generator is connected to the turbine to transform the mechanical power output to electricity.
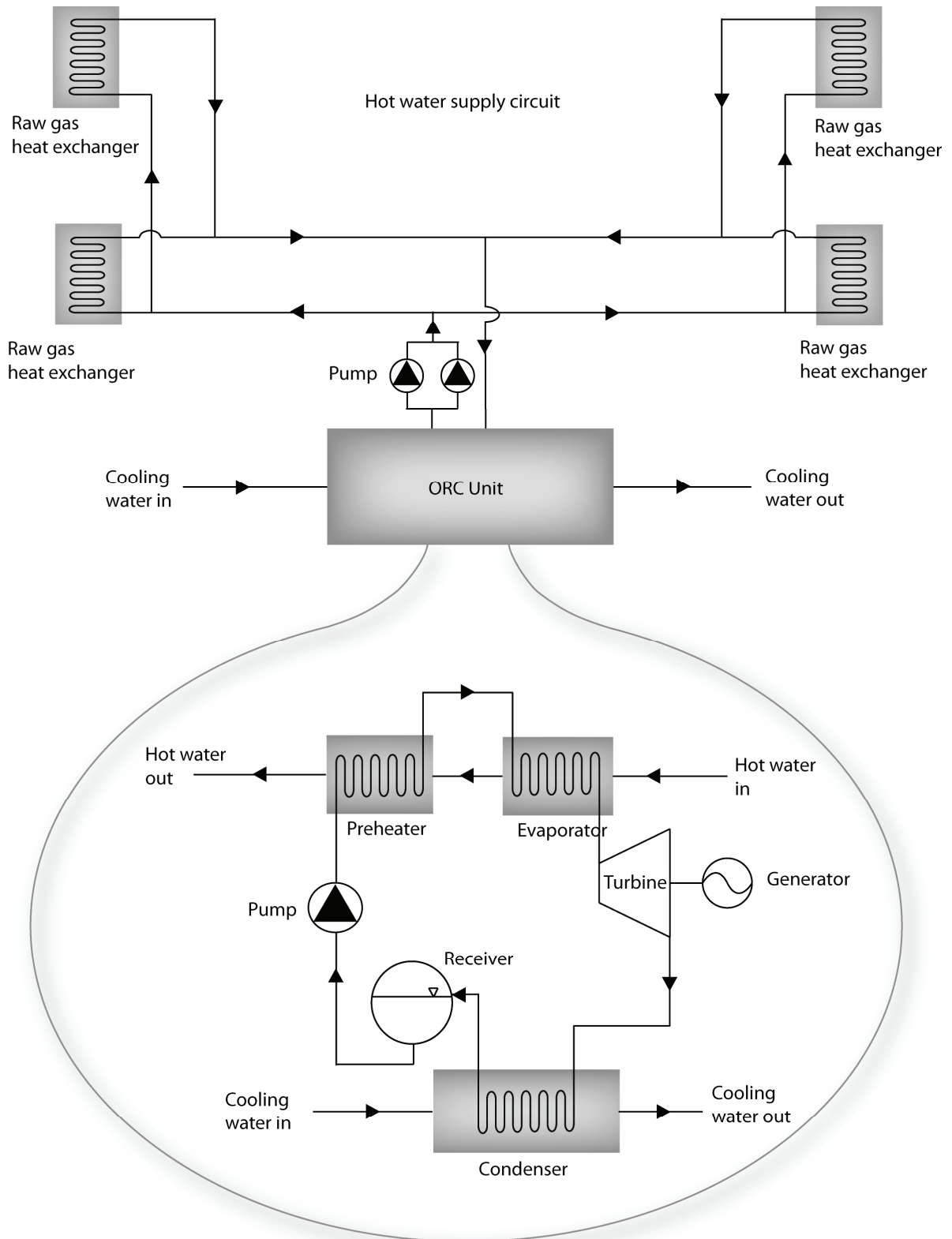
Figure 4.11: Final system design

4.2 PPU Performance Estimate

4.2.1 Choice of Working Fluid

The choice of working fluid is a difficult task as several working fluids have the necessary qualifications to succeed as heat transfer media in the given ORC (see Chapter 3.2.2). It is therefore chosen to look at similar existing installations and to consult the major producers of ORC units for low temperature heat source applications. Table 4.5 displays three ORC producers and their preferred working fluids for low temperature heat source applications.

Table 4.5: Working fluids used for low temperature heat source applications by ORC producers

Working Fluid	Company
Ammonia	Opcon
R134a	Opcon, Turboden, Infinity Turbines
R245fa	Turboden, Infinity Turbines

R227ea, which had the highest power output in the simulations do not appear on the list. According to Turboden, R227ea has the same critical temperature of R134a, but has a lower critical pressure and an inferior system performance. Calculations performed by Turboden using R227ea (with the Årdal system specifications) showed a 2 % lower performance than using R134a. As all three companies use R134a and it is a well known refrigerant on the market, it is selected as the working fluid for the present ORC performance estimate.

4.2.2 ORC Component Efficiencies

The same irreversibilities as for the simulations performed in Chapter 3 also applies for the final system design. These include pinch point in heat exchangers and turbine and pump efficiencies. In addition, an internal pressure loss of 0.5 bar is included to make a more realistic image of the final system. Heat loss in the heat exchangers, and the ORC cycle in general, are not accounted for as they are negligible compared to the other losses. To be able to display the net power output from the ORC unit, the generator connected to the turbine is included in the simulation by adding a 95 % efficiency to the simulated mechanical power output from the turbine. The generator efficiency is set to be quite high because of the steady state operation of the ORC unit.

As for the simulation in Chapter 3, the loss-parameter's magnitude is only approximated to a general value based on experience (Næss and Ladam, 2009). The irreversibilities used in the simulation model are displayed in Table 4.6.

Table 4.6: ORC energy loss-parameters

Pinch point, raw gas heat exchanger	15	°C
Pinch point pure fluid heat exchangers	5	°C
Turbine efficiency	80	%
Pump efficiency	70	%
Internal pressure losses	0.5	bar
Generator efficiency	95	%

4.2.3 ORC Power Production

The ORC power production is found by doing a simulation in Excel using REFPROP 8.0 similar to the ones done in Chapter 3. As for the simulations in Chapter 3 the simulation is done for a winter and a summer scenario. There are however, some additional constraints put on the final ORC system. These include a finite cooling water mass flow rate, a minimum requirement of superheating in the evaporator and a given condensation depression in the condenser. To prevent condensate pump cavitation, the condensate depression in the ORC is set to 2 °C. And because R134a has a negatively sloped liquid saturation line the minimum superheating requirement is also set to 2°C. Table 4.7 gives an overview of all the criteria.

Table 4.7: ORC system criteria

Raw gas temperature, summer	110	°C
Raw gas temperature, winter	100	°C
Cooling water temperature, summer	12	°C
Cooling water temperature, winter	2	°C
Raw gas mass flow rate	522.54	kg/s
Cooling water mass flow rate	500	kg/s
Minimum superheating in evaporator	2	°C
Condensation depression	2	°C

In addition to the system criteria, the simulation also has to include the component efficiencies displayed in Table 4.6. In the simulation, the internal pressure loss is distributed in the cycle as a 0.25 bar pressure loss in the evaporator and a 0.25 bar pressure loss in the condenser. The results from the simulation are displayed in Table 4.8.

Table 4.8: Simulation results for final system design

	Summer scenario	Winter scenario
Power output		
Gross electric power output (kWe)	1781	1783
Captive consumption[i] (kWe)	152	110
Net electric power output (kWe)	**1629**	**1672**
Thermal efficiency (%)	7.53	7.84
Cycle properties		
Condensation pressure (bar)	0.60	0.43
Evaporation pressure (bar)	1.80	1.39
Condensation temperature (°C)	21.50	11.33
Evaporation temperature (°C)	62.83	52.00
Mass flow working fluid (kg/s)	106.81	99.90
Discharge hot water temperature (°C)	55.26	45.78
Q_h (kW)	21643	21332
Q_c (kW)	19920	19566

i) This is just for the ORC module and does not take into account power consumption from auxiliary systems.

Compared to the performance of R134a in the preliminary simulations (Table 3.10 and 3.11), the alterations to real life system have reduced the system efficiency by 21%. This is mainly due to the quantity limitation set on the cooling water supply that went from infinity to 500 kg/s. One thing to notice is the hot water discharge temperature, that is, the temperature of the hot water leaving the preheater. In both scenarios the temperature is clearly above the 40 °C. This indicates that the acid dew point is not a limiting factor to the ORC power output. Figure 4.12 displays the final system configuration in a T-s diagram.
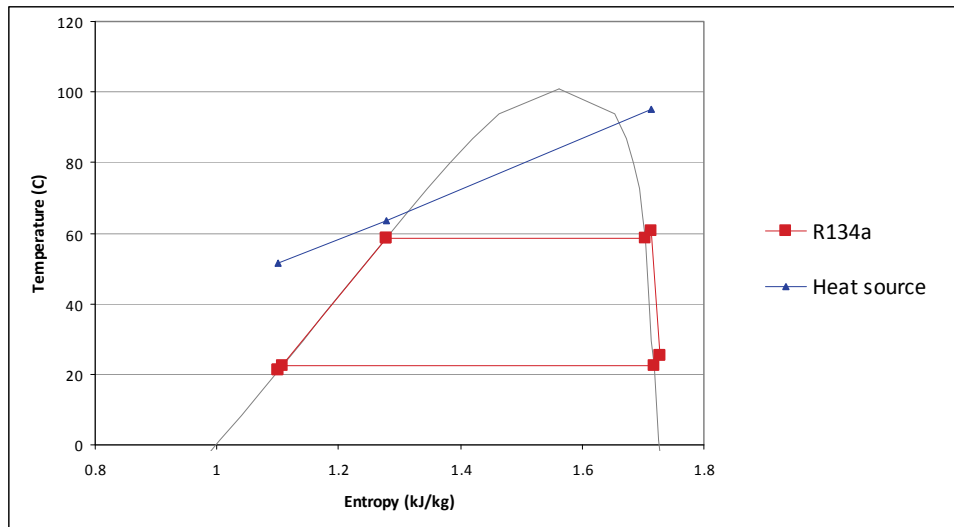
Figure 4.12: Final ORC system, summer scenario

4.2.4 Auxiliary Systems Power Consumption

The net electric power output from the ORC unit in Chapter 4.2.3 does not take into account power consumption from auxiliary systems. To find the net power output of the entire power production unit (PPU) the power consumption of the auxiliary systems has to be mapped. The main consumers of electrical power excluding the ORC unit are pumps and fans in the heat supply and heat discharge system.

Hot Water Supply Pump

The pump work is expressed as:

$$P_{pump} = \frac{\Delta p_{loss} \cdot \dot{m}_{water}}{\rho_{water}} \cdot \frac{1}{\eta_{pump}} \qquad\qquad (4.5)$$

where Δp_{loss} is the total pressure loss in the hot water supply circuit.

The total pressure loss is produced by friction in the pipes, bends, valves and heat exchangers in the circuit. The pressure loss due to surface friction in the pipes and pipe bends only makes up about 0.16 bar (see Appendix A for the entire calculation). This is only a small part of the total pressure loss, which usually is closer to 2 bar (Næss, 2009). The additional pressure loss is produced by the four heat exchangers and the mass flow control valves in the circuit. The control valves creates and equals out pressure differences in the system in order to distribute the hot water in a way that stabilizes the system and contributes to a good power output.

With a pressure loss of 2 bar and a pump efficiency of 75 % the hot water supply pump has a power consumption of 35 kW, which represents only 2% of the net electric power output from the ORC unit. This is only an estimate, but demonstrates that the pump in the hot water supply circuit reduces the net power output from the ORC unit marginally. The parameters used in the calculation are displayed in Table 4.9.

Table 4.9: Parameters used to calculate pump power consumption

Pressure loss	200000	Pa
Massflow water	130	kg/s
Density water	1000	kg/m3
Pump efficiency	0.75	

Fan Work

The fan work is expressed as:

$$P_{fan} = \Delta p_{loss} \cdot \dot{V}_{rawgas} \cdot \frac{1}{\eta_{fan}}$$

(4.6)

Where Δp_{loss} is the total pressure loss in the fume treatment plant and $\dot{V}$ is the volume flow of the raw gas entering the fan.

When installing a heat exchanger, the friction and form drag of the heat exchanger surface creates a pressure drop which has to be compensated for by the fan. The surface area of the heat exchanger, and thereby the heat exchanger design, is therefore a determining factor of the heat exchanger pressure drop. Normally the design is limited by cost and size. In this report it is assumed that the pressure drop of the raw gas heat exchanger on the gas side is 1000 Pa (Næss, 2008). The pressure drop is somewhat higher than in regular heat exchangers because of the higher velocities required in order to avoid fouling in the heat exchanger.

In addition to the added pressure drop, installing a heat exchanger changes the operating conditions of the FTP. This is mostly due to the temperature reduction downstream to the heat exchanger. This temperature is dependent on the amount of heat extracted from the flue gas. The total impact of installing a heat exchanger on fan power consumption needs to be determined in order to find the net benefit of installing the power production unit. To find the total impact, the current fan operating conditions have to be established.

The fan operating conditions for the summer scenario were mapped in the project thesis "Energy Flow Analysis in an Aluminium Plant and Survey of Material Balance", by Tabuk and Børgund 2008. The existing pressure difference across the fan was found to be 5 023 Pa at 110 °C raw gas temperature, and the total volume flow rate was found to be 1 456 000 Nm³/h. As the volume flow rate increases with temperature the volume flow rate entering the fan is somewhat higher than at standard temperature (0 °C). It can be approximated by the equation:

$$\dot{V}_2 = \dot{V}_1 \cdot \frac{T_2}{T_1}$$

(4.7)

Table 4.10 shows the assumed temperature profile in the FTP after installing the heat exchanger (HE) together with the current temperatures. The temperature difference between the raw gas and the clean gas exiting the dry scrubber is assumed to be 20 °C. The temperature out of the heat exchanger is set to be 15 °C higher than the hot water inlet temperature corresponding to the given scenario (see Table 4.8), because of the raw gas heat exchanger pinch point.

Table 4.10: Temperature progression in degrees Celsius

Scenario	Before HE	After HE	Before fan	After fan
Summer	110	110	90	93
Summer + HE	110	70.26	50.26	53.26
Winter	100	100	80	83
Winter + HE	100	60.78	40.78	43.78

The resulting pressure difference across the fans together with the total volume flow is displayed in Table 4.11. The volume flow rate was found by using equation (4.7), while the total pressure loss was found by using the method described in the project thesis, Chapter 6.4.2 Fan Power Consumption.

Table 4.11: Fan power consumption with and without heat exchanger (HE)

Scenario	Δp [Pa]	$\dot{V}$ [m³/s]	P [kW]	$P_{increase}$ [kW]
Summer	5023	563	3969	-
Summer + HE	5446	504	3849	**-120**
Winter	4873	547	3739	-
Winter + HE	5310	488	3638	**-101**

In both scenarios the fan work increase, $P_{increase}$, is negative. It signifies that the net power gain of the reduced volume flow rate is greater than the power loss produced by the increased pressure loss of installing the heat exchanger. However, this is just a preliminary calculation which assumes a pressure drop of 1000 Pa in each raw gas heat exchanger together with turbulent flow in the pipes and laminar flow through the dry scrubber filters to mention some. Thus, the calculation only serves as an indication of the influence of a heat exchanger installation in the raw gas.

Apart from the increased fan work, the heat exchangers influences component sizes and required maintenance in the FTP. As the volume flow rate of the raw gas decreases after the heat exchanger, the gas ducts and FTP components can be made smaller in size, reducing investment costs. Moreover, the reduced temperature reduces the strain on the filter bags in the dry scrubber, increasing their lifetime and reducing maintenance costs.

Cold Water Supply Pump

The cold water supply pipe is not assumed to have a pump as the Tya power station is situated higher up in the terrain than the ORC unit. The altitude difference will create a natural pressure difference between the water source and the ORC unit.

4.2.5 Actual Power Output

The actual power output from the power production unit is the net power output from the ORC unit minus the power consumption of the hot water supply pump and the increased power consumption of the fan. It was found to be approximately 1.5 MW for both the winter and the summer scenario. The exact values are displayed in Table 4.12.

Table 4.12: Actual power output from the power production unit

	Summer	Winter
Net electrical power output, ORC (kWe)	1629	1672
Hot water supply pump power consumption (kWe)	35	35
Increased fan power consumption (kWe)	-120	-101
Net electrical power output, PPU (kWe)	**1714**	**1738**

With an availability of 95%, the yearly electrical power production becomes 14.36 GWh. The yearly electrical power consumption at ÅI is 1699 GWh/year (HERE database 2007). The power recovered from the raw gas will therefore only represent 0.8 % of the electrical power required to produce aluminium at ÅI. On the other hand, the power recovered also represents the electricity consumption of 884 households in Norway (based on a yearly consumption of 16.24 MWh/year (Statistics Norway, 2008)). It should be noted that the result is based on a constant heat sink and heat source temperature in the summer and in the winter. In real life, fluctuations in temperature occur, and the power output during a year is dependent on the climate, the aluminium production and the availability of the ORC unit.

Comments to the Power Output Results

The net power output from the final system is based on working fluid simulations where the goal was to find the system solution with highest power output. In real life, the optimum system is not always the one with the highest power output, as the cost of producing the power also has to be taken into consideration. As more heat is extracted from the heat source, the ORC components have to grow in size because of an increased flow of energy that has to go through the system. A simulation was done to find the relationship between the amount of heat extracted from the source, Q_h, and net ORC power output, P_{net}. The hot water inlet temperature was held constant at 95 °C while the water discharge temperature, T_{W2}, was varied between 55 °C and 80 °C. The result is shown in Table 4.13.

Table 4.13: Simulation results for marginal power output simulation

T_{W2} (°C)	Q_h (kW)	P_{net} (kW)
55	21643	1629
60	19073	1595
65	16352	1497
70	13632	1337
75	10911	1128
80	8187	880

As expected, the power output is highest with a 55 °C water discharge temperature and decreases as the heat transferred to the ORC decreases. However, while Q_h decreases with 2720 kW for each step in the simulation, the power output follows a different trend. In Figure 4.13, the power output for varying Q_h is plotted. From the figure it can be seen that the extra power output gained by decreasing the hot water discharge temperature from 60 °C to 55 °C is quite small compared to the extra power gained by decreasing the discharge temperature from 80 °C to 75 °C. To incorporate this finding in the optimization of the ORC system is not possible in this thesis as it would require knowledge about the cost of the individual ORC components at different pressures and mass flow rates. However, it is an important point that has to be included in a real life optimization model.
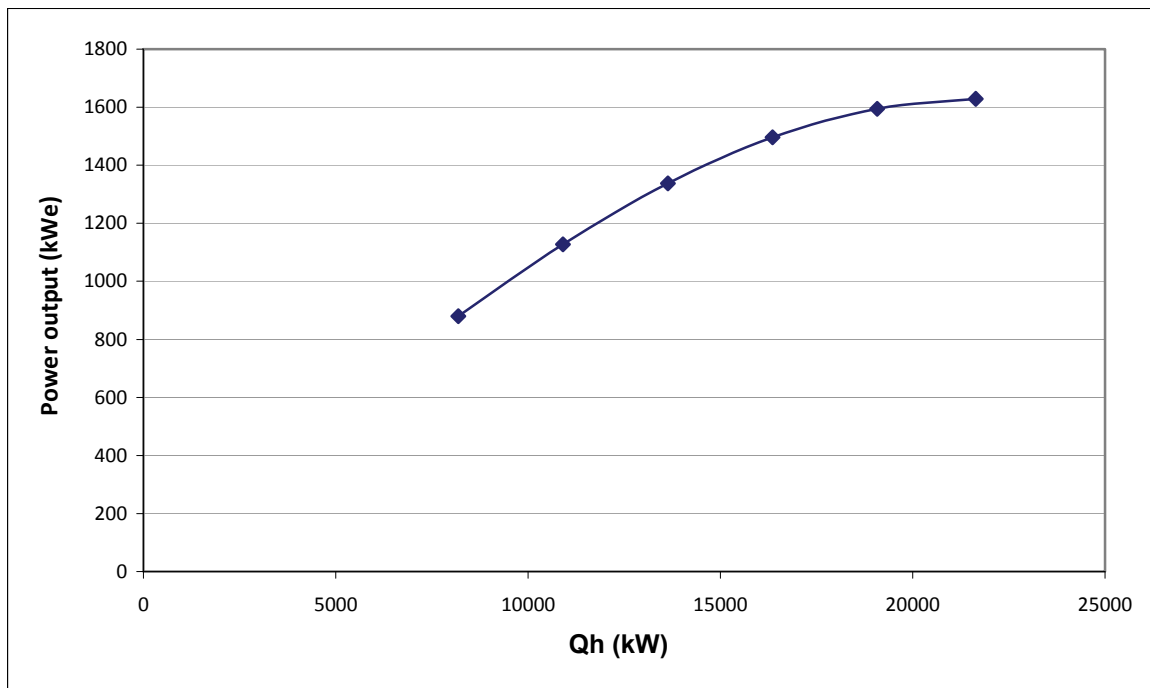
Figure 4.13: Heat transferred to ORC unit versus power output

Another point to make is that the discharge hot water temperature, and therefore the raw gas temperature exiting the raw gas heat exchanger, does not only dictate the power output of the ORC. The raw gas outlet temperature has a large impact on fan work and the dimensions of the FTP unit.
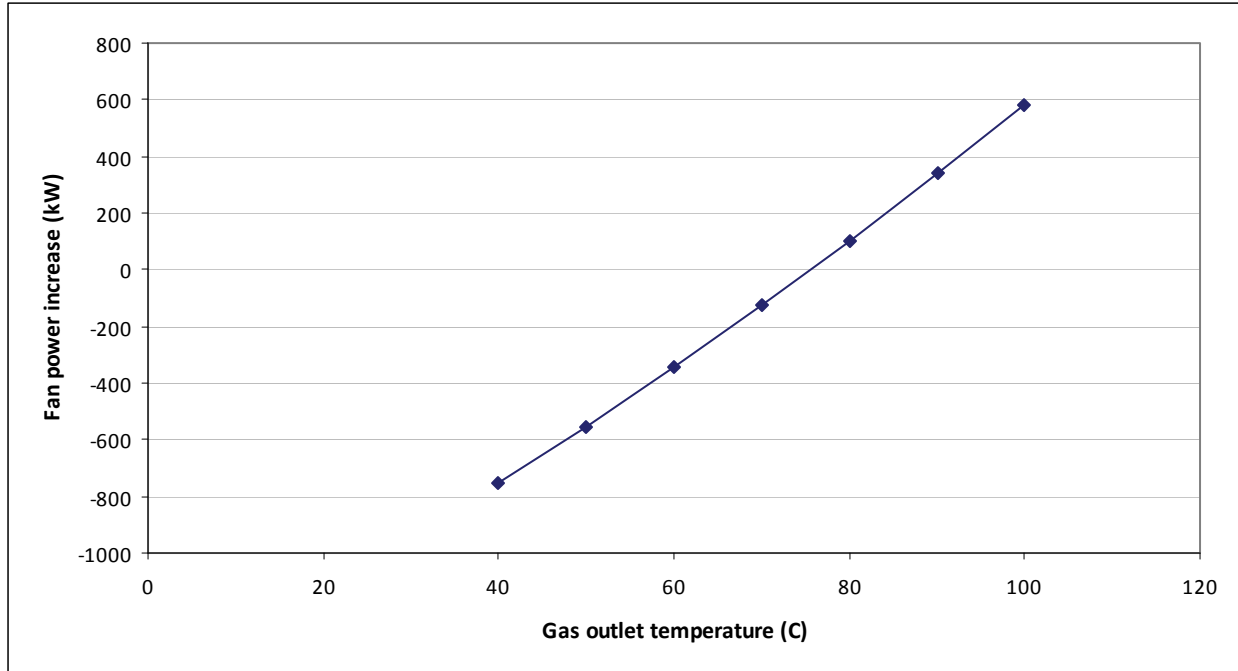
Figure 4.14: Influence of raw gas temperature on fan power consumption

Figure 4.14 displays the fan power consumption increase after installing a raw gas heat exchanger with different gas outlet temperatures. The graph indicates that the fan power consumption is extremely sensitive to temperature changes. If the raw gas is cooled down to 75 °C the fan power consumption remains unchanged. If the outlet raw gas temperature increases beyond this point the fan power consumption will increase. At 90 °C the fan power consumption has increased 338 kWe, equal to 21 % of the net power output from the ORC unit.

The raw gas temperature also has an impact on the capacity needed in the FTP as the volume gas flow decreases with temperature. Experience data implies that the investment costs increase with a factor of 0.7 to an increase in volume flow rate the plant must handle.

From an ORC point of view, to extract as much heat as possible from the heat source might not seem to be economically favorable. However, when including the net benefits the low raw gas temperature has on FTP design and operation, a low hot water discharge temperature might still be the optimal solution. As such, the FTP also has to be taken into consideration when optimizing the ORC operation for best profitability.

4.3 Commercially Available Systems

Several ORC module producers were contacted in order to find a commercially available system fit for electricity production from aluminium electrolysis raw gas in Årdal. Of the initial six companies contacted (Ormat, Infinity Turbines, GMK, Opcon, Turboden and UTC power) only two companies came with a proposition. The system solutions proposed by Turboden and Opcon are displayed below. The two companies have very different profiles (see Chapter 2.3.3), it is therefore interesting to compare them in according to system performance and economic viability. If not stated otherwise, all information on the Turboden ORC unit is received from Sabrina Santarossa (Sabrina.santarossa@turboden.it), sales engineer at Turboden. All information regarding the Opcon ORC modules is received from Tony Gustavsson (tony.gustavsson@opcon.se), business developer in the division of renewable energy at Opcon.

4.3.1 System Performance

For the system performance the companies were sent a set of preliminary calculation data as seen in Table 4.14.

Table 4.14: Preliminary calculation data

Data:	Value	Unit
Exhaust gas temperature	110	°C
Exhaust gas flow rate	1456000	Nm3/h
Mean ambient temperature	5.7	°C
Heat sink temperature (water)	7	°C
Restrictions:		
gas/water HE surface temp	40	°C min
Raw gas heat exchanger pinch point	20	°C min
Gas composition:		
O2	20	vol%
N2	78	vol%
CO2	1	vol%
Ar	1	vol%
Others:		
H2O	4	g/Nm3
Particles	640	mg/Nm3
HF	260	mg/Nm3
SO2	200	mg/Nm3

The heat sink temperature and the raw gas heat exchanger pinch point given in the data set deviates from the values previously presented in this report (For the summer scenario with an exhaust gas temperature of 110 °C, the heat sink temperature was 12 °C and the raw gas heat exchanger pinch point was set to be 15 °C in the preceding calculations). The reason for the

inconsistent use of data is that the data set was sent to the ORC manufacturers at an early stage, before all data values were confirmed. The small differences are assumed not to have a predominant effect on the power output, but should be noted.

Turboden

Turboden offers a customized ORC unit with an indirect system design. The heat supply circuit is filled with water and the working fluid is R134a. The dimensioning cycle parameters are shown in Table 4.15.

Table 4.15: Dimensioning cycle parameters, Turboden system design

Data:	Value	Unit
Inlet hot water temperature	90	°C
Outlet hot water temperature	70	°C
Inlet cooling water temperature	7	°C
Outlet cooling water temperature	17	°C
Net electric power output[i]	920	kWe
Thermal efficiency	8.66	%
Dimension	17 x 7 x 5	m

i) +/- 5 %, excluding power consumption of pump in hot water circuit and raw gas fan.

Opcon

Opcon offers prefabricated ORC modules with either R134a or ammonia (NH_3) as working fluid, named the Opcon Powerbox. As for the system proposed by Turboden, the Powerbox has an indirect system design. The dimensioning cycle parameters for the R134a and the NH_3 system solution can be found in Table 4.16 and Table 4.17, respectively.

Table 4.16: Dimensioning cycle parameters, Opcon R134a system design

Data:	Value	Unit
Inlet hot water temperature	90	°C
Outlet hot water temperature	74	°C
Inlet cooling water temperature	7	°C
Outlet cooling water temperature	16	°C
Net electric power output[i]	690	kWe
Thermal efficiency	8.13	%
Dimension	7 x 3 x 3.5	m

i) +/- 5 %, e xcluding power consumption of pump in hot water circuit and raw gas fan

Table 4.17: Dimensioning cycle parameters, Opcon ammonia system design

Data:	Value	Unit
Inlet hot water temperature	90	°C
Outlet hot water temperature	68	°C
Inlet cooling water temperature	7	°C
Outlet cooling water temperature	16	°C
Net electric power output[i]	750	kWe
Thermal efficiency	8.39	%
Dimension	7 x 3 x 3.5	m

i) +/- 5 %, e xcluding power consumption of pump in hot water circuit and raw gas fan

As seen from Table 4.16 and Table 4.17, ammonia gives a better power output than R134a for the given system configuration. Ammonia is categorized as a B2 fluid (See chapter 3.1.6 for safety classification) and is both poisonous and flammable. If ammonia is to be used in the ORC module several safety measures have to be implemented in case of a leakage. However, ammonia is a commonly used working fluid and the safety installations and routines regarding the use of ammonia are well documented.

Opcon's turbine has a max shaft power of 0.89 MW, which limits the power output from one module. The ammonia system design displayed in Table 4.17 cannot exploit the entire hot water supply for this reason. One solution is to install two modules that use 50 % of the hot water supply each. The system configuration of such as system is displayed in Table 4.18.

Table 4.18: Dimensioning cycle parameters, Opcon ammonia x2 system design

Data:	Value	Unit
Inlet hot water temperature	90	°C
Outlet hot water temperature	62	°C
Inlet cooling water temperature	7	°C
Outlet cooling water temperature	21	°C
Net electric power output[i]	1 100	kWe
Thermal efficiency	7.33	%
Dimension	14 x 6 x 3.5	m

i) +/- 5 %, e xcluding power consumption of pump in hot water circuit and raw gas fan

Auxiliary Systems Power Consumption

Also the commercial units require a hot water supply circuit and have an effect on fan power consumption. The hot water supply pump will have the same power consumption as for the simulation model as the same amount of water is circulated in both cases, namely 35 kWe. The increased fan power consumption depends on the raw gas temperature leaving the raw gas heat exchanger and will vary in the four cases. The same method as described in Chapter 4.2.4 is used to calculate the increased fan work displayed in Table 4.19.

Table 4.19: System solution influence on fan power consumption

System	Raw gas outlet temperature (°C)	Fan power increase (kW)	Fan power increase[i] (%)
Turboden, R134a	90	339	37
Opcon, R134a	94	436	63
Opcon, NH$_3$	88	290	39
Opcon, NH$_3$ x2	82	149	14

i) as percentage of net power output

As seen from Table 4.19, the fan power increase of installing one of the proposed solutions reduces the final power output from the power production unit drastically. If any of the proposed solutions are to be used, the raw gas has to be further cooled down by other means

to avoid the fan power increase. One solution is to install an additional heat exchanger in the hot water supply circuit directly heat exchanging with the cooling water. In the case of the Turboden R134a solution, the ORC heat exchanger would take hot water from 90 °C to 70 °C before the water was additionally cooled by the cooling water heat exchanger. Because of the large fan power increase introduced by using the proposed ORC units with the heat supply system described earlier in the chapter, it is assumed that the heat supply system for the ORC units have a different design and the power consumption of the hot water supply pump and the raw gas fan power increase is ignored.

Comments on System Performance

The system solutions proposed by Turboden and Opcon have much lower power outputs than the simulated result in Chapter 4.2.3, which had a net power output from the ORC unit of 1629 kWe with a raw gas temperature of 110 °C.

One explanation could be that the simulation model has more lenient system requirements. However, a simulation done with Turboden's system configuration gave a 958 kWe net power output from the simulation model, only 4.1 % more than Turboden's power output. This demonstrates that the system configuration of the simulation model is not so wrong compared to Turboden's system configuration. The simulation model is further apart from the Opcon R134a unit with a power output of 807 kWe for the given operational conditions (17 % more than Opcon's solution). The cause of the deviation might be that Opcon's units are prefabricated and has inferior efficiencies compared to the Turboden unit and the simulation model. All in all the simulation model seems to have adequate system requirements compared to the commercial systems.

The main reason for the power output difference is thus the difference in thermal power recovered from the raw gas, Q_h. While the simulation model brings the raw gas from 110 °C down to 70 °C, the commercial units brings it down to only 82 °C – 90 °C. It seems like the companies do not find it economically just to utilize more of the heat source to produce power. As discussed in Chapter 4.2.5, the net benefit of increasing the source utilization and increasing power output does not weigh up for the increased investment costs of large system dimensions and complicated turbine designs.

4.3.2 Profitability Analysis

Hydro Årdal has an 11% minimum requirement on the internal rate of return of their investments (Rørvik, 2009). The profitability analysis will analyze the four offers received from Turboden and Opcon to see if they can meet the internal rate of return requirement.

General assumptions

- Lifetime of the ORC units is set to be 20 years based on indications received from Opcon and Turboden.
- Price increase on electricity production and maintenance costs per year is set to be 2%, based on the consumer price index of Norway the last 10 years (Statistics Norway, 2009)
- Investment costs, excluding ORC unit is set to be 10 MNOK and includes 4 raw gas heat exchangers, the heat supply and heat discharge system, transportation and installation. This item is beyond the scope of this report, hence only a rough estimate is quoted.
- Price of electricity is set to be 0.25 NOK/kWh the first year. This is only an estimate as Hydro Årdal does not wish to share their current electricity price.
- Availability is assumed to be 95 %, i.e. 8322 hours per year.

Turboden

Table 4.20: Turboden profitability analysis input data

ORC module price excl. VAT	20 000 000 ± 10 %	NOK
Maintenance costs	200 000	NOK/year
Net power output	920 ± 5 %	kWe

Table 4.20 displays the input data to the profitability analysis gathered from Turboden. The custom made ORC module will have a price tag of approximately 20 MNOK excluding VAT, transport and installation. It is estimated to produce 920 kWe of net electric power, excluding consumption from hot water pump and exhaust gas fan. Turboden offers maintenance packages with different degree of service included ranging in price from approx. 177 000 NOK to 355 000 NOK a year. The different service plans are shown in Figure 4.15. In the profitability analysis the maintenance cost is set to the same price as the Opcon service plan, namely 200 000 NOK/year.
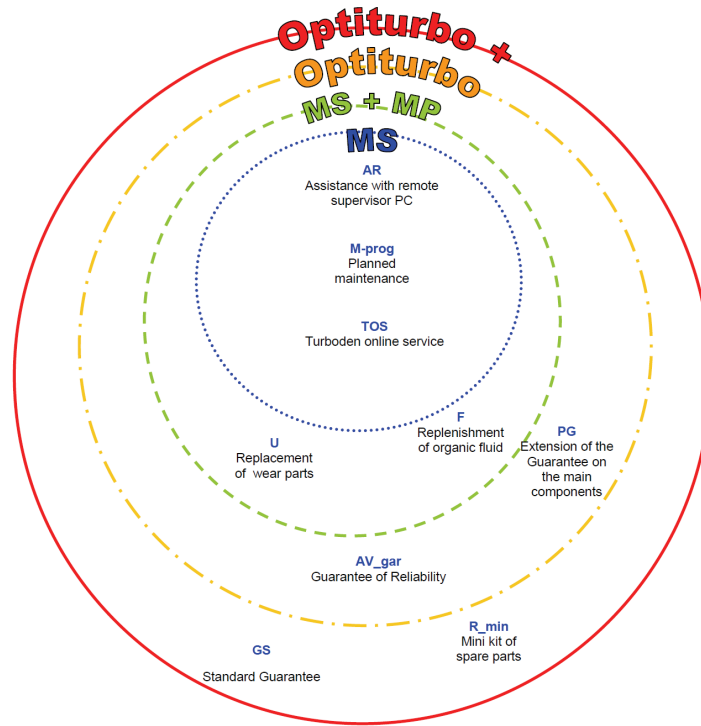
Figure 4.15: Turboden service plans

Opcon

Opcon offers two different prefabricated modules for operation in Årdal, one with R134a and one with ammonia (NH_3) as working fluid. The modules have net power outputs of 690 kWe and 750 kWe, respectively, excluding power consumption from hot water pump and exhaust gas fan. Both units have a price of 7.5 MNOK excluding VAT, transport and installation. Two modules can also be combined for a higher power output, the price will then be 15 MNOK and the power output from two units with ammonia as working fluid becomes 1100 kWe. The yearly maintenance costs of the Opcon ORC module is approximately 200 000 NOK according to the producer. Table 4.21 displays the Opcon input data to the profitability analysis.

Table 4.21: Opcon profitability analysis input data

ORC module price excl. VAT	7 500 000 ± 10 %	NOK
Yearly maintenance costs	200 000	NOK/year
Net power output, R134a	690 ± 5 %	kWe
Net power output, NH_3	750 ± 5 %	kWe
Net power output NH_3 x2	1 100 ± 5 %	kWe

The rate of return is the ratio of money gained or lost on an investment relative to the money invested. In the case of the ORC unit installation in Årdal, the rate of return should be over 11 % for the investment to be profitable. Because of the low electricity prices in Norway (especially for the industry) an ORC installation will most probably not be profitable without financial aid.

In Norway financial aid for projects related to energy efficiency and renewable energy can be gained from Enova. Enova SF is a public enterprise owned by the Royal Norwegian Ministry of Petroleum and Energy. Its main goal is to contribute to the environmentally friendly and efficient use and production of energy. Enova gives financial aid to companies in the industry sector to implement measures leading to reduced energy use and/or to an increased use of renewable energy sources. In 2009, by appointment of Enova, Norsk Energi and NEPAS published a report on the use of waste heat from the Norwegian industry. One of the conclusions in the report emphasized the need for ORC and Sterling motor technology competence in Norway through pilot installations (Sollesnes and Helgerud, 2009). Enova can finance up to 20 % of the investment cost related to the energy efficiency measure, in this case the ORC power production unit.

The profitability analysis was performed with three financial support scenarios: 0 %, 10 % and 20 % of the total investment costs. The results are displayed in Table 4.22.

Table 4.22: Rate of return for the Turboden and Opcon system solutions with 0 %, 10 % and 20 % of investment costs financed by Enova

Financial Support	Turboden	Opcon		
	R134a	R134a	NH3	NH3 x2
0 %	3.44	6.00	7.28	8.31
10 %	4.68	7.40	8.77	9.87
20 %	6.16	9.08	10.57	11.78

As seen from Table 4.22 only one of the proposed system solutions reached the 11 % rate of return target set by Hydro. With 20 % financial support two Opcon Powerbox modules with ammonia as working fluid is economically viable for Hydro. The module also achieves the highest power output and recovers the most energy from the raw gas of the system solutions presented. Table 4.23 displays the minimum required financial support to obtain the set rate of return for the modules. All solutions proposed by Opcon are more economically favorable than Turboden's solution. Because Opcon uses prefabricated parts they manage to sell their modules to a fairly low price. Even though the power output from one Opcon module is less than the power output from Turboden's customized unit, it achieves a better rate of return.

Table 4.23: Required financial support to obtain an 11% rate of return

Financial aid	Turboden	Opcon		
	R134a	R134a	NH3	NH3 x2
NOK	12 803 647	5 087 764	3 883 789	4 062 708
%	42.68	29.07	22.19	16.25

Only one of the proposed systems seems to be economically profitable when the ORC units are seen as individual investments. However, the ORC unit can also be regarded as part of the new FTP design. If the raw gas is to be cooled down independent of the ORC unit, just to give a better FTP performance, the cost of the gas cooling system can be deducted from the cost of the ORC unit. As a consequence, the initial investment cost will be lower and less financial support is needed to reach Hydro's rate of return requirement.

5 Conclusion

Of the four thermodynamic cycles investigated in Chapter 2; Stirling, steam Rankine, organic Rankine (ORC) and Kalina, the ORC proved to be the best suited technology for power production from low temperature waste heat. This is due to its superior thermodynamic properties to the steam Rankine cycle. Furthermore, the cycle is better developed and documented than the Stirling and the Kalina cycle. However, the industry for producing power from industrial waste heat is under rapid development, and the same conclusion might not be valid in a couple of years.

In the preliminary working fluid simulation, R227ea proved to be the best performer both in the direct and the indirect system design with an average power output of 2262 kW and 2153 kW, respectively. This resulted in a 5 % lower power output for the indirect design. For a direct system solution it is necessary to install an internal heat exchanger (IHE) for optimal cycle performance. The indirect system has a broader selection of relevant working fluids than the direct design because of the absence of the IHE.

The best system design for a power production unit in connection to the ÅI FTP is an indirect system with four raw gas heat exchangers connected in parallel to a water circuit supplying hot water to the ORC unit. Even tough R227ea proved to be the best performer in the working fluid simulations, R134a was chosen as the working fluid for the final system design based on ORC manufacturer's practical experience with the working fluids. The final system design has an average net power output of 1726 kW, 21% lower than in the preliminary indirect design. This is mainly due to the applied cooling water mass flow limitation of 500 kg/s. The raw gas fan power consumption was estimated to decrease on average 110 kW after the ORC installation. In fact, as long as the raw gas is cooled down to under 75 °C, the installation of an ORC unit decreases the raw gas fan power consumption.

The ORC performance estimates done by Opcon and Turboden both had inferior power outputs to the simulated ORC. This was partially due to different system constraints, but mostly due to the different simulation targets. While the commercial units are optimized for minimum cost per kW, the simulations done in this thesis are optimized for maximum power output.

Only one of the commercial performance estimates fulfilled the minimum rate of return requirement set by Hydro (11 %). The installation of two Opcon Powerbox modules with ammonia as working fluid is profitable with a financial support of 16.25 % (4 062 708 NOK). Moreover, if the ORC unit is to be installed in connection to the construction of a new FTP, the investment costs of the ORC are expected to be smaller as a gas cooling system is likely to be installed nevertheless.

For future work the influence of the raw gas temperature on FTP operation and design should be thoroughly investigated and documented. This includes mapping the relationship between gas composition and acid dew point and finding a financial relationship between raw gas temperature and FTP costs. Futhermore, the temperature and quantity of cooling water available, together with the practical lay out of the supply pipes have to be found. This because the ORC unit needs substantial amounts of cooling water to operate, so without a cooling water source an ORC installation would not be feasible. Moreover, the profitability analysis documented that financial support is required in order to make the energy recovery system financially viable. Hence funding possibilities should be further investigated.

6 References

Air Liquide, 2005
>
> Hydrogen Sulphide Safety Data Sheet (MSDS). Air Liquide SA 2005, [PDF], available from:
> http://encyclopedia.airliquide.com/sds/en/073_AL_EN.pdf

Air Products, 2008
>
> Safetygram #20 Nitrous Oxide (N_2O). Air Products 2008, [PDF], available from:
> http://www.airproducts.com/nr/rdonlyres/8c46596e-2f7d-4895-b12a-e54cd63e1996/0/safetygram20.pdf

Badr et al., 1985
>
> Badr O, Probert S D, O'Callaghan P W. Selecting a Working Fluid for a Rankine-Cycle Engine. Applied Energy 1985;21:1-42.

Bronicki, 2007
>
> Bronicki L Y. Organic Rankine Cycles in Geothermal Power Plants – 25 years of Ormat Experience. GRC Transactions 2007;31:499-502

Dai et al., 2008
>
> Dai Y, Wang J, Gao L.. Parametric Optimization and Comparative Study of Organic Rankine Cycle (ORC) for Low Grade Waste Heat Recovery. Energy Conversion and Management 2008;50:433-854.

Dippipo, 2004
>
> Dippipo R. Second Law Assessment of Binary Plants Generating Power from Low-temperature Geothermal Fluids. Geothermics 2004;33: 565-586.

Exorca, 2008
>
> Exorca. High Output from Low Temperatures – The Kalina Cycle, [Internet], available from
> http://www.exorka.com/index.php/kalina-cycle.html (accessed April 27, 2009)

Glava, 2008
>
> Glava. Glava AluComfort Rørskål – Produktdata, [PDF], available from
> http://www.glava.no/filesystem/2008/11/alucomfort_rrskal__6015.pdf (accessed May 20, 2009)

GMK, 2009
>
> GMK. ORC Waste Heat Recovery – INDUCAL, [Internet], available from:
> http://www.gmk.info/ORC_waste_heat.523.html (Accessed April 3, 2009)

Gustavsson, 2009
>
> Gustavsson, T, Opcon Energy Systems. Personal communication, April 16, 2009.

HERE database, 2007
>
> HERE database. Hydro's database over all data related to their production units. Data used are from 2007.

Holdman, 2007
> Holdman G. Chena Geothermal Power Plant Project, Final report prepared by Chena Power Company.

Hornnes and Bolland, 1991
> Hornnes A, Bolland O. Power Cycles Working Fluids. SINTEF Energy Research 1991. ISBN 82-595-6407-6.

Høeg, 2009
> Høeg A, Single Phase Power. Personal communication March and April 2009.

Incompera et al., 2007
> Incopera F P, DeWitt D P, Bergman T L, Lavine A S. Fundamentals of Heat and Mass transfer, sixth edition, John Wiley and Sons, Inc 2007. ISBN 0-471-45728-0.

International Institute of Refrigeration, 2006
> International Institute of Refrigeration. Classification of Refrigerants, [PDF], available from: www.iifiir.org/en/doc/1027.pdf (accessed May 29, 2009)

Kolderup and Juliussen, 2001
> Kolderup H, Juliussen O. Varmegjenvinning fra rågass i elektrolyseprosessen. SINTEF Kjemi 2001. Report no. STF66 F01047.

Kontragool and Wongwises, 2003
> Kontragool B, Wongwises S. A Review of Solar-powered Stirling Engines and Low Temperature Differential Stirling Engines. Renewable and Sustainable Energy Reviews 2003;7:131-154.

Ladam, 2009
> Ladam Y. Personal communication throughout the spring semester 2009.

Lakew, 2009
> Lakew, A. A. Working Fluid Selection for Low Temperature Heat Source. Norwegian University of Science and Technology, 2009.

Milora and Tester, 1977
> Milora S L, Tester J W. Geothermal Energy as a Source of Electric Power. The Massachusetts Institute of Technology Press 1977. ISBN 0-262-13123-4.

Norwegian Meteorological Institute, 2009
> Norwegian Meterological Institute. eKlima – weather database, weather station # 54110 Lærdal IV. [Internet] available from: http://eklima.met.no (accessed May 3, 2009).

Næss, 2009
> Næss, E. Personal communication throughout the spring semester 2009.

Renz, 2006
> Renz M. The New Generation Kalina Cycle, contribution to the conference 'Electricity Generation from Enhanced Geothermal Systems', [Presentation], 2006.

Saleh et al., 2007
> Saleh B, Koglbauer G, Wendland M, Fischer J. Working Fluids for Low-Temperature Organic Rankine Cycles. Energy 2007;32:1210-1221.

Sollesnes and Helgerud, 2009

Sollesnes G, Helgerud H E. Utnyttelse av spillvarme fra norsk industri – en potensialstudie, Norsk Energi and NEPAS 2009, [PDF], available from: http://www.enova.no/minas27/publicationdetails.aspx?publicationID=423 (accessed April 20, 2009).

Statistics Norway, 2008
Statistics Norway. Gjennomsnittlig energiforbruk, totalt og fordelt på energibærere. 1993 – 1995, 2001, 2004 og 2006. kWh tilført energi per husholdning. Statistics Norway, [Internet], available from: http://www.ssb.no/emner/01/03/10/husenergi/tab-2008-04-28-01.html (accessed June 3, 2009)

Statistics Norway, 2009
Statistics Norway. Konsumprisindeksen fra 1865. Statistics Norway, [Internet], available from: http://www.ssb.no/kpi/tab-01.html (accessed June 5, 2009)

Tabuk and Børgund, 2008
Tabuk M, Børgund M. Energy Flow Analysis in an Aluminium Plant and Survey of Material Balance. Project thesis at the Norwegian University of Science and Technology 2008.

Thombare and Verma, 2008
Thombare D G, Verma S K. Technological Development in the Stirling Cycle Engines. Renewable and Sustainable Energy Reviews 2008;12:1-38.

Turboden, 2009a
Turboden. ORC technology for distributed energy production, [PDF], available from: http://www.turboden.eu/en/public/downloads/TD_wasteheat_english.pdf (accessed April 20, 2009).

Turboden, 2009b
Turboden. Company Presentation, [PDF], available from: http://www.turboden.eu/en/public/downloads/Turboden_presentation_09Z00156_e.pdf (accessed April 20, 2009).

UNEP, 2006
UNEP (United Nations Environment Programme). Montreal Protocol on Substances that Deplete the Ozone Layer 2006 Assessment. Prepared by the Refrigeration, Air Conditioning and Heat Pumps Technical Options Committee, available from: http://ozone.unep.org/Assessment_Panels/TEAP/Reports/RTOC/index.shtml (accessed May 10, 2009)

UTC Power, 2009a
UTC Power. PureCycle Power System – Overview, [Internet] Available from: http://www.utcpower.com/fs/com/bin/fs_com_Page/0,11491,0167,00.html (accessed February 28, 2009)

UTC Power, 2009b
UTC Power. Chena Hot Springs Resort, [PDF] Available from: http://www.utcpower.com/fs/com/Attachments/Project_Profiles/PP0114_Chena.pdf (accessed February 28, 2009)

Valdimarsson, 2006
Valdimarsson P. The Kalina Power Plant in Husavik. Why Kalina and What Has Been Learned. ENGINE workshop, September 5,2006.

Åmand et al., 2006
Åmand L E, Leckner B, Eskilsson D, Tullin C. Deposits on Heat Transfer Tubes during Co-combustion of Biofuels and Sewage Sludge. Fuel 2006;85:1313-1322

7 Appendices

Appendix A - Pressure Loss in Hot Water Supply Pipes due to Surface Friction and Pipe Bends

For simplicity, it is only chosen to look at the pressure losses for the summer scenario as the pressure loss will not change much from 95 °C to 85 °C.

 The circuit is divided into two parallel connected branches as seen in Chapter 4, Figure 4.5. Each branch continues for about 100 m before it is further divided into two sections each connected to a raw gas heat exchanger. After the raw gas heat exchanger the two sections are reconnected and run back to the ORC unit. As most of the pressure loss happens in the 100 m branches going to and from the four raw gas heat exchangers, the rest of the piping is neglected in this calculation. The friction loss in the pipes can be approximated according to the equation:

$$\Delta P_{loss} = 4 \cdot C_f \cdot \frac{L}{d} \cdot \frac{\rho v^2}{2}$$
(A-1)

Where
C_f = friction coefficient (dimensionless)
ρ = density (kg/m^3)
v = velocity (m/s)
L = length of pipe (m)
d = diameter of pipe (m)

The main friction loss is in the two main branches. Each branch carries 65 kg/s of water with an assumed velocity of 1 m/s, as used earlier in the thesis. This amounts to an inner pipe diameter of 28.77 cm. All parameters in Equation A-1 are therefore known except the friction coefficient. The friction coefficient behaves differently for laminar and turbulent flows. The Reynholds number is an indication as to wether the flow is laminar or turbulent and is expressed as:

$$Re = \frac{\rho v d}{\mu}$$

Where μ is the water viscosity (Pa.s)

The viscosity of a fluid varies with temperature. And the incoming water at 95 °C will have a different viscosity than the discharge water at 40 °C. Table A-1 displays the viscosity (Incompera et al., 2007) and Reynholds number of water at 40 °C and 95 °C.

Table A-1: Viscosity and Reynholds number of water at 95°C and 40°C

Temperature (°C)	95	40
Viscosity (mPa.s)	0.295	0.660
Re	975 191	435 881

As both flows have Reynholds numbers far above 10 000, they are turbulent. For turbulent flows the friction coefficient can be found by using a Moody diagram. This results in a friction coefficient of 0.0046 and 0.0050 for 95 °C and 40 °C, respectively. Using Equation A-1, the total pressure drop of the supply and discharge branches becomes 13348 Pa, or 0.13 bar. How this is divided between the four pipes is displayed in Table A-2.

Table A-2: Pressure loss due to surface friction

| Pipe	Pressure loss (Pa)
100 m water pipe at 95 °C	3 198
100 m water pipe at 40 °C	3 476
200 m pipe at 95 °C plus 200 m pipe at 40 °C	13 348

Pressure loss because of bends in the circuit can be approximated by the equation

$$\Delta P_{loss} = C_{f\_bends} \cdot \frac{\rho v^2}{2}$$

which is a modification to Equation A-1. A good value for the C_{f_bends} factor is 0.25 (Næss, 2009). Assuming there are 5 bends in each pipe section, there are 20 bends all together. This equals a pressure loss of 2500 Pa. The total pressure loss due to surface friction and pipe bends then equals 15848 Pa or 0.16 bar.

Appendix B – cooling water temperature variation throughout the year

The graph below displays the annual temperature fluctuations as recorded at the entrance to Tya cast house from June 4th 2008 to June 4th 2009. From the graph it can be seen that the water temperature stays between 2 °C and 3 °C from the end of November to the beginning of April. Whereas during the rest of the year it is more unstable, but rises just until about 12 °C in the beginning of August and stays over 10 °C until the middle of September. It should be noted that this is only data from one year. The water temperatures differ from year to year dependent on the amount of precipitation in the area and temperature fluctuations. The data were received from Hans Jakob Dolmen, June 4th 2009.
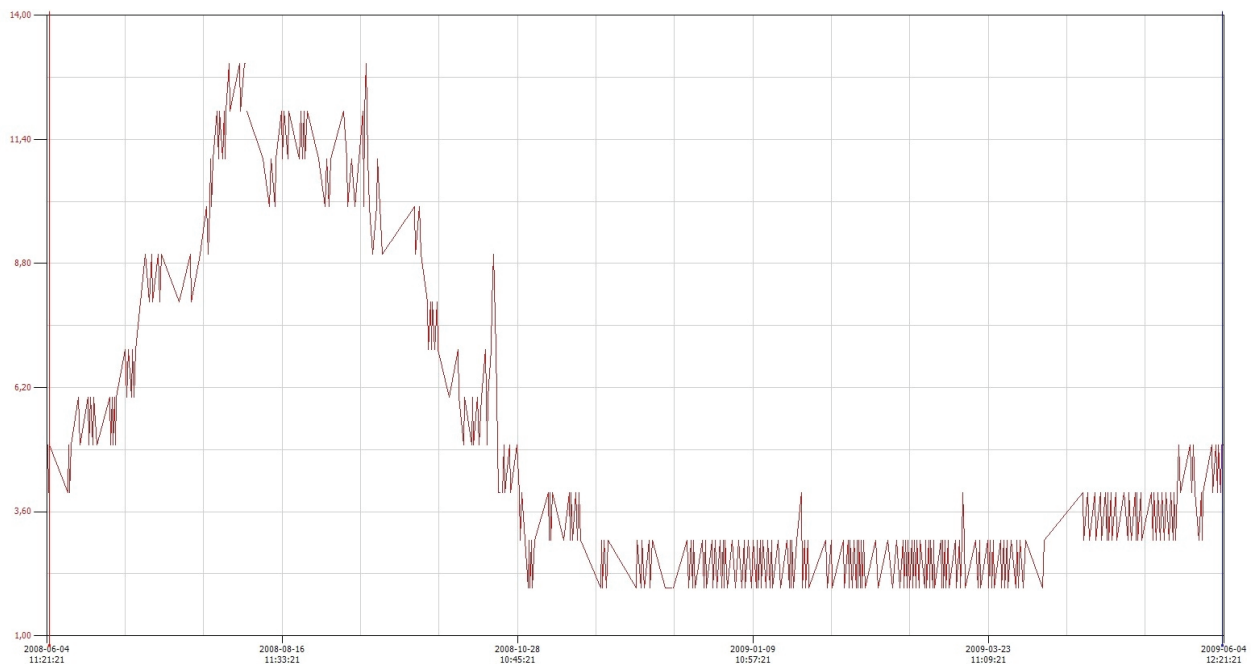
Appendix C – Received Performance Estimates

Opcon – E-mail communication

Hej Monica!

Ledsen att mina svar tar lite tid, men det är mycket hektiskt just nu! (Hoppas att bilden duger)

Du frågade också hur mycket mer el du kan få med den uppdaterade turbinen på 0,89MW axeleffekt:

En PowerBox med R134a:

Data varma sidan:

90c in, 74c ut
457 m3/h

Data kalla sidan:

7c in 16c ut
720 m3/h

Med dessa data ger en PowerBox 0,69MW el!

Om vi kan använda oss av NH3 (ammoniak):

En PowerBox med NH3:

Data varma sidan:

90c in, 68c ut
350 m3/h (kan inte ta hela flödet)

Data kalla sidan:

7c in 16c ut
720 m3/h

Med dessa data ger en PowerBox 0,75MW el!

Jag hoppas att detta enkla förfarande är OK för dig, har du fler frågor är det bara att höra av sig som vanligt! (dock kan det ta lite tid just nu)

Med vänlig hälsning/Best regards

Tony Gustavsson

Från: Monica Andrea Børgund [mailto:monicbo@stud.ntnu.no]
Skickat: den 8 juni 2009 15:49

Till: OES Tony Gustavsson
Ämne: Re: Opcon Powerbox and waste heat from Norwegian aluminiumindustry

Hei igjen Tony!

Er det mulig å få et bilde av Powerboxen? Enten en sketch eller et bilde av en powerbox ferdig montert? Ser det er ett bilde på hjemmesiden deres, men da dette er av den første powerboxen, tenkte jeg at den kanskje ser litt anderledes ut nå?

Monica

----- Original Message -----
From: OES Tony Gustavsson
To: Monica Andrea Børgund
Sent: Tuesday, June 02, 2009 11:30 AM
Subject: SV: Opcon Powerbox and waste heat from Norwegian aluminiumindustry

Hej Monica!

Det är alltid netto elen som vi diskuterar i våra förslag, brutto elen är bara intressant om det finns såsom i Sverige sk. gröna elcerifikat som kan nyttjas.

Priset som jag satt kan tänkas variera +-10% från 9 milj SEK + VAT beroende på materialval på värmeväxlarna.

Livstiden på en OPCON PowerBox är svårt att sia om men 20år är inget problem, årliga vedlikeholdskostnader på Ca 250.000 SEK/år (uppskattningen är gjord på en 5 årsplan med ett planerat turbinbyte efter Ca 30-50.000 timmars drift, utbytesturbiner har vi på lager).

Vi har nu möjlighet att höja axeleffekten till 0.89 MW för att kunna nyttja mer av den energi Ni har tillgänglig till PowerBoxen i ett flöde istället för att dela upp det som jag nämnde förut.

Vill du har mer info vet du att det är bara att höra av sig!

MVH

Tony Gustavsson

Från: Monica Andrea Børgund [mailto:monicbo@stud.ntnu.no]
Skickat: ti 2009-06-02 10:59
Till: OES Tony Gustavsson
Ämne: Re: Opcon Powerbox and waste heat from Norwegian aluminiumindustry

Hei igjen Tony!

Nå har jeg endelig fått tid til å se på det du sendte meg og jeg har noen spørsmål:

- Er det net eller gros el produksjon du refererer til i ditt forslag?
- Hva er usikkerheten i anslaget (+/- 5-10 % ?)
- Vet du noe om anslått livstid og årlige vedlikeholdskostnader?

Hilsen Monica

----- Original Message -----
From: "OES Tony Gustavsson" <Tony.Gustavsson@opcon.se>

To: "Monica Andrea Børgund" <monicbo@stud.ntnu.no>
Sent: Tuesday, May 12, 2009 12:05 PM
Subject: SV: Opcon Powerbox and waste heat from Norwegian aluminiumindustry

OBS!

Frakt och VAT tillkommer!

Med vänlig hälsning/Best regards

Tony Gustavsson

-----Ursprungligt meddelande-----
Från: OES Tony Gustavsson
Skickat: den 12 maj 2009 12:05
Till: 'Monica Andrea Børgund'
Ämne: SV: Opcon Powerbox and waste heat from Norwegian aluminiumindustry

Hej Monica!

Nu börjar det här bli bra!

En PowerBox med R134a:

Data varma sidan:

90c in, 74c ut
450 m3/h

Data kalla sidan:

7c in 19c ut
520 m3/h

Med dessa data ger en PowerBox 0,65MW el!

Om vi kan använda oss av NH3 (ammoniak):

En PowerBox med NH3:

Data varma sidan:

90c in, 69c ut
355 m3/h (kan inte ta hela flödet)

Data kalla sidan:

7c in 20c ut
520 m3/h

Med dessa data ger en PowerBox 0,7MW el!

Med NH3 kan du använda 2PowerBoxar på hela flödet och få ut Ca 1,1MW el!

Data varma sidan:

90c in, 62c ut
2*230 m3/h

Data kalla sidan:

7c in 21c ut
2*400 m3/h

Anledningen till att vi inte kan ta hela flödet genom PowerBoxen är att
Turbinens axeleffekt är begränsad till 0,8MW.

Pris uppskattning per box är Ca 9 milj svenska pesetas (kronor) per Box,
storlekar och dylikt ser du i broschyren. Att jag inte kan ge ett mer exakt
pris beror på materialval i Växlarna beroende på vatten kvaliteerna på varma
och kalla sidan.

Vad som tillkommer är kabel till ett ställverk, rördragning till BowerBoxen
varma och kalla sidan, Upställningsplats (gjuten platta, väger 30ton),
styrkabel från Hydro och lite ström från Hydro för uppstart och dyl.

Låter det intressant?

Med vänlig hälsning/Best regards

Tony Gustavsson

-----Ursprungligt meddelande-----
Från: Monica Andrea Børgund [mailto:monicbo@stud.ntnu.no]
Skickat: den 12 maj 2009 10:55
Till: OES Tony Gustavsson
Ämne: Re: Opcon Powerbox and waste heat from Norwegian aluminiumindustry

Det tycker jeg også! Det finnes nemligen en røykgass varmevekser som et
utviklet av Alstom som passer presis i dette temperatur området.
Kunne jeg fått et mer detaljert forslag fra dere med kostnadsestimat og
anleggstørrelse? Vi kan anta at røykgassvarmeveksleren har en
dimensjonerende minimum temperaturdifferanse på 20 grader. Da vil vannet som
tilføres Powerboxen være 90 grader og ha en massestrøm på 457,35 Nm3/h
(røykgass: 1456000 Nm3/h, Cp = 1.01 kJ/kgK, tetthet: 1,3 kG/Nm3, vann: Cp =
4.18, tetthet =1000).

Vennlig hilsen

Monica

----- Original Message -----
From: "OES Tony Gustavsson" <Tony.Gustavsson@opcon.se>
To: "Monica Andrea Børgund" <monicbo@stud.ntnu.no>
Sent: Tuesday, May 12, 2009 10:17 AM
Subject: SV: Opcon Powerbox and waste heat from Norwegian aluminiumindustry

Hej Monica,

Kan man göra på det viset du beskriver så går det hur bra som helst!

En snabb kalkyl gör att får du Ca 0,6MW/h vid ett varmt flöde (80C) på 360m3/h och 720m3/h vid 7C (kalla sidan). Får du upp temperaturen till 90C så ökar elen till 0.72MW/h!

Detta medför att du få mellan 5-6GWh/år tillbaka till processen, vilket är fantastiskt!

Med vänlig hälsning/Best regards

Tony Gustavsson

Turboden

(Next page)

Date: 16/04/2009
Doc.: 09J022820

TURBODEN
clean energy ahead

Heat recovery from aluminium production exhaust gas employing a Turboden ORC unit

We studied the heat recovery from exhaust gas with data reported in table 1.
We supposed to recover the heat contained in the exhaust gas through a hot water circuit.

Table 1: technical characteristics of the Hot Source

Hot Source		
Exhaust gas flow	1.456.000 Nm3/h	Ms Borgund
Exhaust gas temperature	110 ℃	Ms Borgund
Average SHC	1,01 kJ/(kg*K)	Turboden
Exhaust gas density	1,3 Kg/Nm3	Turboden
Gas cooled down to	90 ℃	Turboden
Thermal power recovered	10.625 kWt	Calculated

In table 2 you can find the preliminary technical characteristics of the Turboden module proposed for the heat recovery.
the working fluid used in the module is HFC 134 fa, no flammable, no corrosive.

Table 2: general technical characteristics of Turboden ORC module

Hot source	Water
Inlet water temperature	90 ℃
Outlet water temperature	70 ℃
Thermal power input in the ORC module	10.625 kWt
Inlet cooling water temperature	7 ℃
Outlet cooling water temperature	17 ℃
Thermal power discharged at the condenser	9.600 kWt
Gross electric power output ORC module	1.035 +/- 5% kWe
Captive consumption ORC module (*)	115 kWe
Net electric power output ORC	**920 +/- 5% kWe**
Specific price ORC module (refered to the gross electric power) (**)	2.100 +/- 10% €/kWe

(*) Captive consumption are refered to the ORC module only. Captive consumption about the hot water pump and the cooling water pump has not been considered in this evaluation.

(**) Scope of supply: main interfaces represented by the inlet and outlet hot water and cooling water flanges and the switch gear.